Estimation of Signal Modulation Based on FM to AM Transduction

by

Wade Patrick Torres

B.S., Electrical Engineering (1995)
B.S., Mathematics (1995)

Southern Illinois University at Carbondale

Submitted to the Department of Electrical Engineering and Computer Science
in partial fulfillment of the requirements for the degree of

Master of Science

at the

MASSACHUSETTS INSTITUTE OF TECHNOLOGY

May 1997

Author .....
Department of Electrical Engineering and Computer Science
May 9, 1997

Certified by .....
Thomas F. Quatieri
Senior Staff, MIT Lincoln Laboratory
Thesis Supervisor

Accepted by .....
Arthur C. Smith
Chairman, Departmental Committee on Graduate Students

Estimation of Signal Modulation Based on FM to AM Transduction

by

Wade Patrick Torres

Submitted to the Department of Electrical Engineering and Computer Science
on May 9, 1997, in partial fulfillment of the
requirements for the degree of
Master of Science

Abstract

In this thesis, we propose methods of estimating the amplitude modulation (AM) and frequency modulation (FM) of the non-stationary sinusoidal components of a signal. The approach is based on the transduction of FM to AM by a bank of filters, motivated by the possibility that the auditory system relies on a similar transduction in perceiving frequency modulation. FM to AM transduction occurs whenever a signal with a time-varying frequency sweeps across the non-flat frequency response of a filter, causing a change in the amplitude envelope of the filter output. When AM is also present, the AM and FM are nonlinearly combined in the amplitude envelope of the filter output. We use the amplitude envelopes of the output of a bank of filters to estimate the AM and FM of an input signal. We first develop a method that refines a current scheme for AM-FM estimation of a single sinusoid by iteratively inverting the AM and FM estimates to reduce error introduced in transduction. The approach is then extended to the case of two sinusoids by reducing the problem to two single-sinusoid AM-FM estimation problems, yielding a closed-form solution that is then improved upon by iterative refinement. For the general multi-component problem, where no closed-form solution has been found, a Newton-type iterative solution is proposed. Error analysis of the methods is performed using a frequency-domain view of transduction. The methods are demonstrated by example for a wide range of AM-FM functions.

Thesis Supervisor: Thomas F. Quatieri
Title: Senior Staff, MIT Lincoln Laboratory

Acknowledgments

I would first like to thank my thesis supervisor, Thomas Quatieri. He has graciously taken the time to oversee my research, providing insight and support along the way. At no point did he show any signs of fatigue or distress due to my continuous stream of questions, concerns, and sometimes bizarre ideas. More importantly, he has been a friend and role-model. Thank you.

I would also like to thank the members of the Speech Systems Technology Group at MIT Lincoln Laboratory for letting me use their facilities, helping me with computer problems, and providing a friendly environment in which to work. In particular, I would like to thank Dr. Bernard Gold for his mentorship, advice, and friendship over the last few years.

I also wish to thank the National Science Foundation, the AT&T Foundation, and the MIT EECS department for the financial support which has allowed me freedom in choosing a thesis topic and an advisor. I also wish to thank Rick Rose of AT&T Labs for his mentorship during my formative, pre-grad-school summer and his continued support.

I thank my family – my parents, Craig and Kathy, my grandmother, Bonnie, and my great-grandmother, Ethel – for always being there for me, believing in me, and giving me the freedom and courage to do whatever I wanted in life.

Last (and definitely not least), I want to thank my wife, Donna, for being there for me. I hope I'm half as supportive for her as she is for me. We've had a wonderful time together, I love you.

This material is based upon work supported under a National Science Foundation Graduate Fellowship. Any opinions, findings, conclusions or recommendations expressed in this publication are those of the author and do not necessarily reflect the views of the National Science Foundation.

Contents

List of Figures

List of Tables

Chapter 1

Introduction

We are surrounded by non-stationary signals. Non-stationary signals consist of components with amplitude envelopes and frequencies that change with time. A familiar example is speech. Whenever we speak, we transform our thoughts into sounds whose components have time-varying amplitudes and frequencies. The changes in the amplitudes and frequencies of those sounds carry the information necessary for a listener to transform the sounds back into thought. Radio broadcasts are another example of non-stationary signals. AM radio broadcasts consist of signals with changing amplitude and a stationary frequency, and FM radio broadcasts consist of signals with a stationary amplitude and a changing frequency. In fact, any signal with a beginning or an end can be considered a non-stationary signal since its amplitude envelope must transition between zero and some non-zero value at some point in time. With this rather broad definition of non-stationary signals, it is apparent that practically any signal of interest is non-stationary.

The goal of this thesis is to estimate the time-varying amplitude and frequency of the components of a signal. To make this mathematically precise, consider a discrete-time signal of the form

$$s[n] = \sum_{k=1}^{N} a_k[n] \cos(\theta_k[n]). \tag{1.1}$$

Our goal is to estimate each $a_k[n]$, which we refer to as the amplitude modulation

(AM), and each $\dot{\theta}_k[n]$, which we refer to as the frequency modulation (FM)[1]. Our approach utilizes the amplitude envelopes of the outputs of a filter bank, which is motivated by the possibility that the auditory system uses this information for separating sound components.

In this chapter, we begin with a description of a few of the more common approaches to AM-FM estimation. We then further introduce our approach and discuss the motivation behind it in more detail. The chapter concludes with a discussion of the contributions of this thesis and an outline of the remainder of the thesis.

1.1 Background

A multitude of approaches have been taken to estimate the AM and FM of signal components. In this section, we describe a few of the more popular methods. The approaches were chosen because together they encompass the majority of the fundamental strategies that have been applied towards AM-FM estimation.

1.1.1 Residual Signal Analysis

Residual Signal Analysis (RSA) was originally proposed by Costas [5, 6]. It is not aimed directly at estimating AM and FM, but rather to track the individual AM-FM sinusoids that make up a complex signal. In the process of tracking the individual components, however, estimates of the AM and FM are obtained and, therefore, RSA can be viewed as an AM-FM estimation method.

In RSA, it is assumed that the signal of interest is of the form

$$s[n] = \sum_{k=1}^{N} a_k[n] \cos(\theta_k[n]) = \sum_{k=1}^{N} x_k[n]. \tag{1.2}$$

The input signal is passed through a bank of N "trackers", one for each AM-FM sinusoid. In order for a given tracker to see only one component of the input signal,

[1] We are abusing the notation here. $\dot{\theta}[n]$ refers to the signal obtained from sampling the derivative of the continuous-time phase, $\theta(t)$, that corresponds to $\theta[n]$.

the value of all other components at the next time instant must be predicted and then subtracted from the incoming sample of the composite signal. Therefore, the input to the kth tracker at time $n = n_0$ is

$$s_k[n_0] = s[n_0] - \sum_{i \neq k}^{N} \tilde{x}_i[n_0], \tag{1.3}$$

where $\tilde{x}_i[n_0]$ is the predicted value of the ith component of $s[n_0]$. This procedure is illustrated in Figure 1-1.

There are two central issues with this approach. First, a component must be acquired before it can be tracked. In other words, at a given instant in time, the system must somehow determine if there is a signal present at some frequency. In most systems based on RSA, this usually involves calculating the energy of the composite signal in a narrow frequency band and assigning a tracker to it if the energy exceeds some threshold. The problem is that there is not an obvious value to choose as a threshold. The second issue involves the estimation of the value of the individual components on the next sample. In Costas' original implementation, the next sample was estimated by simply advancing the phase of the estimate of the current sample, which assumes that there is negligible change in both the amplitude and the frequency of each component of $s[n]$. A more effective method of estimation has been proposed by Ramalingam [17].

1.1.2 The Teager Operator

The Teager operator is a nonlinear operator that estimates the amplitude modulation and frequency modulation of a single sinusoid, i.e.

$$s[n] = a[n]\cos(\theta[n]). \tag{1.4}$$

In discrete-time, the Teager operator,$\Psi(s[n])$, is defined as

$$\Psi(s[n]) = s^2[n] - s[n-1]s[n+1] \tag{1.5}$$

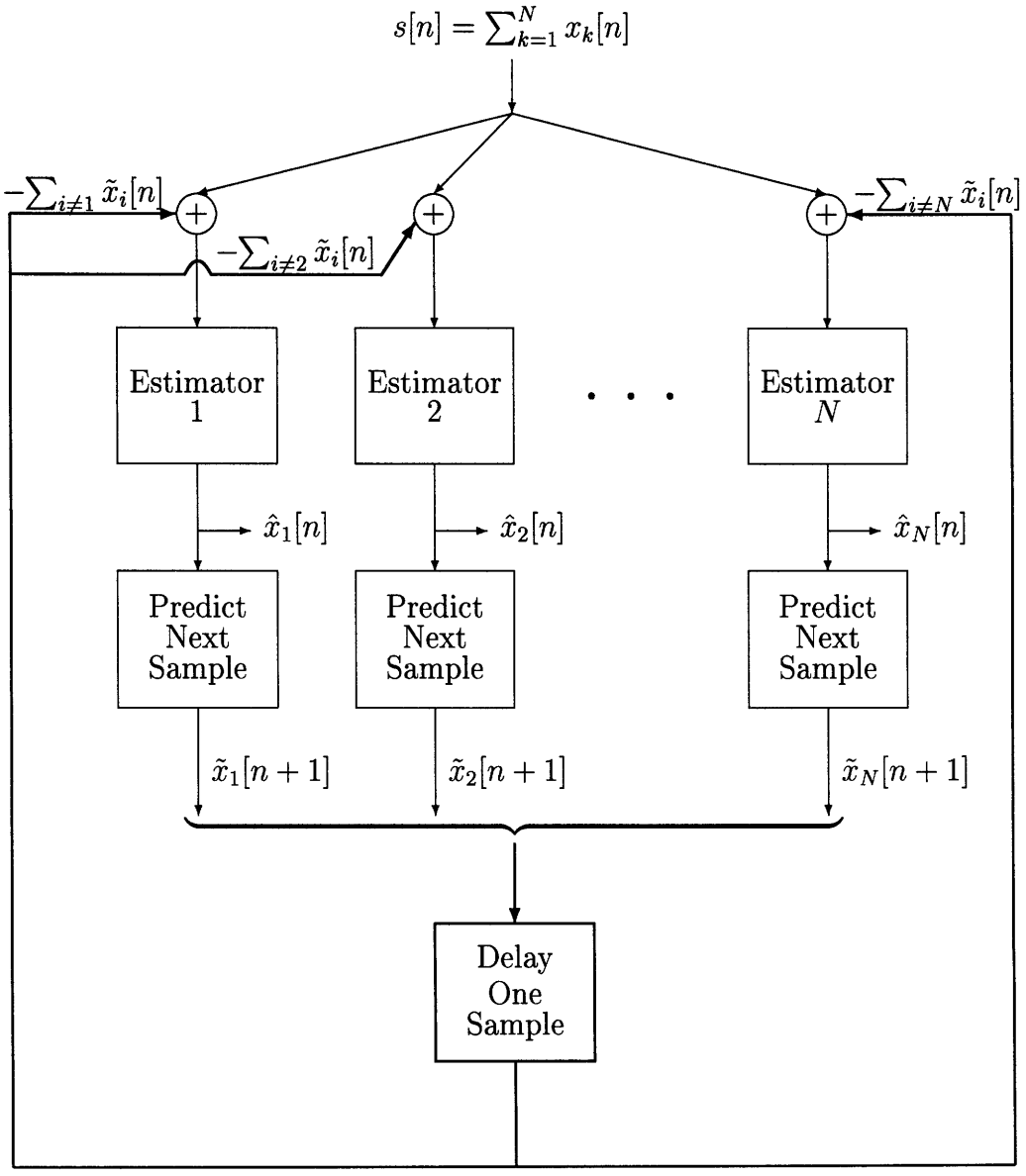

Figure 1-1: A block diagram of residual signal analysis system.

with the property that [10, 11]

$$\Psi(s[n]) \approx a^2[n]\dot{\theta}^2[n] \tag{1.6}$$

under the conditions

$$\Omega_f \ll 1 \tag{1.7}$$

and

$$\sin^2\left(\frac{\Omega_a}{2}\right) \ll \max_n \left[\sin^2(\dot{\theta}[n])\right], \tag{1.8}$$

where Ω_f and Ω_a are the bandwidths of $\dot{\theta}[n]$ and $a[n]$, respectively. $\Psi(s[n])$ is also referred to as the *energy operator* because it is proportional to the energy required for a harmonic oscillator to generate $s[n]$.

Using the Teager operator, the Discrete Energy Separation Algorithms 1 and 2 (DESA-1 and DESA-2) have been developed [10] that estimate the AM and FM of Eq. (1.4). For example, the DESA-1 algorithm uses the Teager operator to estimate $a[n]$ and $\dot{\theta}[n]$ in the following manner:

$$\begin{aligned} a[n] &\approx \frac{2\Psi[x(n)]}{\sqrt{\Psi[x(n+1)-x(n-1)]}} \\ \dot{\theta}[n] &\approx \arcsin\left(\sqrt{\frac{\Psi[x(n+1)-x(n-1)]}{4\Psi[x(n)]}}\right) \end{aligned} \tag{1.9}$$

which holds again under bandwidth constraints on the AM and FM. Both DESA-1 and DESA-2 are intended only for signals that consist of a single AM-FM sinusoid. There have been attempts to generalize this method to multi-component signals [9, 12, 19], but even stronger constraints on the rate of change of the AM and FM must be imposed than the constraints of DESA-1 and DESA-2.

1.1.3 Time-Frequency Distributions

A Time-Frequency Distribution (TFD) is a two dimensional function, $P(t, \omega)$, that describes the energy of a signal in time and frequency simultaneously. It is usually displayed as a three dimensional plot, the axes being time, frequency, and energy. This method does not directly estimate the AM and FM of the components that make up a signal, but it does display this information in an accessible form. One approach to obtaining the AM and FM from such a function is to simply track the peaks of $P(t, \omega)$ on the time-frequency plane, while another method relies on moments of the TFD [2].

TFDs are quite popular and are used in a wide range of applications. Some examples of common TFDs include the spectrogram, the Wigner distribution, and the Choi-Williams distribution. These particular TFDs belong to a large class, all of which can be obtained from [4]

$$C(t,\omega) = \frac{1}{4\pi^2} \int\int\int x^*(u - \frac{1}{2}\tau)x(u + \frac{1}{2}\tau)\phi(\theta,\tau)e^{-j\theta t - j\tau\omega + j\theta u} du d\tau d\theta \qquad (1.10)$$

where $\phi(\theta, \tau)$ is called the "kernel".

There are some significant drawbacks to TFDs. First, the best distribution to use depends on the signal being analyzed. For example, the Wigner distribution works particularly well for FM-chirp signals, but not as well for other FM functions. Also, various types of artifacts occur, especially when the signal consists of more than one component. The most common artifact is the appearance of cross-terms, i.e. there is energy in the time-frequency plane when it is known that no energy is actually in those locations.

1.2 An Approach Motivated by the Auditory System

The methods of the previous section show that the problem of AM-FM estimation can be approached from a variety of viewpoints. RSA is reminiscent of feedback systems used in control theory. The Teager operator was derived by considering the energy required for a harmonic oscillator to generate the AM-FM signal. TFDs can be thought of as generalizations of traditional analysis techniques such as the Fourier transform in the sense that they project some form of the signal onto a set of basis functions. In this thesis, we use yet another approach, based on FM to AM transduction, that is fundamentally different from those mentioned above.

1.2.1 Motivation

The human auditory system has the ability, to a certain extent, to track the amplitude modulation and frequency modulation of a sound. This is essentially our goal. Admittedly, the auditory system is not a perfect AM-FM estimator, but in a general sense, it seems to do what we hope to accomplish. We cannot show that the auditory system actually estimates AM and FM. We can only say that, through our experience, the auditory system somehow gives rise to the sensation of AM and FM. Our goal, however, is not to show how or if the auditory system estimates AM and FM. Instead, our goal is to develop an approach to AM-FM estimation, motivated by a simple model of auditory processing.

1.2.2 Some Properties of the Auditory System

Although the auditory system is a very complex system and much of it is not completely understood, there are a few basic properties that are well known:

1. The first processing stage consists of a large bank of broad, overlapping filters.
2. There is FM to AM transduction from filtering [8, 18]. As the FM sweeps across the frequency response of a filter, a change is induced in the amplitude envelope

of the filter output.

3. The outputs of the overlapping filters are rectified resulting in an amplitude envelope.

4. The rectified signal is transmitted to higher auditory processes.

These properties indicate that one signal used by the higher auditory system is the amplitude envelopes of the filter outputs and that these envelopes are dependent upon the AM and FM functions. A block diagram of this simple auditory model is shown in Figure 1-2.

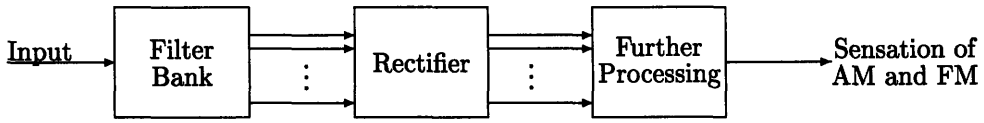

Figure 1-2: A simple block diagram of the auditory system.

1.2.3 Approach

The auditory model in Figure 1-2 is the motivation for our approach. The first step is to filter the signals with a bank of broad, overlapping filters that have a non-flat frequency response followed by a rectification stage in which we calculate the amplitude envelopes of the output. The output envelopes are not only functions of the amplitude modulation of the input, but they are also functions of the frequency modulation due to the FM to AM transduction. In the case where the input consists of a single AM-FM sinusoid, we obtain a closed form solution for the AM and the FM from the amplitude envelopes. When the input consists of a sum of two AM-FM sinusoids, we reduce the problem into two single-sinusoid AM-FM estimation problems and thereby derive a closed-form solution. In the case where there are more than two AM-FM components in the input signal, we are unable to find a

closed-form solution. We do, however, propose a method that still utilizes FM to AM transduction, but instead of a closed form solution, the solution is obtained using standard numerical methods. Although motivated by auditory modeling, we do not claim that the auditory system uses these specific methods for AM-FM estimation.

1.3 Thesis Contribution

This thesis contributes to the area of signal processing in several ways. First, it improves upon the algorithms based on FM to AM transduction implemented by Quatieri et al. [16] by improving the accuracy of AM and FM estimates. Second, the method is extended to the case where the signal consists of two AM-FM sinusoids. Third, a method for estimating the AM and FM of a signal with an arbitrary number of components is proposed. Last, we introduce a frequency domain interpretation of filtering non-stationary signals with linear, time-invariant filters which allows us to perform error analysis of the AM-FM estimation algorithms.

1.4 Thesis Organization

In the current chapter, we have described some of the more popular methods of AM-FM estimation and discussed the motivation behind our approach. In Chapter 2, we discuss some issues related to AM-FM estimation such as uniqueness, the concept of instantaneous frequency, and general constraints on the types of signals that can be analyzed. In Chapter 3, we describe FM to AM transduction and give an approximation for the output of linear, time-invariant filters when the input is non-stationary. Chapter 4 covers the case in which a signal consists of only one AM-FM sinusoid, providing the foundation of the next two chapters. Chapter 5 presents a technique that improves performance of the algorithm of Chapter 4 based on inverting the modulation to reduce transduction error. Issues of robustness with respect to the center frequency and filter shape are discussed in Chapter 6. We also present a frequency domain analysis of the approximation used for the output of a linear, time-invariant

filter when the input is a non-stationary signal. In Chapter 7, an algorithm for estimating the AM and FM of a signal composed of two AM-FM sinusoids is presented and refinements are then made based on generalization of inverse modulation techniques of Chapter 5. Chapter 8 shows how AM-FM estimation can be performed on signals composed of multiple AM-FM sinusoids by posing the problem as a system of nonlinear equations and solving these equations using standard numerical techniques. The last chapter summarizes the thesis and gives suggestions for future work.

Chapter 2

Preliminaries

Before we describe the AM-FM estimation algorithms, we introduce a few concepts, definitions, and subtle issues associated with AM-FM signals. The first topic is the analytic signal, which is important for both establishing the uniqueness of the AM-FM estimates and avoiding complications that often arise when using real signals. We then discuss the concept of instantaneous frequency and some difficulties in formulating its definition. The last section addresses the ambiguity in writing a signal in terms of AM-FM components.

2.1 The Analytic Signal

We use the following definition for the analytic signal.

DEFINITION 2.1 (ANALYTIC SIGNAL)
The continuous-time (CT) analytic signal, $s(t)$, and the discrete-time (DT) analytic signal, $s[n]$, have Fourier transforms that are identically zero over the negative frequency range, i.e.

$$S(\omega) = \int_{\infty}^{\infty} s(t)e^{-j\omega t}dt = 0 \qquad \text{for } \omega \in (-\infty, 0] \quad \text{(CT)} \tag{2.1}$$

$$S(e^{j\omega}) = \sum_{n=-\infty}^{\infty} s[n]e^{-j\omega n} = 0 \qquad \text{for } \omega \in [-\pi, 0] \quad \text{(DT)}. \tag{2.2}$$

For the discrete-time case, for example, $s[n]$ is an analytic signal if and only if its spectrum is identically zero for negative frequencies. From this definition, it follows

that there is only one analytic signal, which we denote $s_a[n]$, corresponding to any signal $s[n]$. This property will be useful when we establish the conditions under which AM-FM estimation gives a unique solution. Also, the envelope of an analytic signal can be determined by simply calculating its magnitude. Since the later algorithms use the amplitude envelope of signals, the analytic signal is a useful form.

Since most signals to be analyzing are real, we discuss the relationship between a real signal and its analytic counterpart in more detail. To calculate the analytic counterpart of a real signal[1], $s[n]$, we zero the negative frequencies of $s[n]$ [4], i.e.

$$s_a[n] = 2\frac{1}{2\pi}\int_0^{\pi} S(e^{j\omega n})e^{j\omega n}d\omega, \tag{2.3}$$

where $S(e^{j\omega})$ is the discrete-time Fourier transform of $s[n]$. Since we are interested in calculating $a[n]$ and $\dot{\theta}[n]$, we desire the analytic signal to have the same amplitude and phase function as the real signal. To establish conditions under which this is true, we introduce the quadrature signal, which is given by

$$s_q[n] = a[n]e^{j\theta[n]}. \tag{2.4}$$

The analytic signal has the same phase as the real signal when

$$s_a[n] = s_q[n] \tag{2.5}$$

Since $e^{j\theta[n]} = \cos(\theta[n]) + j\sin(\theta[n])$,

$$S_q(e^{j\omega}) = S(e^{j\omega}) + j\sum_{n=-\infty}^{\infty} a[n]\sin(\theta[n])e^{-j\omega n} \tag{2.6}$$

$$S_q^*(e^{-j\omega}) = S^*(e^{-j\omega}) - j\sum_{n=-\infty}^{\infty} a[n]\sin(\theta[n])e^{-j\omega n}. \tag{2.7}$$

[1]The analytic signal is twice the inverse Fourier transform of the positive frequencies of $s[n]$ so that $\mathrm{Re}\{s_a[n]\} = s[n]$.

When $s[n]$ is real, $S(e^{j\omega}) = S^*(e^{-j\omega})$. Therefore,

$$S_q(e^{j\omega}) + S_q^*(e^{-j\omega}) = 2S(e^{j\omega}). \tag{2.8}$$

Since

$$S_a(e^{j\omega}) = \begin{cases} 0 & \text{for } -\pi \leq \omega < 0 \\ 2S(e^{j\omega}) = S_q(e^{j\omega}) + S_q^*(e^{-j\omega}) & \text{for } 0 \leq \omega < \pi \end{cases} \tag{2.9}$$

we have the condition that $S_a(e^{j\omega}) = S_q(e^{j\omega})$ if $S_q(e^{j\omega}) = 0$ for $-\pi \leq \omega < 0$. Therefore,

$$s_a[n] = a[n]e^{j\theta[n]}$$

if

$$\sum_{n=-\infty}^{\infty} a[n]e^{j\theta[n]}e^{-j\omega n} = 0 \qquad \text{for } -\pi < \omega < 0 \tag{2.10}$$

In other words, the real signal $s[n] = a[n]\cos(\theta[n])$ has a corresponding analytic signal $s_a[n] = a[n]e^{j\theta[n]}$ when the spectrum of $a[n]e^{j\theta[n]}$ contains no negative frequencies. Throughout this thesis, we assume this to be true.

2.2 Instantaneous Frequency

Instantaneous frequency is a peculiar concept because it is very easy to understand on an intuitive level, but very difficult to describe mathematically. As an example of what is meant by the instantaneous frequency, consider a signal that is one second in duration and starts at frequency of 100Hz and steadily climbs to 200Hz. At half of a second into the signal, we say that the signal is at a frequency of 150Hz. Representing this intuition mathematically, however, is not straightforward.

A standard definition of instantaneous frequency is the derivative of the phase of

the analytic signal [4]. For some signals, this definition of instantaneous frequency matches our intuition, as shown in the next example.

EXAMPLE 2.1
Consider a signal

$$s(t) = \cos\left(2\pi(100t + 50t^2)\right) \qquad \text{for } 0 \leq t \leq 1, \tag{2.11}$$

with the corresponding quadrature signal

$$s_q(t) = e^{j2\pi(100t+50t^2)} \qquad \text{for } 0 \leq t \leq 1. \tag{2.12}$$

The phase derivative is $2\pi(100 + 100t)$ and at $t = .5$ seconds, we obtain a frequency of 150Hz.

In the above example, the result is what we expect. If a signal consists of two sinusoids, however, this definition in terms of the phase derivative no longer meets our intuition.

EXAMPLE 2.2
Suppose $s(t)$ consists of a sum of two stationary sinusoids

$$s(t) = \cos(2\pi 10t) + 2\cos(2\pi 20t) \tag{2.13}$$

which has the corresponding quadrature signal

$$s_q(t) = e^{j2\pi 10t} + 2e^{j2\pi 20t}. \tag{2.14}$$

To determine the phase derivative, we first need $s_q(t)$ in a form with one phase term. Doing so gives us

$$s_q(t) = (5 + 4\cos(2\pi 10t))\, e^{j \arctan\left(\frac{\sin(2\pi 10t)+2\sin(2\pi 20t)}{\cos(2\pi 10t)+2\cos(2\pi 20t)}\right)} \tag{2.15}$$

and a resulting instantaneous frequency function

$$\text{IF} = \frac{1}{2}(2\pi 30) + \frac{1}{2}(2\pi 10)\frac{3}{(5 + 4\cos(2\pi 10t))^2} \tag{2.16}$$

A plot of the instantaneous frequency is shown in Figure 2-1.

Thus, according to our definition of instantaneous frequency, the frequency of the signal varies between approximately 17Hz and 30 Hz. There are some obvious problems with the instantaneous frequency obtained in Example 2.2. First, one of the sinusoids

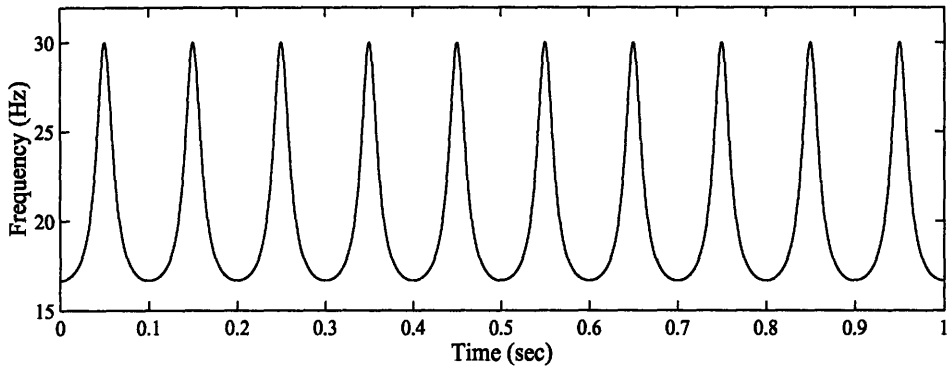

Figure 2-1: An example of the instantaneous frequency of a sum of two sinusoids.

that made up our signal was at 10Hz, yet the instantaneous frequency never equals this value. Second, when shown the plot of the frequency, we would expect that if we heard such a signal it would waver rapidly in frequency. However, it is actually perceived as a tone with no modulation. Cohen has summarized [4] a few of the "paradoxes" of the definition we have given for instantaneous frequency:

1. Frequencies that are in the spectrum might not appear in the instantaneous frequency.

2. For a signal that consists of only a few frequencies, the instantaneous frequency might vary over a large range of frequencies.

3. For an analytic signal, i.e. a signal with no negative frequencies, the instantaneous frequency might be negative.

4. For a band-limited signal, the instantaneous frequency might go outside of the band.

5. To calculate the instantaneous frequency, the analytic signal must be obtained because the instantaneous frequency has been defined as the derivative of the phase of the analytic signal. Since calculating the analytic signal is dependent upon the signal over the entire time axis, the instantaneous frequency indirectly depends on future and past values.

It is obvious that this popular definition for the instantaneous frequency does not lead to the desired results since it does not account for the possibility of more than one instantaneous frequency. If we were asked to describe the signal given in Eq. 2.14, we would say that it consists of *two* sinusoids, one with an instantaneous frequency of 10Hz and the other with an instantaneous frequency of 20Hz. Therefore, we must allow for the possibility of the signal having multiple instantaneous frequencies, one for each sinusoid present in the signal. We redefine instantaneous frequency to be a *set* of phase derivatives, with each phase derivative corresponding to a particular AM-FM component of the signal being analyzed.

2.3 Representing a Signal as a Sum of AM-FM Sinusoids

Although allowing multiple instantaneous frequencies might avoid some of the "paradoxes" listed in the previous section, we are now faced with the problem of determining how many AM-FM sinusoids make up a signal. This is not a simple matter. In fact, if the signal of interest is white noise, representing it as a sum of AM-FM sinusoids is probably not much more enlightening than representing it as a sum of stationary sinusoids, as in standard Fourier techniques. In this section, we discuss the problem of determining how many sinusoids make up a signal and describe some constraints that ensure that the signal lies within the framework of the methods developed in this thesis.

2.3.1 Two Extremes

An arbitrary signal can be expressed in an uncountably infinite number of ways. At one end, it can be written as a single AM-FM sinusoid in an infinite number of ways and, at the other end, it can be written in only one way as a sum of infinite number of AM-FM sinusoids. We begin with the first case. Suppose we are given a real signal,

$s[n]$, that is non-zero for $-N \leq n \leq N$ and we want to represent it in the form

$$s[n] = a[n]\cos(\theta[n]). \tag{2.17}$$

One way to to do this would be to simply choose any value for $a[n]$ at each n with the constraint that $a[n] \geq |s[n]|$. This implies that $\theta[n]$ is equal to $\arccos\left(\frac{s[n]}{a[n]}\right)$. Since the only constraint is that $a[n] \geq |s[n]|$, there are an infinite number of possible choices for $a[n]$ and $\theta[n]$ at each sample point. Note, however, that an analytic signal, $s_a[n]$, can be expressed as an AM-FM sinusoid in *only one way.* This is due to the fact that if $s_a[n] = a[n]e^{j\theta[n]}$, it must be true that $|s_a[n]| = |a[n]e^{j\theta[n]}| = a[n]$ and therefore, $a[n]$ is uniquely defined. This implies that $\theta[n] = -j\ln\left(\frac{|s_a[n]|}{a[n]}\right)$, which is also unique (modulo 2π).

We can also represent $s[n]$ as a sum of an infinite number of AM-FM sinusoids. One way[2] is to take the discrete-time Fourier transform of $s[n]$, i.e.

$$s[n] = \frac{1}{2\pi}\int_{-\pi}^{\pi} S(e^{j\omega})e^{j\omega n}d\omega, \tag{2.18}$$

where we are viewing the integral as the limit of a summation. We can also take M stationary sinusoids obtained from the Fourier transform and express the remaining sinusoids as a single AM-FM sinusoid. This gives a representation of $s[n]$ consisting of $M+1$ AM-FM sinusoids. In this fashion, we can write an arbitrary signal as a sum of any number of AM-FM sinusoids.

After making these observations, we see that from a strictly mathematical point of view, it is meaningless to say that a signal consists of a certain number of sinusoids. There is, however, for a given signal, a particular representation in terms of AM-FM signals that is more "natural" and intuitive, as in Example 2.2. There it seemed more natural to view the signal as a sum of two stationary sinusoids rather than one sinusoid with both AM and FM. Determining the correct number of sinusoids is a rather complex issue and not the topic of this thesis. Therefore, we assume that the

[2]We consider stationary sinusoids to be a member of the class of AM-FM sinusoids; they are AM-FM signals with constant modulation functions.

correct number of sinusoids, N, is known beforehand and our goal is to determine the AM and FM of the signal under the assumption that $s[n]$ is the sum of N non-stationary sinusoids.

2.3.2 Signal Constraints

Throughout the remainder of the thesis, it is assumed that the signals being analyzed satisfy two constraints. These constraints are necessary to ensure that the algorithm produces the expected results. First, the signal must always be present and consist of the same number of AM-FM sinusoids. This constraint allows us to avoid the problem of signal detection. Second, the quadrature signal, described in Section 2.1, must equal the analytic signal. If this condition is not met, an increasing difference between the quadrature signal and the analytic signal results in an increasing amount of error in the estimates. This constraint indirectly places constraints on the the AM and FM because it constrains the spectrum of $a_i[n]e^{j\theta_i[n]}$ to be confined to the interval $[0, \pi]$. To establish when this constraint is violated, we determine the manner in which the FM and AM contribute to the width of the spectrum of $a_i[n]e^{j\theta_i[n]}$. We denote the Fourier transform of the amplitude as $S_{AM}(e^{j\omega})$ and the Fourier transform of $e^{j\theta_i[n]}$ as $S_{FM}(e^{j\omega})$. Since multiplication in the time domain corresponds to convolution in the frequency domain,

$$S_q(e^{j\omega}) = \int_{-\pi}^{\pi} S_{AM}(e^{j(\omega-\tilde{\omega})}) S_{FM}(e^{j\tilde{\omega}}) d\tilde{\omega}, \tag{2.19}$$

which means that the width of the spectrum of the quadrature signal is equal to the sum of the widths of $S_{AM}(e^{j\omega})$ and $S_{FM}(e^{j\omega})$. Therefore, to state the constraint more explicitly, the sum of the widths of $S_{AM}(e^{j\omega})$ and $S_{FM}(e^{j\omega})$ must be less than π, otherwise the spectrum of the quadrature signal cannot be confined to frequencies between 0 and π. Note that this constrains the spectral content of the AM and FM functions, but not necessarily their rate of change.

2.4 Summary

We began with a discussion of the analytic signal and the relationship between real signals and their analytic counterparts. We then introduced the concept of instantaneous frequency and gave reasons, through a few examples, for defining it so that it allows a signal to have multiple instantaneous frequencies. Next, we addressed the issue of representing an arbitrary signal as a sum of AM-FM sinusoids. In particular, we showed that it is possible to express a signal with any number of AM-FM sinusoids and that for a given number of AM-FM sinusoids, there is not, in general, a unique expression. We did show, however, that if the signal consists of one analytic component, the amplitude and phase derivative are uniquely specified. We then gave constraints in order to ensure that the signals being analyzed fit within the framework of our algorithms.

Chapter 3

FM to AM Transduction

This chapter introduces the fundamental idea behind this thesis – FM to AM transduction. FM to AM transduction was first used in FM broadcasting by Armstrong [1] for FM demodulation in a device referred to as a *balanced frequency discriminator.* Recently, evidence of FM to AM transduction has been observed in the early processing stages of the auditory system [18].

In the first section, we give a general description of FM to AM transduction and how it arises in filtering. The following section covers an important relation called the *transduction approximation.* The last section describes the circumstances under which the transduction approximation is valid.

3.1 Filtering and FM to AM Transduction

FM to AM transduction occurs when an FM signal passes through a filter that has a non-flat spectral shape. As the frequency of the signal sweeps across the passband of the filter, the amplitude envelope of the filter output changes. In this fashion, the amplitude envelope of the filter output is a function of both the AM and the FM of the filter input. This idea is best illustrated by a few examples.

EXAMPLE 3.1
Consider the signal,

$$s[n] = e^{j(1.1n+2\sin(.1n))}, \tag{3.1}$$

passed through a filter with frequency response

$$H(e^{j\omega}) = \begin{cases} \omega & 0 \leq \omega < \pi \\ 2\pi - \omega & \pi \leq \omega < 2\pi \end{cases} . \tag{3.2}$$

Due to the change in frequency of $s[n]$, the signal moves across the frequency response of the filter as a function of time. This movement induces a change in amplitude envelope of the output, as shown in Figure 3-1.

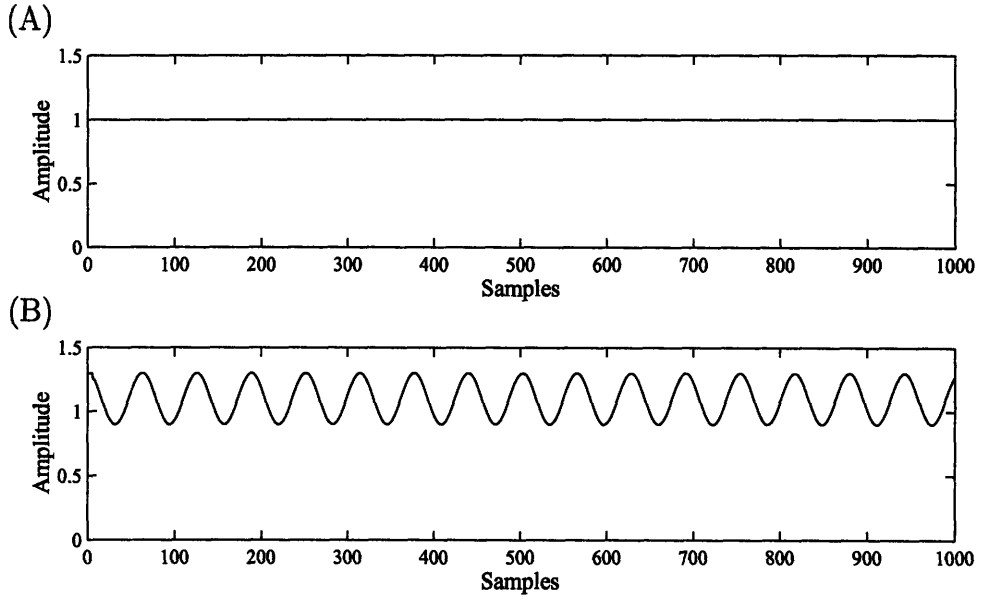

Figure 3-1: An example of FM to AM transduction, (A) the amplitude envelope of the filter input, and (B) the amplitude envelope of the filter output.

EXAMPLE 3.2

Now suppose that we add amplitude modulation to the signal,

$$s[n] = \left[e^{-.00001(n-500)^2}\right] e^{j(1.1n+2\sin(.1n))}, \tag{3.3}$$

and use the same filter from Example 3.1. The amplitude envelope of $s[n]$ and the amplitude envelope of the filter output is shown in Figure 3-2. The amplitude envelope of the output of the filter depends both on the AM and the FM of $s[n]$.

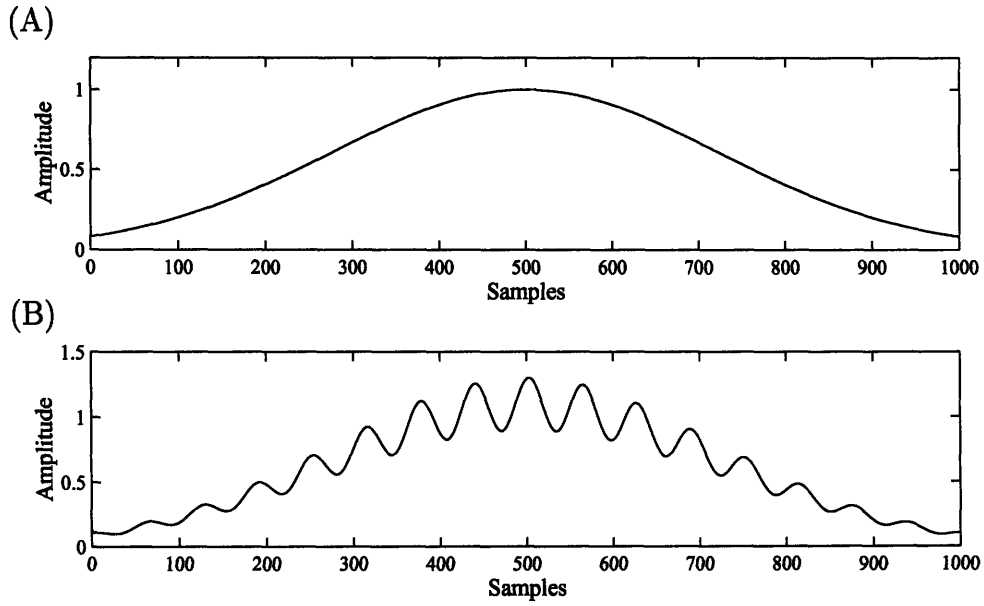

Figure 3-2: An example of FM to AM transduction when both AM and FM are present, (A) the amplitude envelope of the filter input, and (B) the amplitude envelope of the filter output.

3.2 The Transduction Approximation

In the previous section, it was shown by way of example how frequency modulation can be transformed into amplitude modulation and that the AM and FM are nonlinearly combined in the amplitude envelope of the filter output. We now show how to approximate the filter outputs.

Since we are interested in obtaining the AM and FM as functions of time, a temporal representation is desired. One possible representation is the convolution sum,

$$y[n] = \sum_{k=-\infty}^{\infty} h[k]x[n-k], \tag{3.4}$$

where $x[n]$ is the input to the filter with impulse response $h[n]$. Unfortunately, this representation is intractable for the type of analysis used to develop the AM-FM estimation algorithms. Instead, the convolution sum is approximated. Suppose the

input to the filter is of the form

$$x[n] = a[n]e^{j\theta[n]}. \tag{3.5}$$

The output of a linear, time-invariant (LTI) filter with frequency response $H(e^{j\omega})$ can then be approximated as

$$y[n] \approx a[n]e^{j\theta[n]}H(e^{j\dot{\theta}[n]}) = x[n]H(e^{j\dot{\theta}[n]}). \tag{3.6}$$

This approximation is referred to as the *transduction approximation.* Here it is assumed that $x[n]$ has been obtained by sampling a continuous time signal and that the phase derivative, $\dot{\theta}[n]$, is the sampled continuous-time phase derivative. Observe that if $x[n]$ has no AM and FM, then this approximation is exact. In fact, this approximation can be viewed as treating all AM-FM signals as if they are eigenfunctions of an LTI filter, which is true only of stationary signals. The above approximation is sometimes referred to as the *quasi-eigenfunction approximation.* The name "transduction approximation" is used here to emphasize FM to AM transduction property.

3.3 Error Bounds for the Transduction Approximation

Error bounds for the transduction approximation have been derived by Bovik et al [3]. Although we do not use these error bounds explicitly, they provide guidelines for the design of the filterbank of Chapter 4. The error bounds are summarized as follows. Consider a signal of the form

$$s[n] = a[n]e^{j\theta[n]}. \tag{3.7}$$

Let $y[n]$ be the actual output of an LTI filter with frequency response $H(e^{j\omega})$ and impulse response $h[n]$, i.e.,

$$y[n] = s[n] * h[n] \tag{3.8}$$

and $\hat{y}[n]$ be the output approximated by

$$\hat{y}[n] \approx s[n]H(e^{j\dot{\theta}[n]}). \tag{3.9}$$

Then the error, defined as

$$\varepsilon[n] = |y[n] - \hat{y}[n]|, \tag{3.10}$$

is bounded by

$$\varepsilon[n] \leq \sum_{\substack{p\in\mathbf{Z} \\ p\neq 0}} |h[p]| \int_{n-p}^{n} \left(|\dot{a}(v)| + a_{max}|p||\ddot{\theta}(v)| \right) dv, \tag{3.11}$$

where $a_{max} = \max_n a[n]$ and $a(v)$ and $\theta(v)$ are the continuous time signals corresponding to $a[n]$ and $\theta[n]$.

This bound indicates that there are three factors that influence the accuracy of the transduction approximation. First, increasing the amount or rate of the AM increases the first term in the integration and thereby increases the error. Likewise, increasing the amount or rate of the FM increases the second term in the integral. Finally, increasing the length of the impulse response of the filter increases the error. Of these three sources of error, the one that can be optimized in our AM-FM estimation algorithms is the length of the filter impulse response, which we desire to be as short in duration as possible. Since the presence of phase in the frequency response of a filter can increase the length of the impulse response, we consider only zero-phase filters throughout this thesis.

Note that *both* AM and FM contribute to error in the transduction approximation. Although the AM is not being "transduced", it does cause error in the approximation.

Therefore, when we refer to "transduction error", we are referring to error in the transduction approximation which is caused by *both* AM and FM.

3.4 Summary

FM to AM transduction, which is the fundamental idea behind the approach of this thesis, was introduced with some examples. Next, we gave an approximation, called the "transduction approximation", that provides a simple expression to approximate the output of an LTI filter when the input is a non-stationary sinusoid. We then bounded the error of this approximation using results obtained by Bovik et al [3]. From this error bound, we argued that filters to be used in our algorithms should have an impulse response that is as short in duration as possible.

Chapter 4

Single-Sinusoid AM-FM Estimation

Some previous work has applied FM to AM transduction to the problem of AM-FM estimation when the input is assumed to consist of a single AM-FM sinusoid. M^{c}Eachern [13, 14] has proposed that the auditory system uses FM to AM transduction for tracking the frequencies of sounds and qualitatively described a method similar to the approach we will take. Quatieri et al. [16] have proposed and implemented algorithms similar to the first algorithm we will describe.

In this chapter, we first describe the implementation of the single-sinusoid AM-FM estimation algorithm which is an integral part of the two-sinusoid AM-FM estimation algorithm of Chapter 7. The second section covers design choices and implementation. We conclude with some examples of algorithm performance.

4.1 Approach

Figure 4-1 shows the structure of the estimation algorithm when the input is assumed to be a single AM-FM sinusoid, i.e.

$$x[n] = a[n]\cos(\theta[n]). \tag{4.1}$$

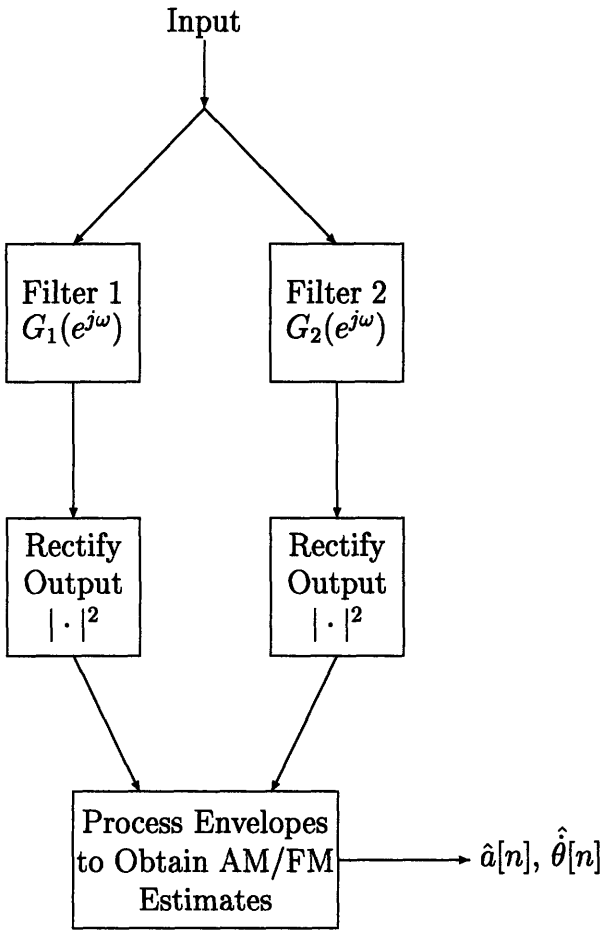

Figure 4-1: Block diagram of the basic single-sinusoid AM-FM estimation algorithm.

As mentioned in the first chapter, this process is modeled after the early stages of the auditory system:

1. The input is processed with a bank of broad, overlapping filters. These filters must have a non-flat pass band so that the FM is transduced to AM.

2. The filter outputs are rectified. The envelopes have the AM and the FM combined in some nonlinear fashion.

3. The envelopes are processed to extract the AM and FM. The method by which the AM and FM is extracted is not based on the auditory system.

4.2 Algorithm

The filtering serves two purposes: to transduce the FM to AM and to make the signal analytic. The signal is made analytic so that the amplitude envelopes can be determined easily and so that the phase derivative and amplitude are unambiguously specified[1]. The FM to AM transduction causes the amplitude envelopes to be functions of $a[n]$ and $\dot{\theta}[n]$, the parameters to be estimated.

In Section 3.1, we described FM to AM transduction and showed that the output of filters $G_1(e^{j\omega})$, and $G_2(e^{j\omega})$ can be approximated as

$$y_i[n] \approx a[n]e^{j\theta[n]}G_i(e^{j\dot{\theta}[n]}) \tag{4.2}$$

where the input is of the form given in Eq. (4.1) and $G_i(e^{j\omega}) = 0$ for $-\pi < \omega < 0$. Thus, the output of the rectification stage is given by

$$|y_i[n]|^2 \approx a^2[n]G_i^2(e^{j\dot{\theta}[n]}). \tag{4.3}$$

Using these filter output envelopes, we can solve for $\dot{\theta}[n]$. By taking the quotient of the amplitude envelopes of the filter outputs, we eliminate the amplitude function, $a[n]$, from the equations, i.e.

$$\frac{|y_2[n]|^2}{|y_1[n]|^2} = \frac{G_2(e^{j\dot{\theta}[n]})}{G_1(e^{j\dot{\theta}[n]})}. \tag{4.4}$$

The filters must be chosen in such a way that the solution to this equation is unique. Therefore, it must be true that

$$\frac{G_2(e^{j\dot{\theta}[n]})}{G_1(e^{j\dot{\theta}[n]})} \neq \frac{G_2(e^{j\dot{\phi}[n]})}{G_1(e^{j\dot{\phi}[n]})} \quad \text{for all } \dot{\theta}[n] \neq \dot{\phi}[n] \text{ on the interval } [0, \pi]. \tag{4.5}$$

In other words, the only constraint for a unique solution is that the quotient, $\frac{G_2(e^{j\omega})}{G_1(e^{j\omega})}$, must be either monotonically increasing or monotonically decreasing on the interval

[1] See Section 2.3

$\omega \in [0, \pi]$. This allows a great deal of freedom in choosing filters that give a unique solution.

We choose, for the sake of analytic simplicity, to constrain the filters to satisfy

$$G_2(e^{j\omega}) = \omega G_1(e^{j\omega}), \tag{4.6}$$

which means that the envelopes of the filter outputs can be approximated as

$$|y_1[n]|^2 \approx a^2[n] G_1^2(e^{j\dot{\theta}[n]}) \tag{4.7}$$

$$|y_2[n]|^2 \approx a^2[n] \dot{\theta}^2[n] G_1^2(e^{j\dot{\theta}[n]}). \tag{4.8}$$

This allows us to estimate the parameters by

$$\hat{\dot{\theta}}[n] = \sqrt{\frac{|y_2[n]|^2}{|y_1[n]|^2}} \tag{4.9}$$

$$\hat{a}[n] = \frac{\sqrt{|y_1[n]|^2}}{G_1(e^{j\hat{\dot{\theta}}[n]})} \tag{4.10}$$

The only remaining design choice is the filter $G_1(e^{j\omega})$. The design must take into account the following:

1. The impulse response of $G_1(e^{j\omega})$ (and $G_2(e^{j\omega})$) must be short in duration so that the transduction approximation, Eq. (3.6), is valid.

2. The filter output must be analytic so that the envelope can be determined. Therefore, we must constrain $G_1(e^{j\omega})$ to be zero for $-\pi < \omega < 0$.

3. $G_1(e^{j\omega})$ must be in a form such that Eq. (4.10) can be evaluated and the analysis is tractable.

The first two requirements are somewhat related. The standard approach used to make a signal analytic is by way of the Hilbert transform. The impulse response of

an ideal Hilbert transformer is

$$h[n] = \begin{cases} \frac{2}{n\pi} & n \text{ odd} \\ 0 & \text{otherwise} \end{cases} \tag{4.11}$$

As shown in Eq. (3.11), however, the transduction error increases as the length of the impulse response of a filter increases. Although the impulse response of the filter described in Eq. (4.11) does decay rapidly, we can choose a filter that has a much shorter impulse response and that also has an analytic output. This is possible because no where in our analysis thus far have we restricted the shape of $G_1(e^{j\omega})$ over the range $0 \leq \omega \leq \pi$. This means that we can choose $G_1(e^{j\omega})$ to be any function on $[0, \pi]$ and zero on $(-\pi, 0)$. The other constraint is that the filter must have a frequency response that we can evaluate to calculate the amplitude function as shown in Eq. (4.10). Taking all of these constraints into consideration, we choose the filters to be

$$G_1(e^{j\omega}) = \begin{cases} \frac{1}{2}(1 - \cos(2\omega)) & 0 \leq \omega \leq \pi, \\ 0 & -\pi < \omega < 0 \end{cases} \tag{4.12}$$

and

$$G_2(e^{j\omega}) = \begin{cases} \omega\frac{1}{2}(1 - \cos(2\omega)) & 0 \leq \omega \leq \pi, \\ 0 & -\pi < \omega < 0. \end{cases} \tag{4.13}$$

Plots of the frequency response and the magnitude of the impulse response of these filters are shown in Figure 4-2 and Figure 4-3.

4.3 Implementation

$G_1[k]$ and $G_2[k]$ are the sampled frequency responses corresponding to $G_1(e^{j\omega})$ and $G_2(e^{j\omega})$. They were obtained by first sampling $G_1(e^{j\omega})$ and $G_2(e^{j\omega})$ with a sample

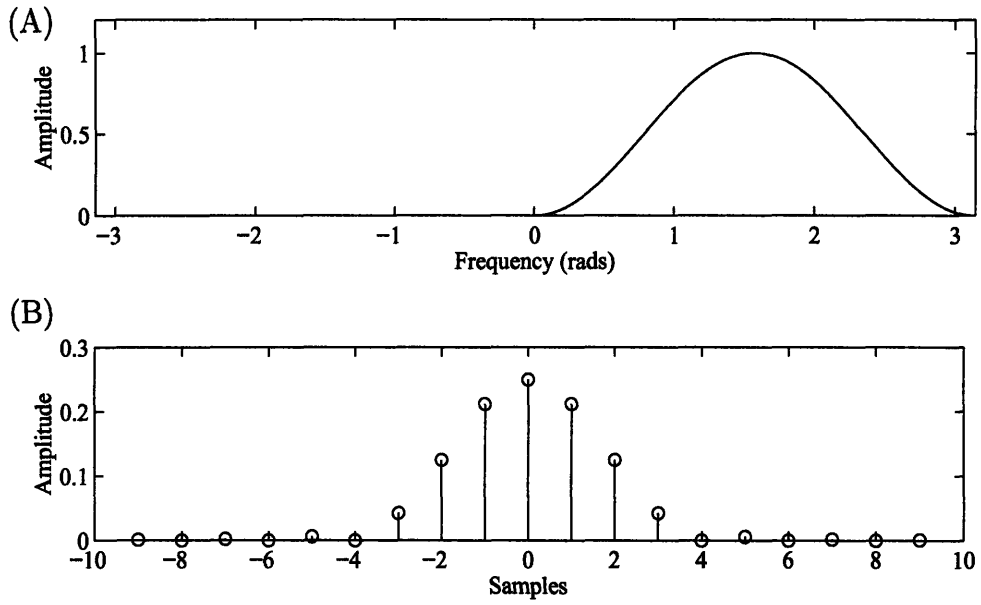

Figure 4-2: Frequency and impulse response of $G_1(e^{j\omega})$, (A) frequency response, (B) impulse response.

interval of $\frac{2\pi}{8192}$.

$$G_i'[k] = G_i(e^{j\frac{2\pi k}{8192}}) \qquad \text{for } k = 0, \ldots, 8191,\ i = 1, 2. \tag{4.14}$$

This interval size was chosen to minimize the amount of aliasing in the impulse response. Experimentation indicated that there was negligible gain in decreasing the interval size any further for these particular filters. The impulse responses corresponding to $G_1'[k]$ and $G_2'[k]$ were then truncated using a 129 point rectangular window,

$$g_i[n] = w[n]g_i'[n] \qquad \text{for } n = 0, \ldots, 8191,\ i = 1, 2. \tag{4.15}$$

where

$$w[n] = \begin{cases} 1 & \text{for } n = -64, \ldots, 64 \\ 0 & \text{otherwise} \end{cases} \tag{4.16}$$

$G_1[k]$ and $G_2[k]$ are then obtained from the impulse responses, $g_1[n]$ and $g_2[n]$.

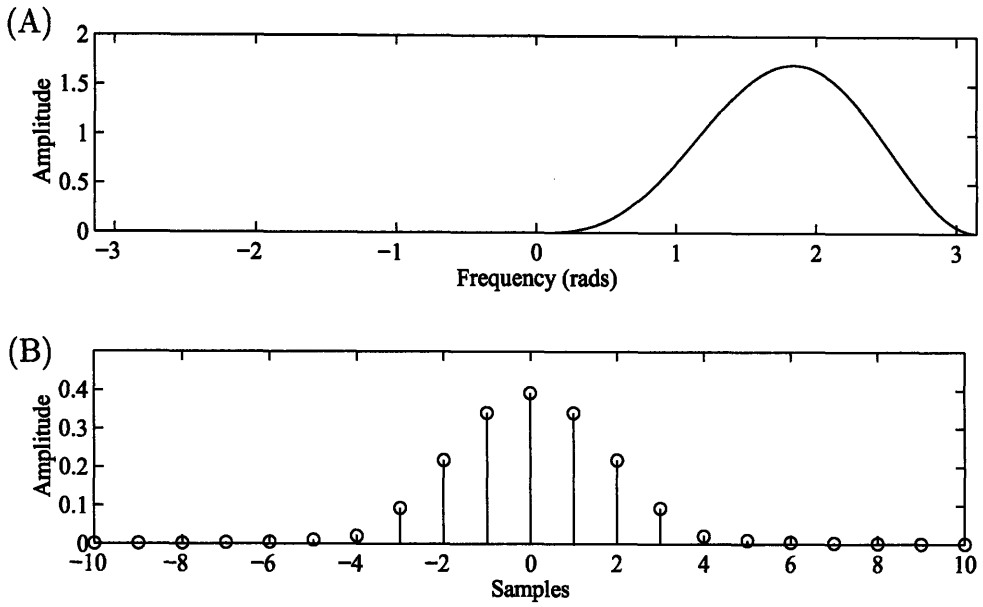

Figure 4-3: Frequency and impulse response of $G_2(e^{j\omega})$, (A) frequency response, (B) impulse response.

The input is processed in blocks of 1,920 samples and the input is filtered by circular convolution using a 2,048 point DFT and the overlap-save method [15]. The amplitude envelopes are obtained by taking the absolute value of the output of the filters at each sample point. The frequency and amplitude estimates are evaluated at each sample point according to Eq. (4.9) and Eq. (4.10).

4.4 Results

In this section, we show examples of the algorithm performance for a variety of signals. Figures showing the estimate of the AM and FM functions have two sets of axis. One set is in terms of samples and radians, the other in terms of time and frequency. Using samples and radians is more general for discrete-time signals because it is independent of an arbitrarily chosen sample frequency. Time and frequency, however, are more common parameters for describing signals. For the axes corresponding to time and frequency, we have chosen 10,000Hz as the sampling frequency.

We give two error criteria, the first one being the mean square error of the estimate

$$e = \frac{1}{N}\sum_{n=1}^{n=N}(f_a[n] - f_e[n])^2. \tag{4.17}$$

where $f_a[n]$ is the actual function, $f_e[n]$ is the estimated function, and N is the length of the signal in samples. The other error criterion is the maximum deviation of the estimate from the true function

$$d = \max_n(|f_a[n] - f_e[n]|). \tag{4.18}$$

Also, there is *no* post-processing on these estimates, which is performed in many AM-FM estimation algorithms.

Another important point is that edge effects have been ignored and are not shown in the figures. As mentioned in Chapter 1, we assume that the signal is always present. Therefore, we truncate the output of the algorithm so that the transient response corresponding to the beginning and ending of the signal are not shown. Since the filters $G_1(e^{j\omega})$ and $G_2(e^{j\omega})$ have impulse responses with energy concentrated in seven adjacent samples, this transient response is very short. Nonetheless, we do not address the issue of transient response and therefore exclude this from the plots.

For the first example, we analyze a signal with constant AM and constant FM.

EXAMPLE 4.1

Figure 4-4 shows the AM and FM estimates for the signal

$$x[n] = \cos\left(\frac{\pi}{2}n\right). \tag{4.19}$$

The error is negligible for this case, illustrating that when our assumptions have not been violated and the transduction equation is exact, there is practically no error.

The next example is a signal with sinusoidal AM and constant FM.

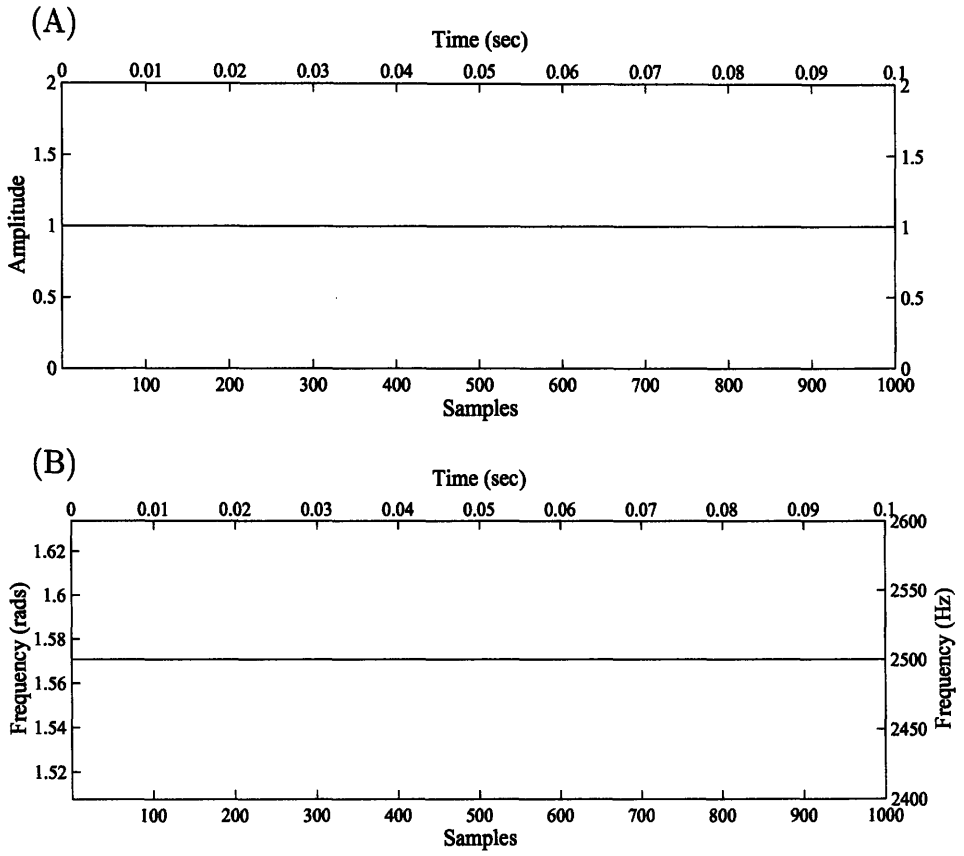

Figure 4-4: Single-sinusoid AM-FM estimates for a signal with constant AM and FM, (A) amplitude estimate, mean square error: 1.078×10^{-16}, max deviation: 1.468×10^{-8}, (B) frequency estimate, mean square error: 4.552×10^{-28} (rad^2/sec), max deviation: 6.994×10^{-14} (rad).

EXAMPLE 4.2

The input is

$$x[n] = \left[1 + .7\cos\left(\frac{\pi n}{20}\right)\right]\cos\left(\frac{\pi n}{2}\right) \tag{4.20}$$

The results are shown in Figure 4-5 where the original (dashed) and estimated (solid) modulation is superimposed. Here we are seeing the effects of the transduction error due to AM.

In the next example, we see the effects of frequency modulation.

EXAMPLE 4.3

The input signal is now

$$x[n] = \cos\left(\frac{\pi n}{2} + 2\sin\left(\frac{\pi n}{10}\right)\right). \tag{4.21}$$

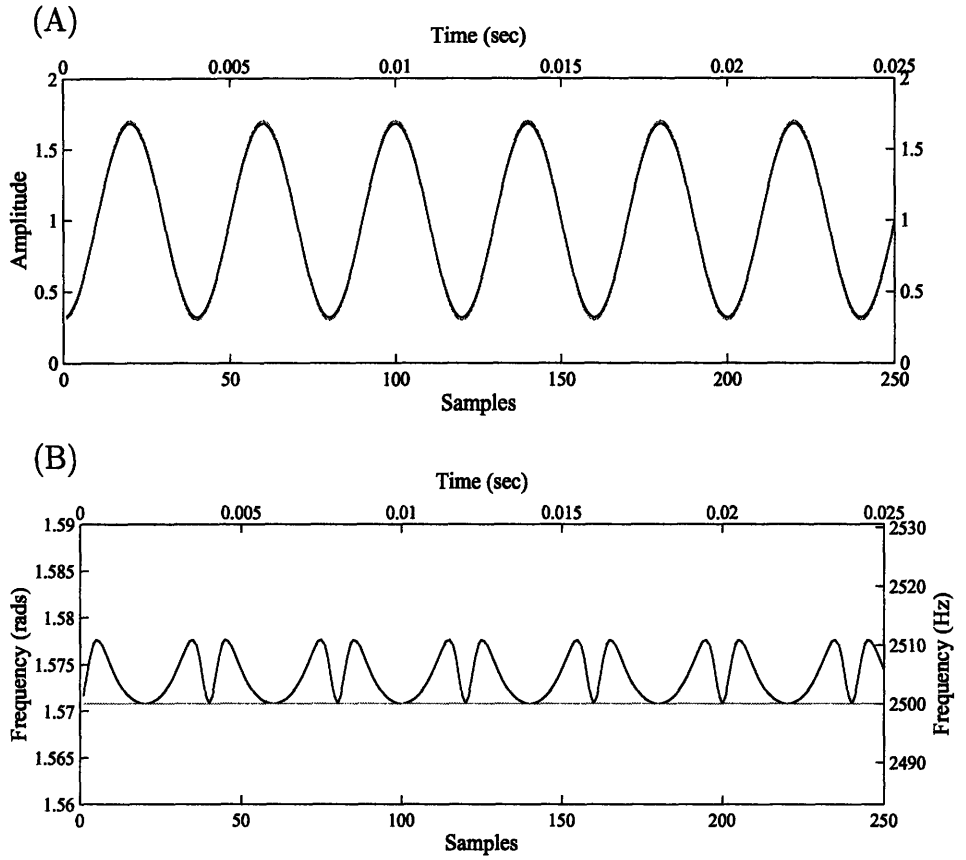

Figure 4-5: Single-sinusoid AM-FM estimates (solid lines) for a signal with sinusoidal AM and constant FM. (A) amplitude estimate, mean square error: 1.468×10^{-4}, max deviation: 1.713×10^{-2}, (B) frequency estimate, mean square error: 1.409×10^{-5} (rad^2/sec), max deviation: 6.832×10^{-3} (rad).

The results are shown in Figure 4-6. Again, the error has increased from that of the first example due to the transduction error caused by the FM.

We now impose the AM and FM of the two previous signals together in one signal.

EXAMPLE 4.4

The input is

$$x[n] = \left[1 + .7\cos\left(\frac{\pi n}{20}\right)\right]\cos\left(\frac{\pi n}{2} + 2\sin\left(\frac{\pi n}{10}\right)\right). \tag{4.22}$$

The results are shown in Figure 4-7. The error in this example might be too large for some applications. At a sampling frequency of 10,000 Hz, the maximum frequency deviation is approximately 160Hz. The modulations we have chosen, however, are somewhat severe in both the rate and extent of modulation. In fact, if we listen to the signal, we do not perceive AM or FM. Instead,

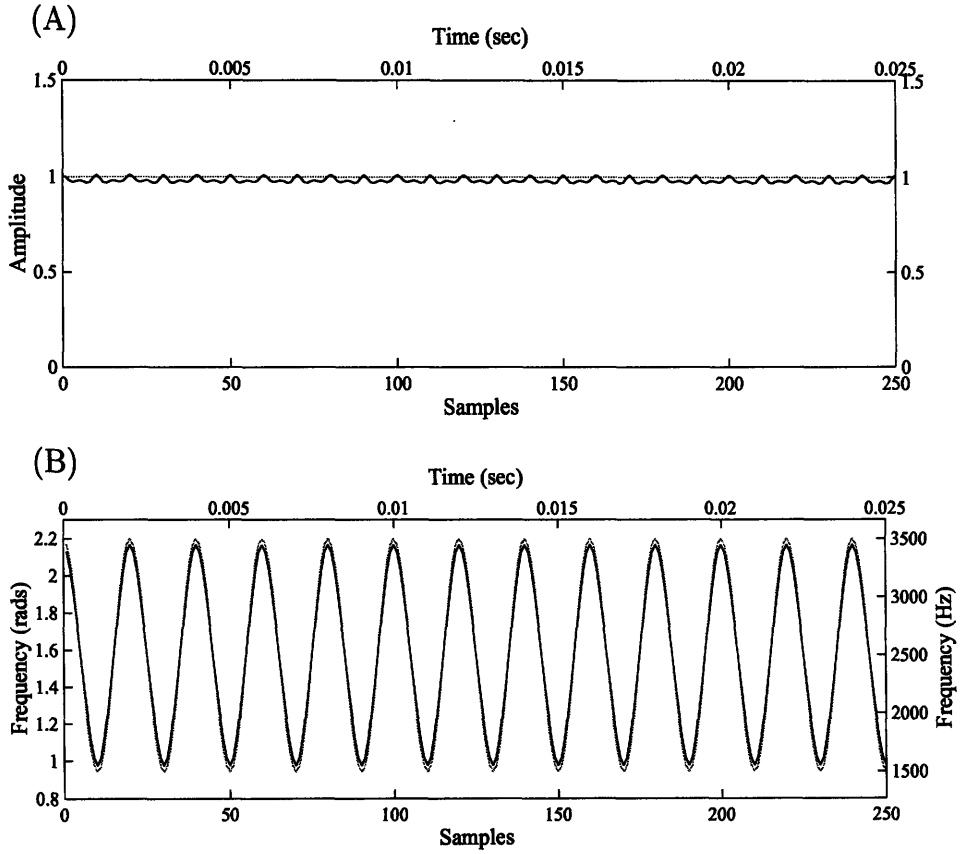

Figure 4-6: Single-sinusoid AM-FM estimates (solid lines) for a signal with constant AM and sinusoidal FM, (A) amplitude estimate, mean square error: 4.522×10^{-4}, max deviation: 3.177×10^{-2}, (B) frequency estimate, mean square error: 1.696×10^{-3} (rad^2/sec), max deviation: 5.602×10^{-2} (rad).

the modulations cause the signal to take on a "buzz" quality. Apparently, the AM and FM modulations are too severe for the human auditory system to track.

As a final example, we add noise to the input signal of the previous example.

EXAMPLE 4.5

The input is now

$$x[n] = \left[1 + .7\cos\left(\frac{\pi n}{20}\right)\right]\cos\left(\frac{\pi n}{2} + 2\sin\left(\frac{\pi n}{10}\right)\right) + w[n]. \tag{4.23}$$

where $w[n]$ is white Gaussian noise and the signal-to-noise ratio is

$$\text{SNR} = 10\log_{10}\left(\frac{x^2[n]}{w[n]}\right) \approx 22\text{dB}. \tag{4.24}$$

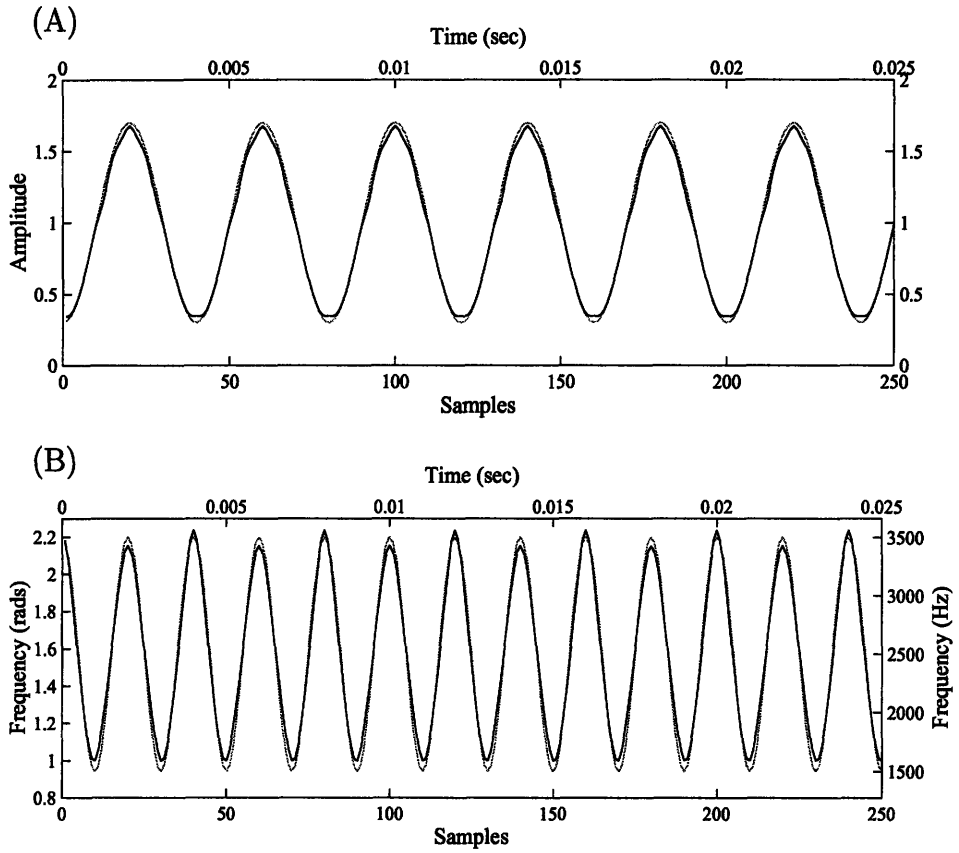

Figure 4-7: Single-sinusoid AM-FM estimates (solid lines) for a signal with sinusoidal AM and sinusoidal FM, (A) amplitude estimate, mean square error: 1.421×10^{-3}, max deviation: 6.694×10^{-2}, (B) frequency estimate, mean square error: 2.835×10^{-3} (rad^2/sec), max deviation: 1.001×10^{-1} (rad).

The results are shown in Figure 4-8, illustrating that the estimates suffer from both transduction error and external noise.

4.5 Summary

We have described and implemented a method of estimating the amplitude and frequency modulation of a signal that is assumed to consist of only one AM-FM sinusoid. The fundamental idea behind our approach is FM to AM transduction, which was motivated by the fact that there is evidence of this phenonemon in early stages of the human auditory system. We concluded with a few examples of how the algorithm

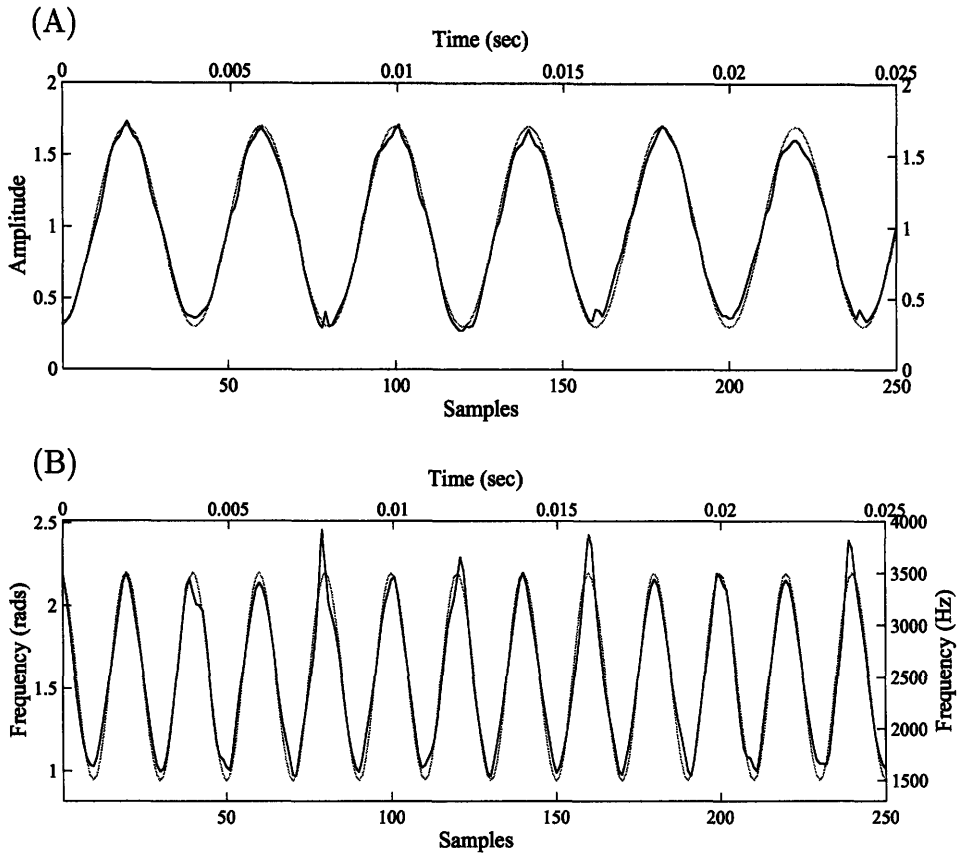

Figure 4-8: Single-sinusoid AM-FM estimates (solid lines) for a signal with sinusoidal AM and sinusoidal FM with additive white Gaussian noise, (A) amplitude estimate, mean square error: 3.009×10^{-3}, max deviation: 1.731×10^{-1}, (B) frequency estimate, mean square error: 5.439×10^{-3} (rad^2/sec), max deviation: 3.313×10^{-1} (rad).

performs with various types of signals and external noise. In the next two chapters, we will discuss methods of reducing the error in the transduction approximation and methods that make the algorithm more robust with respect to external noise.

Chapter 5

Inverse Modulation

The performance of the algorithm presented in the previous chapter degrades as the rate and extent of AM and FM increase due to the fact that as the modulation is increased, the transduction approximation becomes less accurate. This can be seen in Eq. (3.11), where the error bounds on the transduction approximation increase as $\dot{a}[n]$ and $\ddot{\theta}[n]$ increase. In this chapter, we propose a method that reduces $\dot{a}[n]$ and $\ddot{\theta}[n]$ by iteratively inverting the modulation with the AM and FM estimates.

We treat separately the cases in which the input is analytic and the case in which the signal is real. We do this because when the input is analytic, the approach is relatively straightforward. When the signal is real, however, complications arise due to the fact that a real signal has negative frequencies; care must be taken in inverting the FM so that negative frequencies are not modulated into the positive frequency region.

In the first section of this chapter, we introduce our approach for the analytic signal and the following section has examples showing the improved performance. The third section discusses the issues that arise when the signal is real and shows how to modify the approach used for the analytic signal. The last section gives examples showing the improved performance with real signals.

5.1 AM and FM Inversion when x[n] is Analytic

To reduce the extent of the AM and FM, we use the estimates obtained from the AM-FM estimation algorithm of the previous chapter to invert the modulation and then re-apply the algorithm to the new demodulated signal. Since the initial estimates are not exact, the demodulated signal still has some modulation. However, we can iterate this procedure to further reduce the modulation that remains in the demodulated signal. The block diagram of this system is shown in Figure 5-1. We denote $x_k[n]$, $k = 0, 1, 2, ...$ as the input on the kth iteration and $\hat{a}_k[n]$ and $\hat{\dot{\theta}}_k[n]$ as the amplitude and frequency estimates corresponding to $x_k[n]$. On the initial iteration, $x_0[n] = x[n]$, $\hat{a}_0[n] = 1$, and $\hat{\dot{\theta}}_0[n] = 0$. The inverse modulation procedure is described by the following equation:

$$\begin{aligned} x_{k+1}[n] &= \frac{1}{\hat{a}_k[n]} x_k[n] e^{j(\omega_c n - \int_0^n \hat{\dot{\theta}}_k[p]dp)} \\ &= \left(\prod_{i=1}^{k} \frac{a[n]}{\hat{a}_i[n]} \right) e^{j(k\omega_c n + \theta[n] - \sum_{m=1}^{k} \int_0^n \hat{\dot{\theta}}_m[p]dp)} \end{aligned} \tag{5.1}$$

The overall estimates after k iterations are given by

$$\hat{\dot{\theta}}[n] = \sum_{i=1}^{k} \hat{\dot{\theta}}_i[n] - k\omega_c \tag{5.2}$$

and

$$\hat{a}[n] = \prod_{i=1}^{k} \hat{a}_i[n]. \tag{5.3}$$

We have modulated by $e^{j\omega_c n}$ to keep the signal in the passband of the filters $G_1(e^{j\omega})$ and $G_2(e^{j\omega})$. In the next chapter we show that the "optimal" modulation frequency is $\omega_c = \frac{\pi}{2}$. The procedure can be summarized as follows:

1. Estimate the modulation of $x_k[n]$.

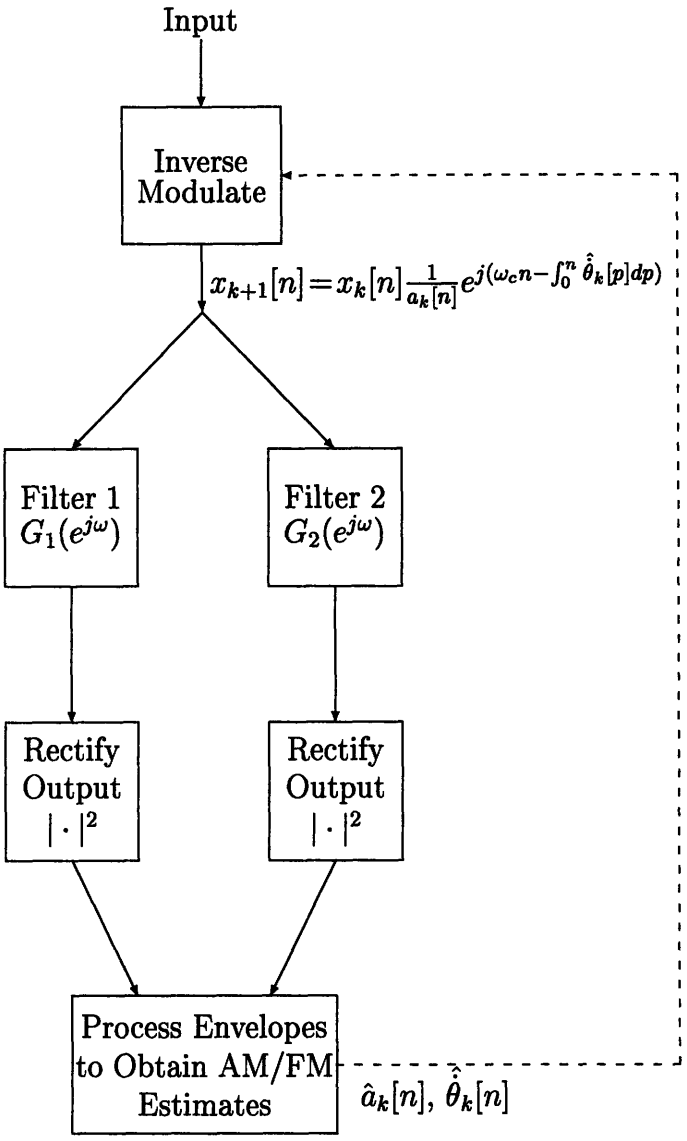

Figure 5-1: Single-sinusoid AM-FM estimation algorithm with inverse modulation. $\hat{\theta}_0[n] = 0$ and $\hat{a}_0[n] = 1$.

2. Divide $x_k[n]$ by the amplitude estimate, $a_k[n]$. If $a_k[n]$ is close to the actual modulation, then dividing by $a_k[n]$ produces a new signal that has almost no amplitude modulation.

3. Estimate the phase, $\theta_k[n]$, by numerically integrating $\hat{\dot{\theta}}_k[n]$.

4. Modulate $x_k[n]$ by $e^{j\hat{\theta}_k[n]}$. If $\hat{\theta}_k[n]$ is close to the actual phase, the resulting signal has a frequency of approximately 0 radians/sec with almost no frequency modulation.

5. Modulate $x_k[n]$ back up to the passband of the filters $G_1(e^{j\omega})$ and $G_1(e^{j\omega})$.

6. Repeat the procedure with the new "inverse modulated" signal.

The first step is performed as described in the previous chapter. In the second step, we assumed that $\hat{a}_k[n] \neq 0$ for all n. As mentioned in Chapter 2, we assume that the signal is always present, and, therefore, $a[n] \neq 0$ for all n. However, it may be the case, due to noise, that the estimate is equal to 0 or perhaps negative. If this occurs, we do not divide by $a_k[n]$ at the point where it is not positive. Instead, we linearly extrapolate between the two nearest values of $a_k[n]$ that are positive.

The third step requires numerical integration. For this step, we use the trapezoidal rule for integration [20]. Since we use only amplitude envelopes, the phase offset is not important and need not be estimated. After inverting the frequency modulation, we are left with a signal that is at 0 radians/sec which must be modulated to the passband of $G_1(e^{j\omega})$ and $G_2(e^{j\omega})$. We will show in the next chapter that the "optimal" modulation frequency is $\frac{\pi}{2}$ rad/sec. In the Section 5.3, we show that, in general, we cannot use this modulation frequency if $x[n]$ is real and discuss a suboptimal alternate procedure.

5.2 Results of the Modified Algorithm for an Analytic Signal

Rather than show error reduction for a few specific examples, we show error reduction after each iteration for a group of signals. The group consists of 625 AM-FM signals that are described as follows:

$$x_{k,l}[n] = \left[1 + .5\sin\left(\frac{2\pi kn}{500}\right)\right] e^{j\left(\frac{\pi n}{2} + \frac{50}{l}\cos\left(\frac{2\pi ln}{500}\right)\right)} \tag{5.4}$$

where $k = 2, 4, \ldots, 50$ and $l = 2, 4, \ldots, 50$. If the sampling frequency is chosen to be 10,000 samples/sec, the above set of signals has sinusoidal amplitude modulation varying from 0.5 to 1.5 over a range of frequencies from 20 Hz to 500 Hz. The frequency modulation varies from 2,000 Hz to 3,000 Hz and the rate of the frequency modulation ranges from 20 Hz to 500 Hz. The average mean square error after one, three, and five iterations is shown in figures 5-2, 5-3, and 5-4 respectively. The average of the mean square error, i.e. the average value of the surface shown in Figure 5-2, Figure 5-3, and Figure 5-4, is shown after each iteration in Table 5.1. There is a large reduction in error after the first iteration and a less significant decrease

Iteration:	1	2	3	4	5
Average AM Estimate Error	3.57×10^{-4}	3.44×10^{-6}	3.67×10^{-7}	1.39×10^{-7}	8.08×10^{-8}
Average FM Estimate Error	2.02×10^{-4}	7.62×10^{-6}	2.16×10^{-6}	1.32×10^{-6}	1.06×10^{-6}

Table 5.1: The average of the mean square error over the signal set in Eq. 5.4 (Frequency error in rad^2/sample)

on subsequent iterations. There is such a significant reduction in error after the first iteration because the estimates obtained on the first iteration are very close to the actual AM and FM functions and therefore the majority of the modulation is eliminated on the first iteration.

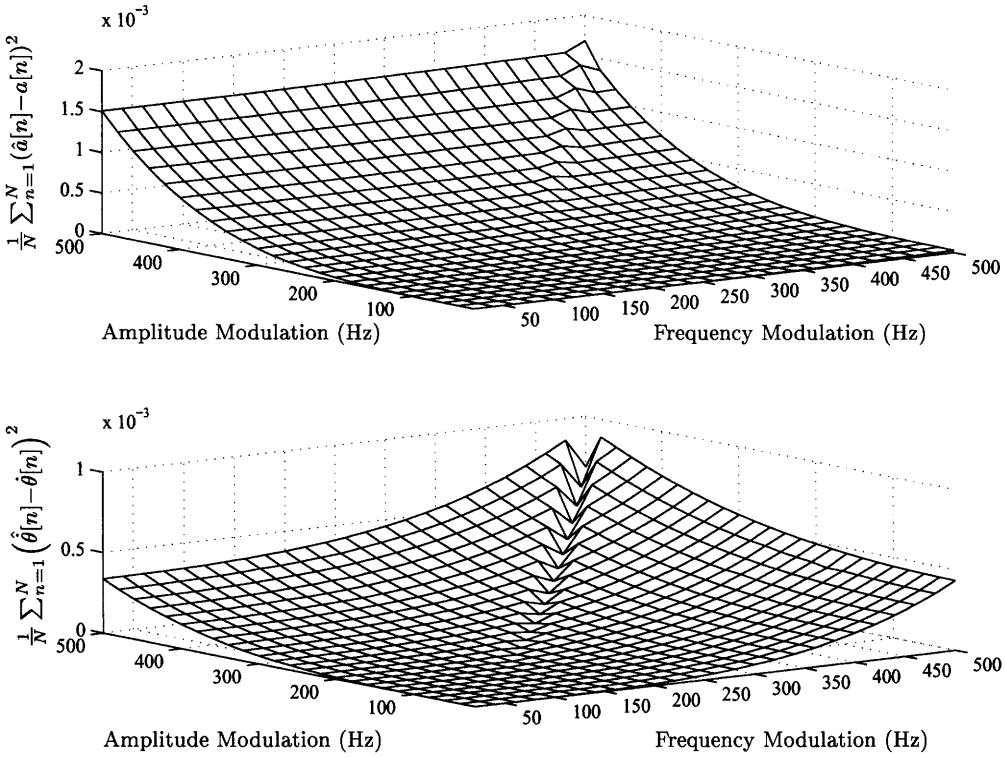

Figure 5-2: Error in the initial amplitude and frequency estimates. Frequency estimate error in rad^2/sample.

5.3 Inverting the AM and FM when x[n] is real

A real signal has negative frequencies and the inverse modulation technique described in Section 5.1 may modulate the negative frequencies to the positive frequency range. This is illustrated in the following example.

EXAMPLE 5.1

Suppose that we have the following signal,

$$x_0[n] = \left[1 + .7\cos\left(\frac{\pi n}{50}\right)\right]\cos\left(\frac{\pi n}{5} + 2\sin\left(\frac{\pi n}{20}\right)\right), \tag{5.5}$$

and we use the same demodulation algorithm as for the analytic input. After the first iteration,

$$x_1[n] = \frac{1}{a[n]}e^{j\left(\frac{\pi n}{2} - \frac{\pi n}{5} - 2\sin\left(\frac{\pi n}{20}\right)\right)}x_0[n], \tag{5.6}$$

and, as shown in Figure 5-5, the negative frequencies are modulated into the positive frequency range.

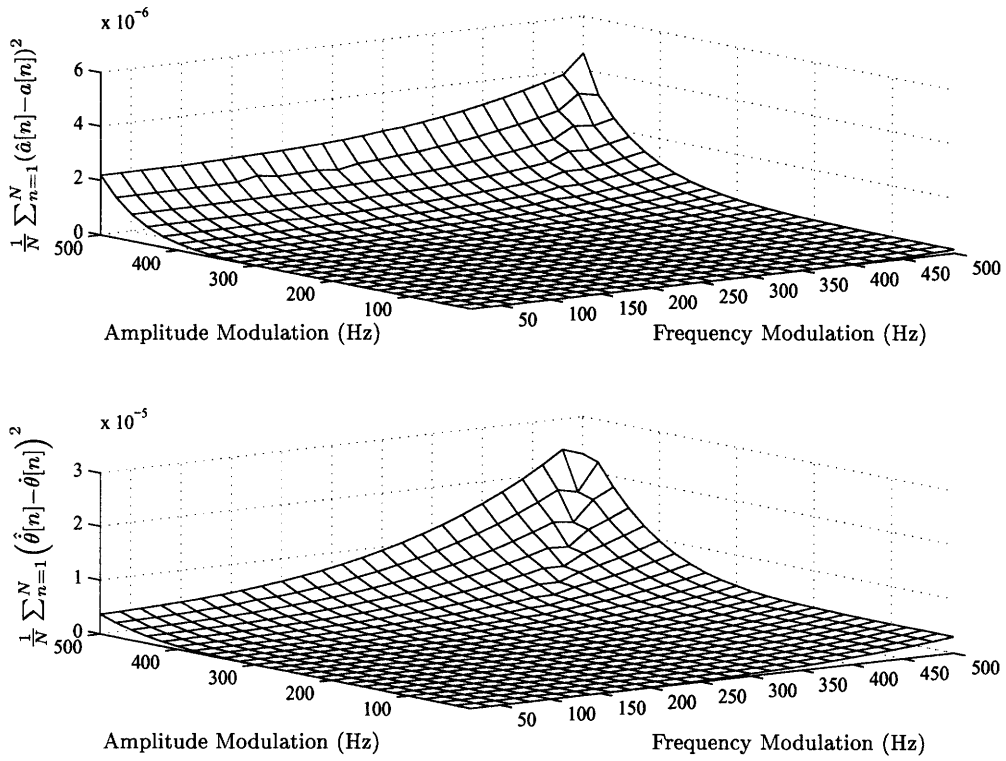

Figure 5-3: Error in amplitude and frequency estimates after the third iteration. Frequency estimate error in rad^2/sample.

If the negative frequencies are modulated to the positive frequency range, then when $x[n]$ is made analytic, it is no longer true that $x_a[n] = x_q[n]$, resulting in incorrect AM and FM estimates[1]. Therefore, we need to restrict the function used to invert the FM so that negative frequencies are not modulated to positive frequencies.

We denote $\dot{\theta}_+[n]$ as the positive FM function of $x[n]$ and $\dot{\theta}_-[n]$ as the negative FM function. If $x[n]$ is real, then

$$x[n] = \frac{1}{2}a[n]\left(e^{j\int_{-\infty}^{n}\dot{\theta}_+[p]dp} + e^{j\int_{-\infty}^{n}\dot{\theta}_-[p]dp}\right) \tag{5.7}$$

and

$$\dot{\theta}_+[n] = -\dot{\theta}_-[n]. \tag{5.8}$$

[1]See Section 2.1 for a description of the quadrature signal, $x_q[n]$.

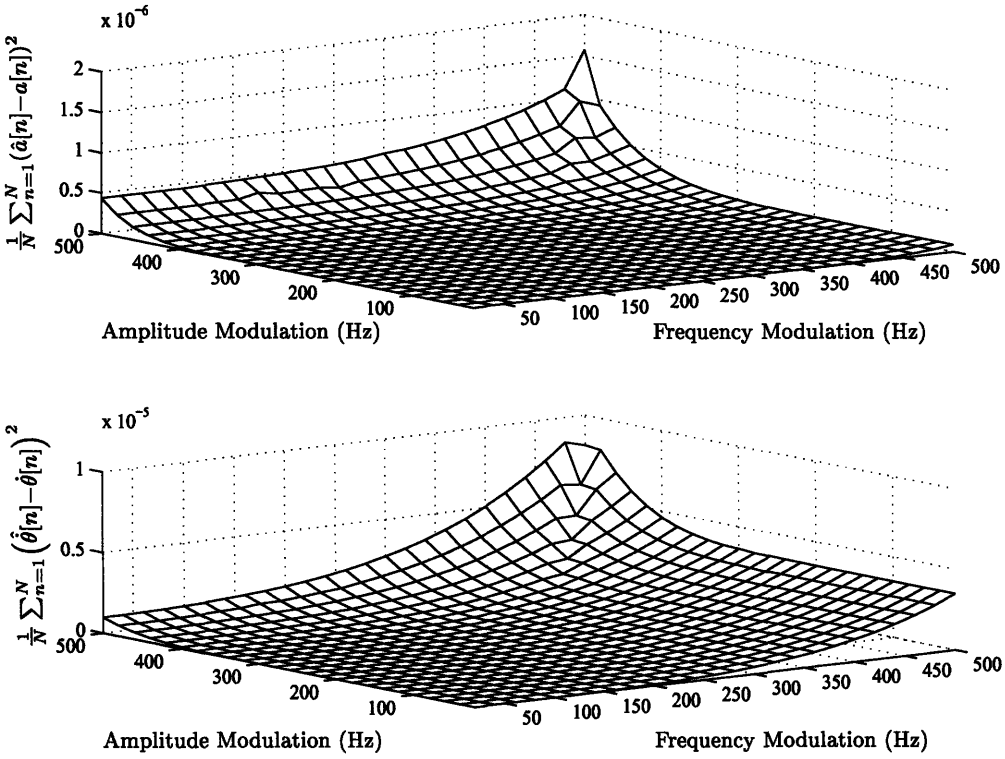

Figure 5-4: Error in amplitude and frequency estimates after the fifth iteration. Frequency estimate error in rad^2/sample.

Demodulating with $\omega_c n - \hat{\dot{\theta}}_+[n]$ results in

$$x[n] = \frac{1}{2}a[n]\left(e^{j\int_{-\infty}^{n}\dot{\theta}_+[p]dp} + e^{j\int_{-\infty}^{n}\dot{\theta}_-[p]dp}\right)e^{j(\omega_c n - \int_{-\infty}^{n}\hat{\dot{\theta}}_+[p]dp)} \tag{5.9}$$

$$\approx \frac{1}{2}a[n]\left(e^{j\omega_c n} + e^{j(\int_{-\infty}^{n}\dot{\theta}_-[p] - \hat{\dot{\theta}}_+[p]dp)}\right) \tag{5.10}$$

To prevent the negative frequencies from being modulated into the positive frequency range, we must force

$$-\pi \leq \dot{\theta}_-[n] - \hat{\dot{\theta}}_+[n] + \omega_c \leq 0 \qquad \text{for all } n. \tag{5.11}$$

This inequality can only be satisfied if

$$|\dot{\theta}_-[n] - \hat{\dot{\theta}}_+[n]| < \pi \qquad \text{for all } n. \tag{5.12}$$

To satisfy this inequality, there are two options. We can scale $\hat{\dot{\theta}}_+[n]$ by some factor $0 < \alpha < 1$, or we can divide the signal into shorter sections in which the frequency variation of $x[n]$ is confined to a smaller region. With the first option, the frequency modulation would never be completely inverted. The second option assumes that the frequency modulation of $x[n]$ does not vary over a range of $\frac{\pi}{2}$ rad/sec within the duration of the impulse response of the filters $G_1(e^{j\omega})$ and $G_2(e^{j\omega})$. This does not impose a significant constraint. For example, if the sampling frequency is 10,000 Hz, a signal that violated this constraint would have to sweep across 2,500 Hz in approximately 1 millisecond. If a signal does violate this assumption, we can use both options, i.e. use a short block of the signal and scale the FM estimate by $0 < \alpha < 1$ to ensure that Eq. (5.12) is not violated. Therefore, we always use option two and, if necessary, combine it with option one.

Once we have satisfied Eq. (5.12), we can now choose ω_c. For reasons given in the next chapter, we select an ω_c that is as close to $\frac{\pi}{2}$ as possible while still satisfying Eq. (5.11). Assuming that Eq. (5.12) is satisfied, ω_c is determined by

$$\omega_c = \begin{cases} 2\min\limits_n(\hat{\dot{\theta}}_+[n]) & \text{if } \min\limits_n(\hat{\dot{\theta}}_+[n]) < \frac{\pi}{4} \\ \frac{\pi}{2} & \text{if } \min\limits_n(\hat{\dot{\theta}}_+[n]) > \frac{\pi}{4} \text{ and } \max\limits_n(\hat{\dot{\theta}}_+[n]) < \frac{3\pi}{4} \\ \pi - 2\max\limits_n(\hat{\dot{\theta}}_+[n]) & \text{if } \max\limits_n(\hat{\dot{\theta}}_+[n]) \geq \frac{3\pi}{4} \end{cases} \tag{5.13}$$

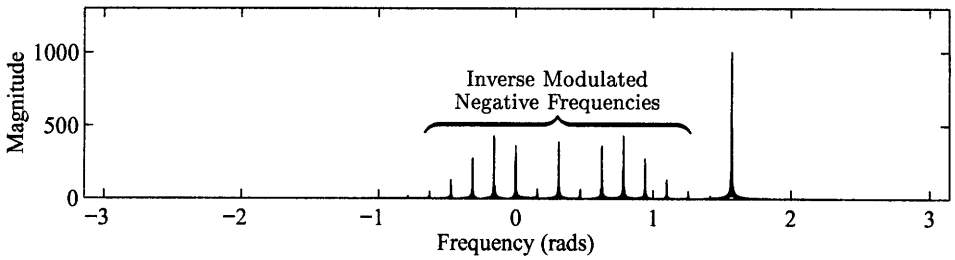

Figure 5-5: An example of the negative frequencies being modulated to the positive frequency range.

5.4 Practical Considerations

In the previous section, we gave constraints that must be satisfied to ensure that the negative frequencies are not modulated to positive frequencies. In deriving that constraint, it was assumed that we knew the actual FM function. Actually, we only have an estimate of the FM function and because this estimate is generally not exact, using it to demodulate the FM might violate the constraint in Eq. (5.12). Also, the spectrum of an FM signal has spectral components outside the range of the instantaneous frequency. This means that although $\dot{\theta}_-[n]$ is confined to $(-\pi, 0)$, $e^{j\dot{\theta}_-[n]}$ might have spectral components in the positive frequency range. Therefore, we must leave some room for error when we demodulate, thus giving the following constraint,

$$-\pi + \varepsilon < \dot{\theta}_-[n] - \hat{\dot{\theta}}_+[n] + \omega_c < 0 - \varepsilon \qquad \text{for all } n. \tag{5.14}$$

where $\varepsilon > 0$. Determining the best ε is a complex issue that involves finding a tight bound for the estimation error and also determining the spectral range of the negative frequencies. Therefore, we choose $\varepsilon = .06$ rad/sec based on experimental results.

It is important to observe that even if a portion of the negative frequency spectrum does get modulated to positive frequencies, the algorithm still produces useful results. This is due the fact that the filters $G_1(e^{j\omega})$ and $G_2(e^{j\omega})$ are close to zero near $-\pi$ and 0. Therefore, any negative frequency spectral components that are modulated to the low or high positive frequency range are approximately filtered out.

5.5 Results of the Modified Algorithm for a Real Signal

The same signal set for the case where $x[n]$ is analytic is used here. The average mean square error after one, three, and five iterations is shown in Figures 5-6, 5-7, and 5-8, respectively. From these plots, it is apparent that this method does result

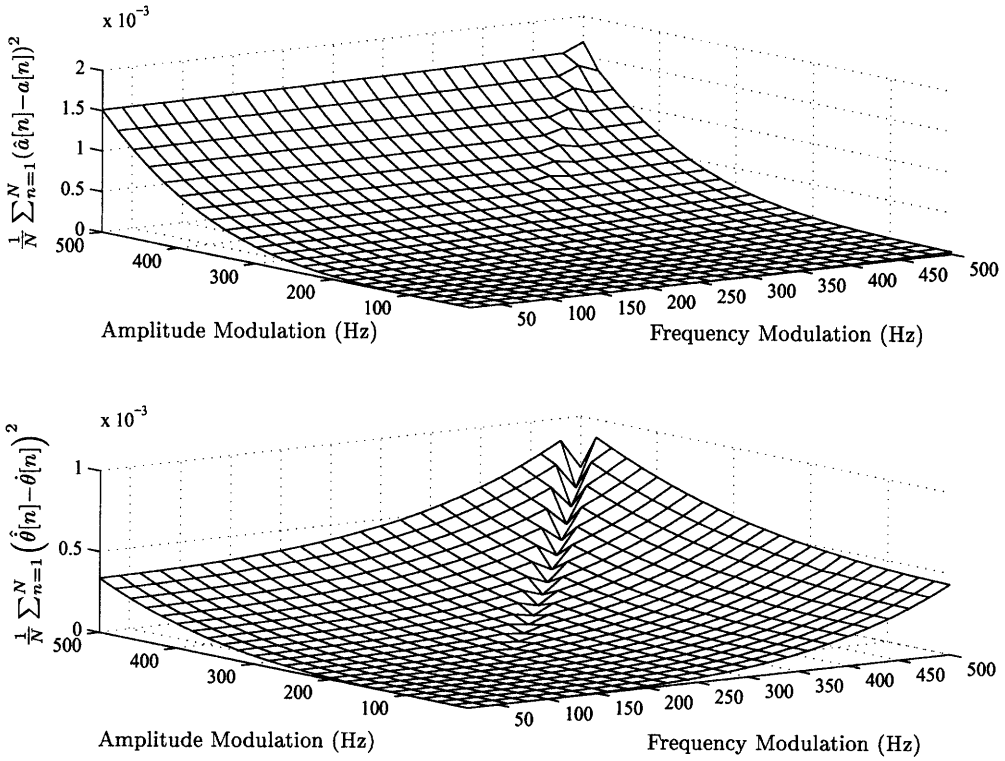

Figure 5-6: Error in amplitude and frequency estimates on the first iteration with $x[n]$ real. Frequency error in rad^2/sample.

in significant error reduction when $x[n]$ is real, although it does not perform quite as well when $x[n]$ is analytic. As a final example, we show how the modifications of this chapter improve upon the results shown in Example 4.4.

EXAMPLE 5.2

The signal in Example 4.4 is

$$x[n] = \left[1 + .7\cos\left(\frac{\pi n}{20}\right)\right]\cos\left(\frac{\pi n}{2} + 2\sin\left(\frac{\pi n}{10}\right)\right). \tag{5.15}$$

The results are shown in Figure 5-9. The mean square error of the amplitude estimate has been reduced by a factor of approximately 40 and the mean square error of the frequency estimate has been reduced by a factor of approximately 20.

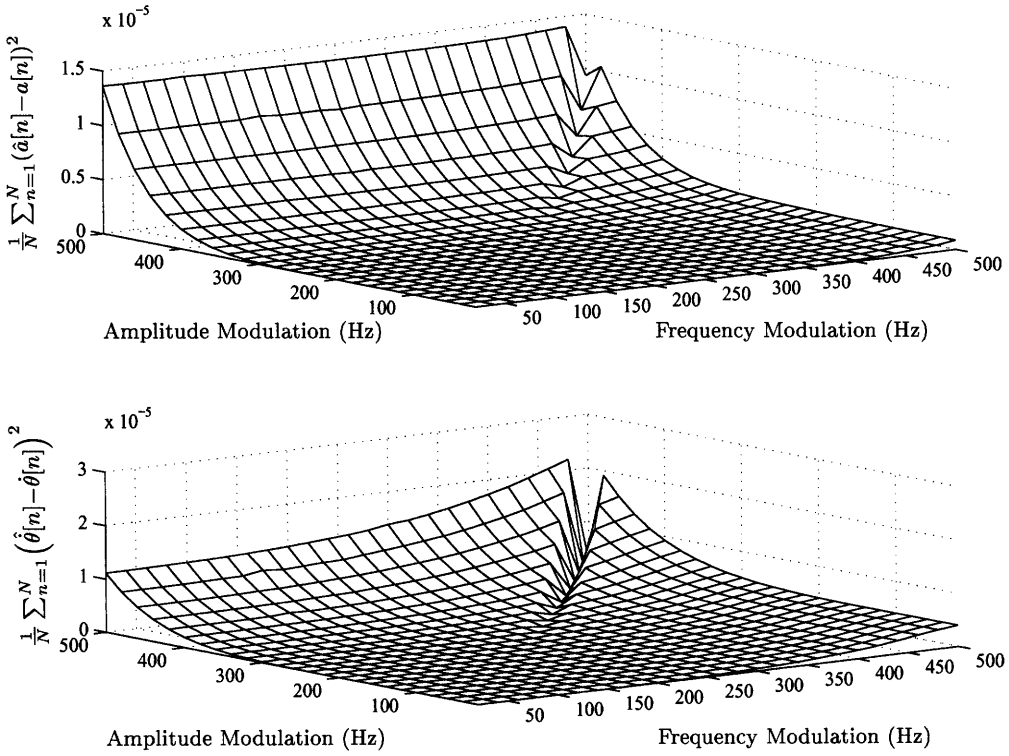

Figure 5-7: Error in amplitude and frequency estimates on the third iteration with $x[n]$ real. Frequency error in rad^2/sample.

5.6 Summary

In this chapter, we proposed a method for reducing the estimation error that is caused by transduction error. The fundamental approach was to invert the modulation with the modulation estimates and then iterate this procedure. When $x[n]$ is real, in contrast to being analytic, care must be taken so that the negative frequencies of $x[n]$ are not modulated into the positive frequency range. The most significant reduction error came after the first iteration. This is due to the fact that the initial estimates are close to the actual modulation functions and, therefore, the most of the modulation is eliminated after the first iteration. Experiments were performed on a group of sinusoidally modulated signals. The mean square error averaged over the group of signals is shown in Table 5.1 for the case in which $x[n]$ is analytic and in Table 5.2 for the case in which $x[n]$ is real.

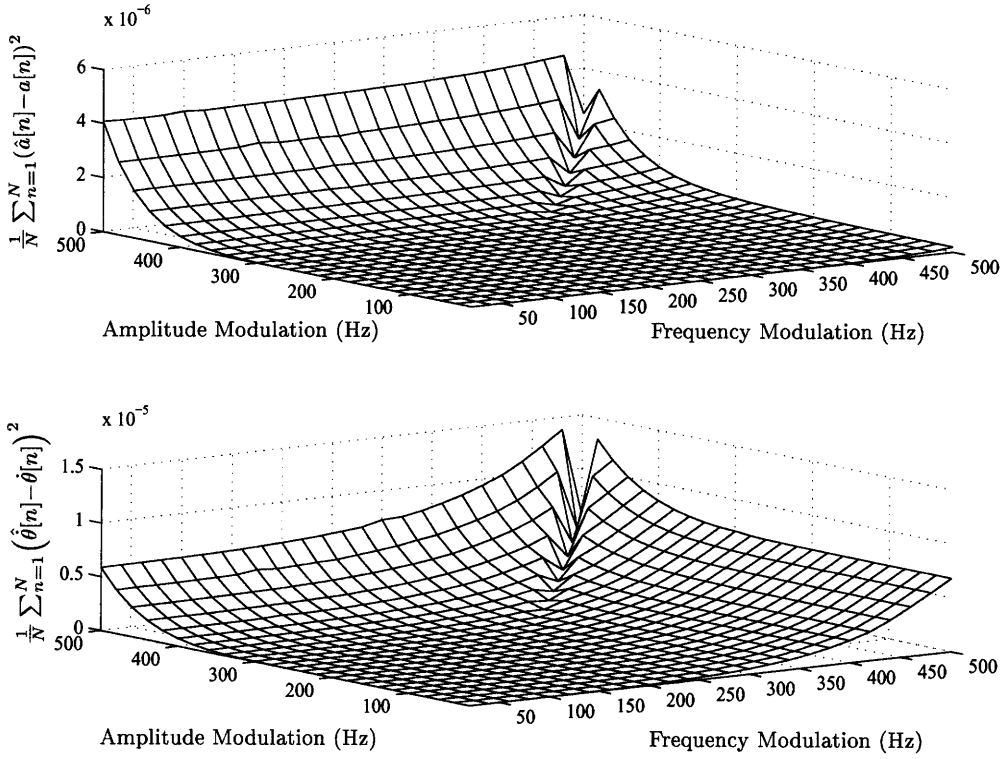

Figure 5-8: Error in amplitude and frequency estimates on the fifth iteration with $x[n]$ real. Frequency error in rad^2/sample.

Iteration:	1	2	3	4	5
Average AM Estimate Error	3.57×10^{-4}	7.10×10^{-6}	1.78×10^{-6}	8.10×10^{-7}	4.92×10^{-7}
Average FM Estimate Error	2.02×10^{-4}	4.54×10^{-6}	2.75×10^{-6}	2.27×10^{-6}	2.05×10^{-6}

Table 5.2: The average of the mean square error over the signal set in Eq. 5.4 for $x[n]$ real. (Frequency error in rad^2/sample.)

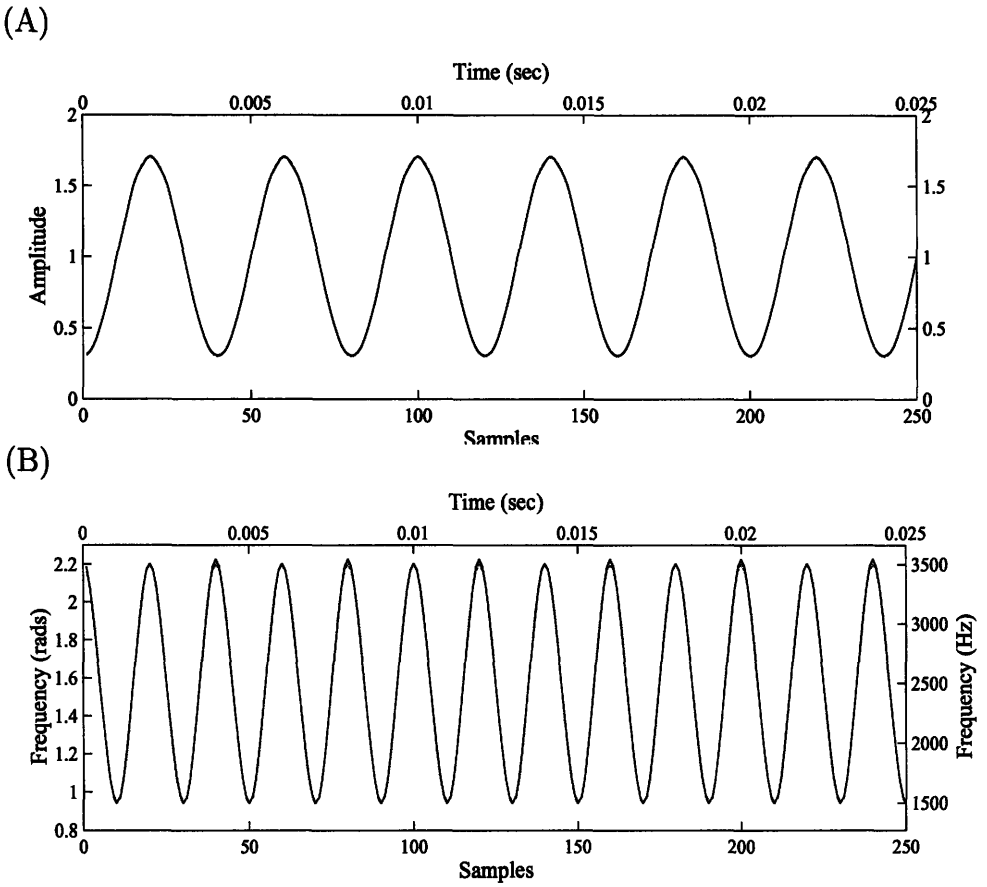

Figure 5-9: An example of the estimated AM and FM (solid lines) after two iterations, (A) amplitude estimate, mean square error: 3.312×10^{-5}, max deviation: 1.101×10^{-2}, (B) frequency estimate, mean square error: 1.646×10^{-4} (rad^2/sec), max deviation: 2.676×10^{-2} (rad).

Chapter 6

Robustness with Respect to Center Frequency

In the previous chapter, we showed that using the AM and FM estimates to demodulate the signal results in improved performance. Recall that when the signal is demodulated with its FM estimate, the signal lies at a center frequency of approximately 0 rad/sec. Therefore, we are required to modulate the signal back up into the passband of the filters $G_1(e^{j\omega})$ and $G_2(e^{j\omega})$. We stated that the optimal frequency to which to modulate was $\omega_c = \frac{\pi}{2}$, or, if $x[n]$ is real, to modulate the signal as close to this frequency as possible without modulating the negative frequencies of $x[n]$ to the positive frequency range. In this chapter, we show separately that $\omega_c = \frac{\pi}{2}$ is optimal in the sense of minimizing the transduction error as well as reducing sensitivity to additive noise.

6.1 Center Frequency and Transduction Error

To show that $\omega_c = \frac{\pi}{2}$ is the best choice in terms of transduction error for our particular choice of $G_1(e^{j\omega})$ and $G_2(e^{j\omega})$, we relate transduction error to the shape of an arbitrary

filter. Consider a filter with a frequency response

$$H(e^{\omega}) = \begin{cases} H_+(e^{j\omega}) & 0 \leq \omega < \pi \\ 0 & \pi \leq \omega < 2\pi \end{cases} \tag{6.1}$$

where $H_+(e^{j\omega})$ is some arbitrary function. We assume that, over the frequency range of the input signal, we can represent $H_+(e^{j\omega})$ as a sum of polynomials, i.e.

$$H_+(e^{j\omega}) = \sum_{k=0}^{\infty} \omega^k f_k. \tag{6.2}$$

Since the output of a filter with shape ω^k is $(-j)^k \frac{d^k}{dn^k} x[n]$ [15], we can analyze the transduction error explicitly by looking at the transduction error that corresponds to each term in Eq. (6.2)[1].

For an input of the form $x[n] = a[n]e^{j\theta[n]}$, we have the following outputs:

[1] $\frac{d^k}{dn^k} x[n]$ corresponds to samples of $\frac{d^k}{dt^k} x(t)$, where $x(t)$ is a band-limited continuous-time signal corresponding to $x[n]$.

Filter		Output
1	$\leftrightarrow$	$y[n] = a[n]e^{j\theta[n]}$
ω	$\leftrightarrow$	$y[n] = \underbrace{\dot{\theta}[n]a[n]e^{j\theta[n]}}_{\substack{\text{Transduction} \\ \text{Approximation}}} - \underbrace{j\dot{a}[n]e^{j\theta[n]}}_{e_1[n]}$
ω^2	$\leftrightarrow$	$y[n] = \underbrace{\dot{\theta}^2[n]a[n]e^{j\theta[n]}}_{\substack{\text{Transduction} \\ \text{Approximation}}} - \underbrace{j\left(\ddot{\theta}[n]a[n] + \dot{\theta}[n]\dot{a}[n]\right)e^{j\theta[n]} - j\frac{d}{dn}e_1[n]}_{e_2[n]}$
ω^3	$\leftrightarrow$	$y[n] = \underbrace{\dot{\theta}^3[n]a[n]e^{j\theta[n]}}_{\substack{\text{Transduction} \\ \text{Approximation}}} - \underbrace{j\left(2\dot{\theta}[n]\ddot{\theta}[n]a[n] + \dot{\theta}^2[n]\dot{a}[n]\right)e^{j\theta[n]} - j\frac{d}{dn}e_2[n]}_{e_3[n]}$
ω^4	$\leftrightarrow$	$y[n] = \underbrace{\dot{\theta}^4[n]a[n]e^{j\theta[n]}}_{\substack{\text{Transduction} \\ \text{Approximation}}} - \underbrace{j\left(3\dot{\theta}^2[n]\ddot{\theta}[n]a[n] + \dot{\theta}^3[n]\dot{a}[n]\right)e^{j\theta[n]} - j\frac{d}{dn}e_3[n]}_{e_4[n]}$
$\vdots$		
ω^n	$\leftrightarrow$	$y[n] = \underbrace{\dot{\theta}^n[n]a[n]e^{j\theta[n]}}_{\substack{\text{Transduction} \\ \text{Approximation}}} - \underbrace{j\left((n-1)\dot{\theta}^{n-2}[n]\ddot{\theta}[n]a[n] + \dot{\theta}^{n-1}[n]\dot{a}[n]\right)e^{j\theta[n]} - j\frac{d}{dn}e_{n-1}[n]}_{e_n[n]}$

We can now make a few observations:

1. As the number of high-order terms in Eq. (6.2) decreases, the transduction error, in general, becomes less severe.

2. If $H(e^{j\omega}) = 1$ over the frequency range of the signal, there is no transduction error.

3. If $H(e^{j\omega}) = c\omega + d$ over the frequency range of the signal, there is no transduction error due to frequency modulation.

These observations complement the results obtained by Bovik[2] et al. [3] in the sense that their results pertain to the time-domain filter response while the above results pertain to the frequency-domain filter response. This raises an interesting point concerning the ideal Hilbert transformer. We argued in Chapter 3 that the ideal Hilbert transformer is not a good procedure for calculating an analytic signal because

[2]See Eq. (3.11)

it has such a long impulse response, and from Eq. (3.11), suffers from transduction error. However, our frequency-domain results suggest that, as long as the signal does not have any energy at 0 rad/sec, there will be no transduction error since the frequency response of the Hilbert transformer is flat everywhere except at 0 rad/sec[3]. The real problem with the Hilbert transformer is that the long impulse response implies a long transient response in the filter output. In other words, the starting point and ending point affect the estimates over a large range of samples. For the particular filters we have chosen, most of the energy is contained in seven samples and therefore we see only the effects of signal endpoints over approximately seven samples.

In order to quantify the performance of a given filter, we define the following measure,

$$E(\omega) = \sum_{k=1}^{\infty} k|f_{\omega,k}|, \tag{6.3}$$

where $f_{\omega,k}$ is the kth coefficient of the Taylor series expansion of the frequency response of the filter evaluated at ω. As the frequency response of a filter requires an increasing number of high order terms, the above measure increases in value. Therefore, this measure corresponds to the amount of transduction error we expect for an arbitrary input signal at a frequency of ω.

Applying this measure to the filters $G_1(e^{j\omega})$ and $G_2(e^{j\omega})$, it is evident from Figure 6-1 that $\omega_c = \frac{\pi}{2}$ is the optimal center frequency with respect to transduction error; the transduction error for $G_1(e^{j\omega})$ and $G_2(e^{j\omega})$, taken together, is minimum at $\omega_c = \frac{\pi}{2}$. This result is consistent with the previous Taylor's series analysis because at $\omega = \frac{\pi}{2}$, $G_1(e^{j\omega}) \approx 1$ and $G_2(e^{j\omega}) \approx \omega$.

[3]The transduction error bounds given in Eq. 3.11 do not directly capture the frequency-domain characteristics of a filter. The analysis that we have presented here complements the time-domain analysis and when choosing filters, *both* the time-domain and frequency-domain aspects should be considered.

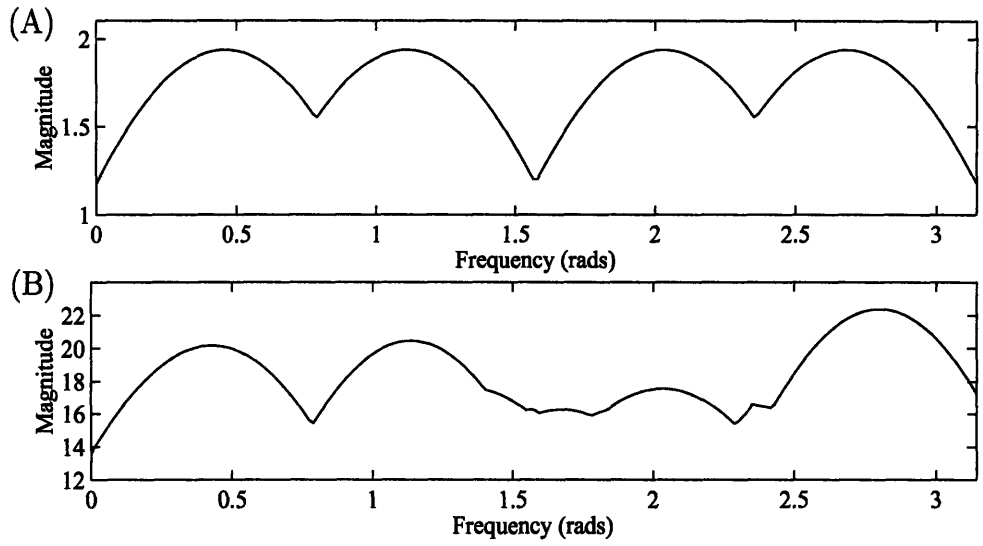

Figure 6-1: A plot of the frequency domain filter error measure for (A) $G_1(e^{j\omega})$ and (B) $G_2(e^{j\omega})$.

6.2 Center Frequency and Additive Noise

An important consideration in performance is robustness in the presence of noise. Suppose that the signal to be analyzed consists of a single AM-FM sinusoid with some additive disturbance,

$$x[n] = a[n]\cos(\theta[n]) + w[n] \tag{6.4}$$

where

$$\max_n(w[n]) < \varepsilon \min_n(a[n]) = \varepsilon\, a_{min}. \tag{6.5}$$

The constraint in Eq. (6.5) ensures that the amplitude of the disturbance never exceeds the amplitude of the signal.

We again denote $g_1[n]$ as the impulse response of the filter described in Eq. (4.12) and $g_2[n]$ as the impulse response of the filter described in Eq. (4.13). The absolute value of these impulse responses were shown in Figure 4-2 and Figure 4-3. As evident in the figures, $g_1[n]$ and $g_2[n]$ have most of their energy confined to the region $-3 \leq$

$n \leq 3$. Therefore, for the following analysis, we define

$$\mathbf{g_1} = \begin{bmatrix} g_1[-3] & g_1[-2] & \dots & g_1[2] & g_1[3] \end{bmatrix}^T \tag{6.6}$$

$$\mathbf{g_2} = \begin{bmatrix} g_2[-3] & g_2[-2] & \dots & g_2[2] & g_2[3] \end{bmatrix}^T \tag{6.7}$$

$$\mathbf{w} = \begin{bmatrix} w[n_0-3] & w[n_0-2] & \dots & w[n_0+2] & w[n_0+3] \end{bmatrix}^T \tag{6.8}$$

Since we are concerned only with the amplitudes of the filter outputs, we assume without loss of generality that $\theta[n_0] = 0$. Therefore, the output of filter $G_i(e^{j\omega})$ is given by

$$y_i[n_0] = \underbrace{a[n_0]G_i(e^{j\dot{\theta}[n_0]})}_{\substack{\text{Transduction} \\ \text{Approximation}}} + \underbrace{e_i[n_0]}_{\substack{\text{Transduction} \\ \text{Error}}} + \underbrace{\mathbf{g_i}'\mathbf{w}}_{\substack{\text{Filtered} \\ \text{Noise}}} \tag{6.9}$$

and the square of the amplitude envelope of the filter output is given by

$$\begin{aligned} |y_i[n_0]|^2 = a^2[n_0]G_i^2(e^{j\dot{\theta}[n_0]}) + 2a[n_0]G_i(e^{j\dot{\theta}[n_0]})\mathrm{Re}\{e_i[n_0]\} + |e_i[n_0]|^2 \\ + 2\mathrm{Re}\left\{\left(a[n_0]G_i(e^{j\dot{\theta}[n_0]}) + e_i[n_0]\right)\mathbf{g_i}'\mathbf{w}\right\} + \mathbf{w}'\mathbf{g_i}\mathbf{g_i}'\mathbf{w}. \end{aligned} \tag{6.10}$$

Because our analysis is in terms of the worst-case noise sequence, we assume that the transduction error is negligible. We then approximate the square of the envelopes of the filter output as

$$|y_i[n_0]|^2 \approx a^2[n_0]G_i^2(e^{j\dot{\theta}[n_0]}) + 2a[n_0]G_i(e^{j\dot{\theta}[n_0]})\mathrm{Re}\{\mathbf{g_i}'\mathbf{w}\} + \mathbf{w}'\mathbf{g_i}\mathbf{g_i}'\mathbf{w}. \tag{6.11}$$

Since we are calculating the error at an arbitrary point in time, we drop the time index to simplify the notation. Also, since the signal-to-noise ratio is the smallest when $a[n] = a_{min}$, the worst-case frequency estimate is

$$\hat{\dot{\theta}^2} = \frac{|y_2|^2}{|y_1|^2} = \frac{a_{min}^2 G_2^2(e^{j\dot{\theta}}) + 2a_{min}G_2(e^{j\dot{\theta}})\mathrm{Re}\{\mathbf{w}'\mathbf{g_2}\} + \mathbf{w}'\mathbf{g_2}\mathbf{g_2}'\mathbf{w}}{a_{min}^2 G_1^2(e^{j\dot{\theta}}) + 2a_{min}G_1(e^{j\dot{\theta}})\mathrm{Re}\{\mathbf{w}'\mathbf{g_1}\} + \mathbf{w}'\mathbf{g_1}\mathbf{g_1}'\mathbf{w}}. \tag{6.12}$$

We now seek two aspects of the performance with respect to the external noise, $\mathbf{w}$.

First, for a given frequency $\dot{\theta}$, we find the disturbance sequence, $\mathbf{w_E}(\dot{\theta})$, that causes the most severe error in the estimate, and second, we find the frequency at which the algorithm is least sensitive to $\mathbf{w_E}(\dot{\theta})$. It is possible to solve for the bounds of $\hat{\dot{\theta}}^2$ and the corresponding disturbance sequence $\mathbf{w_E}(\dot{\theta})$ by using optimization techniques. Namely, we minimize and maximize $\hat{\dot{\theta}}^2[n_0]$ over all possible disturbances, $\mathbf{w}$, subject to the constraint given in Eq. (6.5). The procedure, sometimes referred to as constrained maximum ascent (to find a maximum) or constrained maximum descent (to find a minimum), is described as follows:

1. Start at some point $\mathbf{w} = \mathbf{x_i}$, with $\mathbf{x_0}$ being a random initial point.
2. Calculate the gradient of $\hat{\dot{\theta}}$ at $\mathbf{x_i}$: $\left.\frac{\partial \hat{\dot{\theta}}}{\partial \mathbf{w}}\right|_{\mathbf{w}=\mathbf{x_i}}$.
3. Step in the (opposite) direction of the gradient to maximize (minimize), restricting the step length to be less than some small constant δ: $\mathbf{x_{i+1}} = \mathbf{x_i} + \mathbf{s_i}$ where $\mathbf{s_i} = \delta \left.\frac{\partial \hat{\dot{\theta}}}{\partial \mathbf{w}}\right|_{\mathbf{w}=\mathbf{x_i}} \left(\mathbf{s_i} = -\delta \left.\frac{\partial \hat{\dot{\theta}}}{\partial \mathbf{w}}\right|_{\mathbf{w}=\mathbf{x_i}}\right)$.
4. If this steps outside of the boundary region given in Eq. (6.5), reduce the length of the step (i.e., reduce the parameter δ) so that x_{i+1} lies within the boundary.
5. Repeat steps 2-4 with a new starting point, $\mathbf{x_{i+1}}$, until the algorithm converges.

The results of this procedure indicate that $\hat{\dot{\theta}}[n]$ is maximized when

$$\mathbf{w_E} = \begin{cases} \varepsilon a_{min}[1 \quad -1 \quad -1 \quad 1 \quad -1 \quad -1 \quad 1]^T & \text{for } \dot{\theta} < \frac{\pi}{2} \\ \varepsilon a_{min}[1 \quad 1 \quad -1 \quad -1 \quad -1 \quad 1 \quad 1]^T & \text{for } \dot{\theta} \geq \frac{\pi}{2} \end{cases} \tag{6.13}$$

and is minimized when

$$\mathbf{w_E} = \begin{cases} \varepsilon a_{min}[-1 \quad 1 \quad 1 \quad -1 \quad 1 \quad 1 \quad -1]^T & \text{for } \dot{\theta} < \frac{\pi}{2} \\ \varepsilon a_{min}[-1 \quad -1 \quad 1 \quad 1 \quad 1 \quad -1 \quad -1]^T & \text{for } \dot{\theta} \geq \frac{\pi}{2} \end{cases} \tag{6.14}$$

Figure 6-2 shows an example of the convergence of the algorithm for the second case in Eq. (6.14) with $\delta = 0.005$, $\sup_n |\mathbf{w}| = 0.1$, $a_{min} = 1$, and $\dot{\theta} = 2$. The initial points

(marked with an 'o') where randomly generated. Similar behavior occurred in the convergence of the other cases.

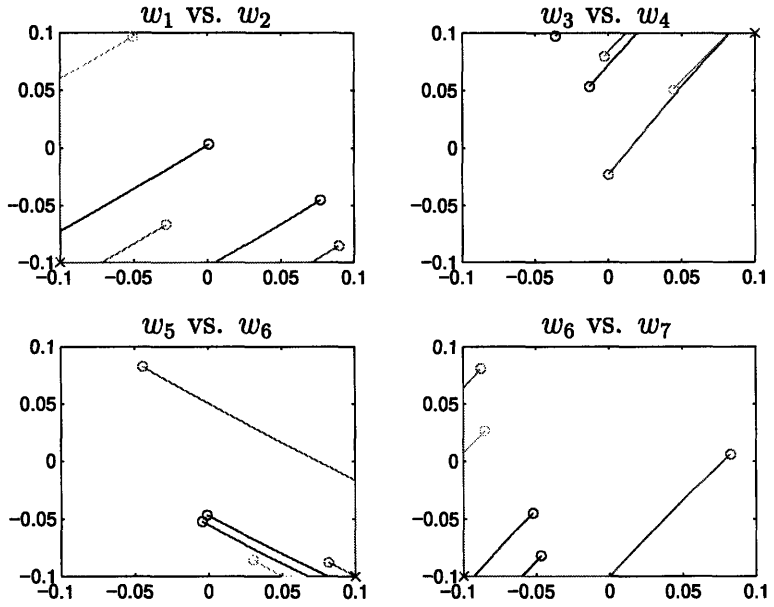

Figure 6-2: An example of the convergence of the constrained maximum descent algorithm for determining the worst case disturbance vector. The o's mark the randomly generated starting points and the x's mark the points to which the algorithm converged ($\delta = 0.005$, $\sup_n |\mathbf{w}| = 0.1$, $a_{min} = 1$, and $\dot{\theta} = 2$).

Now that we have determined the worst-case error vector, $\mathbf{w_E}$, we find the frequency, ω_c, at which the algorithm is least sensitive to the disturbance vector, $\mathbf{w_E}$. One possible approach is to set $\frac{\partial}{\partial \dot{\theta}} \left| \hat{\dot{\theta}} - \dot{\theta} \right|$ equal to zero and solve for $\dot{\theta}$. This calculation, however, is rather cumbersome, so we determine ω_c by plotting $\left| \hat{\dot{\theta}} - \dot{\theta} \right|$ as a function of $\dot{\theta}$ with $\mathbf{w} = \mathbf{w_E}$. This function is shown in Figure 6-3 over the range of $.0001 \leq \varepsilon \leq .01$ and $.3 \leq \dot{\theta} \leq \pi - .3$, from which it is evident that $w_c = \frac{\pi}{2}$ is the optimal choice in terms of reducing the sensitivity to external noise.

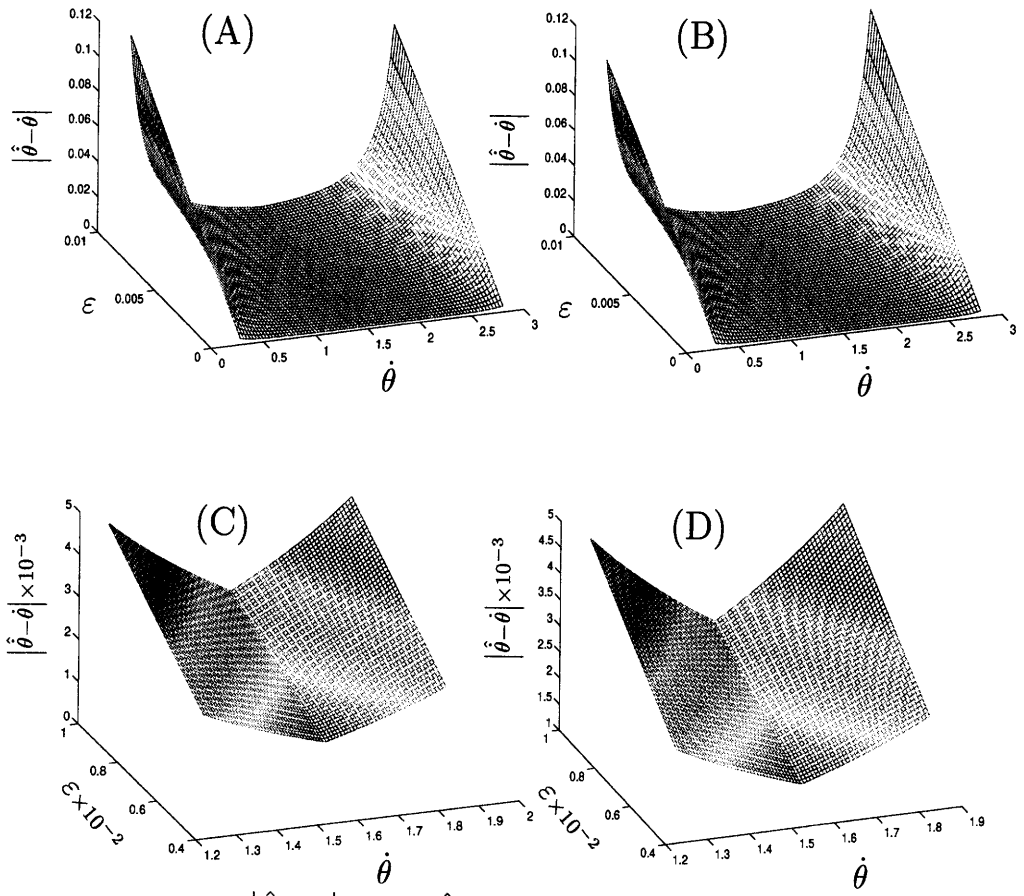

Figure 6-3: Plot of $\left|\hat{\dot{\theta}}-\dot{\theta}\right|$: (A) $\hat{\dot{\theta}}$ is minimized (Eq. (6.14)), (B) $\hat{\dot{\theta}}$ is maximized (Eq. (6.13)), (C) a zoom-in of (A), and (D) a zoom-in of (B).

6.3 Summary

In this chapter, we showed that $\omega_c = \frac{\pi}{2}$ is optimal for both transduction error reduction and robustness in the presence of additive noise. We also introduced a frequency domain perspective on the transduction approximation which was used in the transduction error analysis.

Chapter 7

Two-Sinusoid AM-FM Estimation

In this chapter, we propose an algorithm for the estimation of the AM and FM functions of a signal that consists of two sinusoids. Our first step in developing this method is to resolve the uniqueness issues discussed in Chapter 2. Recall that there are an infinite number of ways to express a signal as a sum of two AM-FM signals, even when the signal is analytic. We show that it is possible to reduce the two-sinusoid estimation problem to two single-sinusoid estimation problems and that this results in the desired uniqueness. In the second section, we discuss the implementation of the algorithm and, in the following section, we illustrate the performance with some examples. We then show how the algorithm can be modified to improve its performance.

7.1 The Two-Sinusoid AM-FM Estimation Algorithm

Consider signals of the form

$$x[n] = a_1[n]\cos(\theta_1[n]) + a_2[n]\cos(\theta_2[n]). \tag{7.1}$$

Our goal is to estimate $a_1[n]$, $a_2[n]$, $\dot{\theta}_1[n]$, and $\dot{\theta}_2[n]$. An immediate difficulty is that, for a given $x[n]$, these functions are not unique, even if $x[n]$ is made analytic. In

the single-sinusoid case, making the signal analytic forces a unique solution. Our approach is to transform the two-sinusoid problem into two single-sinusoid problems and thereby establish uniqueness.

7.1.1 Approach

If the input is passed through the filters $G_1(e^{j\omega}) = \frac{1}{2}(1 - \cos(2\omega))$ and $G_2(e^{j\omega}) = \omega G_1(e^{j\omega})$, then from the transduction approximation the filter outputs can be approximated as

$$y_1[n] \approx a_1[n]G_1(e^{j\dot{\theta}_1[n]})e^{j\theta_1[n]} + a_2[n]G_1(e^{j\dot{\theta}_2[n]})e^{j\theta_2[n]} \tag{7.2}$$

and

$$\begin{aligned} y_2[n] &\approx a_1[n]G_2(e^{j\dot{\theta}_1[n]})e^{j\theta_1[n]} + a_2[n]G_2(e^{j\dot{\theta}_2[n]})e^{j\theta_2[n]} \\ &\approx a_1[n]\dot{\theta}_1[n]G_1(e^{j\dot{\theta}_1[n]})e^{j\theta_1[n]} + a_2[n]\dot{\theta}_2[n]G_1(e^{j\dot{\theta}_2[n]})e^{j\theta_2[n]} \end{aligned} \tag{7.3}$$

The square of the amplitude envelopes of the filter outputs are given by

$$\begin{aligned} |y_1[n]|^2 \approx\ & a_1^2[n]G_1^2(e^{j\dot{\theta}_1[n]}) + a_2^2[n]G_1^2(e^{j\dot{\theta}_2[n]}) \\ & + 2a_1[n]a_2[n]G_1(e^{j\dot{\theta}_1[n]})G_1(e^{j\dot{\theta}_2[n]})\cos(\theta_2[n] - \theta_1[n]) \end{aligned} \tag{7.4}$$

and

$$\begin{aligned} |y_2[n]|^2 &\approx a_1^2[n]G_2^2(e^{j\dot{\theta}_1[n]}) + a_2^2[n]G_2^2(e^{j\dot{\theta}_2[n]}) \\ &\quad + 2a_1[n]a_2[n]G_2(e^{j\dot{\theta}_1[n]})G_2(e^{j\dot{\theta}_2[n]})\cos(\theta_2[n] - \theta_1[n]) \\ &\approx a_1^2[n]\dot{\theta}_1^2[n]G_1^2(e^{j\dot{\theta}_1[n]}) + a_2^2[n]\dot{\theta}_2^2[n]G_1^2(e^{j\dot{\theta}_2[n]}) \\ &\quad + 2a_1[n]a_2[n]\dot{\theta}_1^2[n]\dot{\theta}_2^2[n]G_1(e^{j\dot{\theta}_1[n]})G_1(e^{j\dot{\theta}_2[n]})\cos(\theta_2[n] - \theta_1[n]) \end{aligned} \tag{7.5}$$

If the first two terms in Eq. (7.4) and Eq. (7.5) are treated as noise terms[1], i.e., we define

$$\nu_1[n] = a_1^2[n]G_1^2(e^{j\dot{\theta}_1[n]}) + a_2^2[n]G_1^2(e^{j\dot{\theta}_2[n]}) \tag{7.6}$$

$$\nu_2[n] = a_1^2[n]\dot{\theta}_1^2[n]G_1^2(e^{j\dot{\theta}_1[n]}) + a_2^2[n]\dot{\theta}_2^2[n]G_1^2(e^{j\dot{\theta}_2[n]}), \tag{7.7}$$

then we are left with two single AM-FM sinusoids with additive noise

$$|y_1[n]|^2 \approx 2a_1[n]a_2[n]G_1(e^{j\dot{\theta}_1[n]})G_1(e^{j\dot{\theta}_2[n]})\cos(\theta_2[n] - \theta_1[n]) + \nu_1[n] \tag{7.8}$$

and

$$|y_2[n]|^2 \approx 2a_1[n]a_2[n]\dot{\theta}_1^2[n]\dot{\theta}_2^2[n]G_1(e^{j\dot{\theta}_1[n]})G_1(e^{j\dot{\theta}_2[n]})\cos(\theta_2[n] - \theta_1[n]) + \nu_2[n]. \tag{7.9}$$

Therefore, if $|y_1[n]|^2$ is passed to the single-sinusoid estimation algorithm, the algorithm gives a unique amplitude estimate

$$\hat{a}_{|y_1|^2}[n] = 2a_1[n]a_2[n]G_1(e^{j\dot{\theta}_1[n]})G_1(e^{j\dot{\theta}_2[n]}) \tag{7.10}$$

and a unique instantaneous frequency estimate

$$\hat{\dot{\theta}}_{|y_1|^2}[n] = \dot{\theta}_2[n] - \dot{\theta}_1[n]. \tag{7.11}$$

Similarly, for $|y_2[n]|^2$, the single-sinusoid estimation algorithm gives a unique amplitude estimate

$$\hat{a}_{|y_2|^2}[n] = 2a_1[n]a_2[n]\dot{\theta}_1^2[n]\dot{\theta}_2^2[n]G_1(e^{j\dot{\theta}_1[n]})G_1(e^{j\dot{\theta}_2[n]}) \tag{7.12}$$

[1]We will discuss when this representation is valid in the next section.

and the same instantaneous frequency estimate

$$\hat{\dot{\theta}}_{|y_2|^2}[n] = \dot{\theta}_2[n] - \dot{\theta}_1[n]. \tag{7.13}$$

The product of the individual instantaneous frequencies can be obtained from

$$\dot{\theta}_2[n]\dot{\theta}_1[n] = \frac{\hat{a}_{|y_2|^2}[n]}{\hat{a}_{|y_1|^2}[n]}. \tag{7.14}$$

Solving for $\dot{\theta}_2[n]$ in Eq. (7.13) and substituting this into Eq. (7.14) gives

$$\begin{aligned} \dot{\theta}_1[n]\left(\dot{\theta}_1[n] + \hat{\dot{\theta}}_{|y_1|^2}[n]\right) &= \frac{\hat{a}_{|y_2|^2}[n]}{\hat{a}_{|y_1|^2}[n]} \\ \dot{\theta}_1^2[n] + \hat{\dot{\theta}}_{|y_1|^2}[n]\dot{\theta}_1[n] - \frac{\hat{a}_{|y_2|^2}[n]}{\hat{a}_{|y_1|^2}[n]} &= 0. \end{aligned} \tag{7.15}$$

This has two possible solutions,

$$\dot{\theta}_1[n] = \frac{1}{2}\left(-\hat{\dot{\theta}}_{|y_1|^2}[n] \pm \sqrt{\hat{\dot{\theta}}^2_{|y_1|^2}[n] + 4\frac{\hat{a}_{|y_2|^2}[n]}{\hat{a}_{|y_1|^2}[n]}}\right). \tag{7.16}$$

Since the frequency is positive, the correct solution is

$$\dot{\theta}_1[n] = \frac{1}{2}\left(-\hat{\dot{\theta}}_{|y_1|^2}[n] + \sqrt{\hat{\dot{\theta}}^2_{|y_1|^2}[n] + 4\frac{\hat{a}_{|y_2|^2}[n]}{\hat{a}_{|y_1|^2}[n]}}\right). \tag{7.17}$$

Substituting this result into Eq. (7.13), we obtain

$$\dot{\theta}_2[n] = \frac{1}{2}\left(\hat{\dot{\theta}}_{|y_1|^2}[n] + \sqrt{\hat{\dot{\theta}}^2_{|y_1|^2}[n] + 4\frac{\hat{a}_{|y_2|^2}[n]}{\hat{a}_{|y_1|^2}[n]}}\right). \tag{7.18}$$

Observe that we always assign the lower valued frequency estimate to $\dot{\theta}_1[n]$ and the higher valued frequency estimate to $\dot{\theta}_2[n]$. It is now possible to estimate the amplitude modulation using the instantaneous frequency estimates and the magnitude of the filter outputs. First we multiply $|y_1[n]|^2$ of Eq. (7.4) by $\dot{\theta}_1\dot{\theta}_2$ and then subtract this

from $|y_2[n]|^2$ of Eq. (7.5), which results in

$$|y_2[n]|^2 - \dot{\theta}_1[n]\dot{\theta}_2[n]|y_1[n]|^2 = a_1^2[n]G_1^2(e^{j\dot{\theta}_1[n]})(\dot{\theta}_1^2[n] - \dot{\theta}_1[n]\dot{\theta}_2[n]) + a_2^2[n]G_1^2(e^{j\dot{\theta}_2[n]})(\dot{\theta}_2^2[n] - \dot{\theta}_1[n]\dot{\theta}_2[n]) \quad (7.19)$$

From Eq. (7.10), we have

$$a_2^2[n]G_1(e^{j\dot{\theta}_2[n]}) = \frac{(\hat{a}_{|y_1|^2}[n])^2}{4a_1^2[n]G_1^2(e^{j\dot{\theta}_1[n]})}. \quad (7.20)$$

We new drop the time subscript so the equations are less cumbersome. Combining Eq. (7.19) with Eq. (7.20), we have

$$|y_2|^2 - \dot{\theta}_1\dot{\theta}_2|y_1|^2 = a_1^2G_1^2(e^{j\dot{\theta}_1})(\dot{\theta}_1^2 - \dot{\theta}_1\dot{\theta}_2) + \frac{(a_{|y_1|^2})^2}{4a_1^2G_1^2(e^{j\dot{\theta}_1})}(\dot{\theta}_2^2 - \dot{\theta}_1\dot{\theta}_2)$$

$$\left[a_1^2G_1^2(e^{j\dot{\theta}_1})\right]^2 - \frac{|y_2|^2 - \dot{\theta}_1\dot{\theta}_2|y_1|^2}{\dot{\theta}_1^2 - \dot{\theta}_1\dot{\theta}_2}\left[a_1^2G_1^2(e^{j\dot{\theta}_1})\right] + \frac{(\hat{a}_{|y_1|^2})^2(\dot{\theta}_2^2 - \dot{\theta}_1\dot{\theta}_2)}{4(\dot{\theta}_1^2 - \dot{\theta}_1\dot{\theta}_2)} = 0. \quad (7.21)$$

The above equation has two roots,

$$a_1^2G_1^2(e^{j\dot{\theta}_1}) = \frac{1}{2}\left(\frac{|y_2|^2 - \dot{\theta}_1\dot{\theta}_2|y_1|^2}{\dot{\theta}_1^2 - \dot{\theta}_1\dot{\theta}_2} \pm \sqrt{\left(\frac{|y_2|^2 - \dot{\theta}_1\dot{\theta}_2|y_1|^2}{\dot{\theta}_1^2 - \dot{\theta}_1\dot{\theta}_2}\right)^2 - 4\frac{(\hat{a}_{|y_1|^2})^2(\dot{\theta}_2^2 - \dot{\theta}_1\dot{\theta}_2)}{4(\dot{\theta}_1^2 - \dot{\theta}_1\dot{\theta}_2)}}\right) \quad (7.22)$$

Because $\dot{\theta}_1 < \dot{\theta}_2$, it is always true that

$$-4\frac{(\hat{a}_{|y_1|^2})^2(\dot{\theta}_2^2 - \dot{\theta}_1\dot{\theta}_2)}{4(\dot{\theta}_1^2 - \dot{\theta}_1\dot{\theta}_2)} > 0,$$

and thus it is always true that

$$\sqrt{\left(\frac{|y_2|^2 - \dot{\theta}_1\dot{\theta}_2|y_1|^2}{\dot{\theta}_1^2 - \dot{\theta}_1\dot{\theta}_2}\right)^2 - 4\frac{(\hat{a}_{|y_1|^2})^2(\dot{\theta}_2^2 - \dot{\theta}_1\dot{\theta}_2)}{4(\dot{\theta}_1^2 - \dot{\theta}_1\dot{\theta}_2)}} > \left|\frac{|y_2|^2 - \dot{\theta}_1\dot{\theta}_2|y_1|^2}{\dot{\theta}_1^2 - \dot{\theta}_1\dot{\theta}_2}\right|. \quad (7.23)$$

Therefore, one of the roots of Eq. (7.22) is always negative and the other one is always positive. The correct root, since $a_1 G_1(e^{j\dot{\theta}_1})$ is real, is the positive root and we have

$$a_1 = \frac{\sqrt{\frac{1}{2}\left(\frac{|y_2|^2 - \dot{\theta}_1\dot{\theta}_2|y_1|^2}{\dot{\theta}_1^2 - \dot{\theta}_1\dot{\theta}_2} + \sqrt{\left(\frac{|y_2|^2 - \dot{\theta}_1\dot{\theta}_2|y_1|^2}{\dot{\theta}_1^2 - \dot{\theta}_1\dot{\theta}_2}\right)^2 - 4\frac{(\hat{a}_{|y_1|^2})^2(\dot{\theta}_2^2 - \dot{\theta}_1\dot{\theta}_2)}{4(\dot{\theta}_1^2 - \dot{\theta}_1\dot{\theta}_2)}}\right)}}{G_1(e^{j\dot{\theta}_1})} \tag{7.24}$$

We can now obtain $a_2[n]$ from Eq. (7.10) and Eq. (7.24),

$$a_2 = \frac{\hat{a}_{|y1|^2}}{2a_1 G_1(e^{j\theta_1})G_1(e^{j\theta_2})}. \tag{7.25}$$

A block diagram of the two-sinusoid AM-FM estimation algorithm is shown in Figure 7-1.

7.1.2 Validity of the Approximations

The two terms, $\nu_1[n]$ and $\nu_2[n]$ described in Eq. (7.6) and Eq. (7.7), will be referred to as *self generated noise* (SGN). In general, noise terms of this magnitude cause severe problems in the single-sinusoid estimation algorithm. However, $\nu_1[n]$ and $\nu_2[n]$ consist primarily of large low-frequency components, which are effectively eliminated at the input of the single-sinusoid algorithm by the filters $G_1(e^{j\omega})$ and $G_2(e^{j\omega})$. In fact, if there is no AM or FM modulation, the noise terms are constant and therefore completely eliminated. This is illustrated in the following example.

EXAMPLE 7.1

Consider an input

$$x[n] = \cos\left(\frac{2\pi n}{5}\right) + \cos\left(\frac{3\pi n}{5}\right). \tag{7.26}$$

Then the magnitude squared of the output of filter $G_1(e^{j\omega})$ is

$$|y_1[n]|^2 = G_1(e^{j\frac{2\pi}{5}})^2 + G_1(e^{j\frac{3\pi}{5}})^2 + G_1(e^{j\frac{2\pi}{5}})G_1(e^{j\frac{3\pi}{5}})\cos\left(\frac{\pi n}{5}\right). \tag{7.27}$$

This signal, $|y_1[n]|^2$, is the input to the single-sinusoid estimation algorithm. The first step in that algorithm is to make the input analytic by filtering with

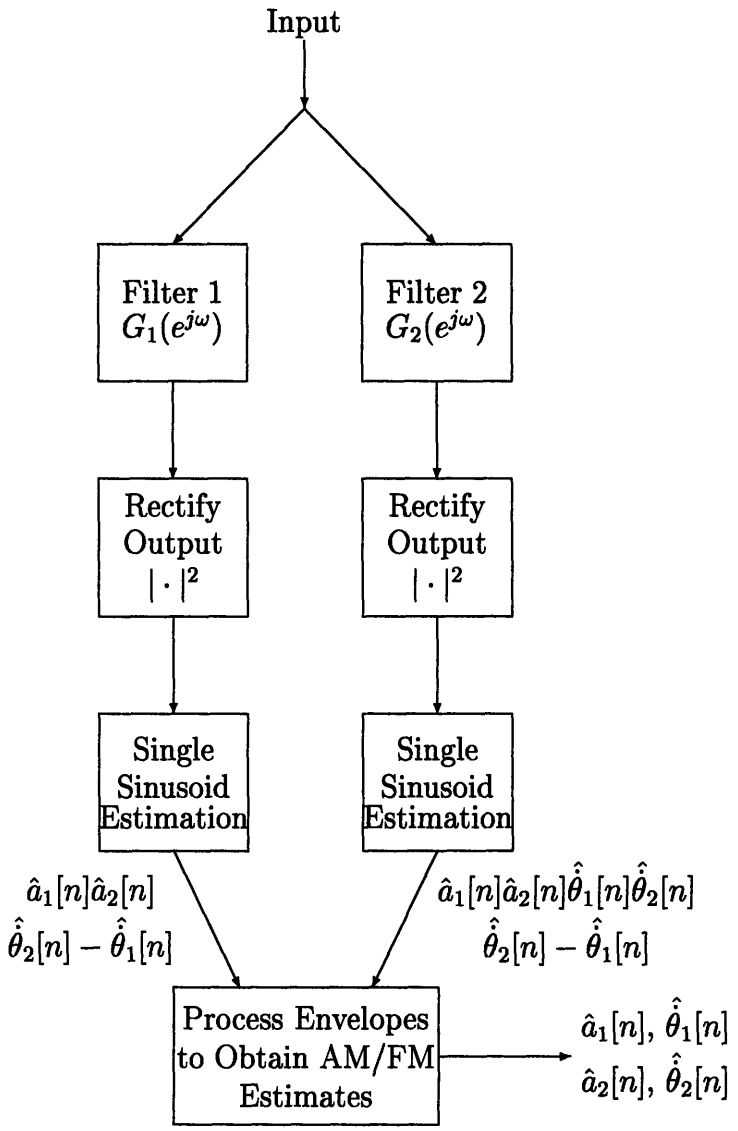

Figure 7-1: Block diagram of basic two-sinusoid AM-FM estimation algorithm.

$G_1(e^{j\omega})$, resulting in

$$|y_1[n]|_a^2 = G_1(e^{j\frac{2\pi}{5}})G_1(e^{j\frac{3\pi}{5}})e^{j\frac{\pi n}{5}}. \tag{7.28}$$

The two terms, $G_1(e^{j\frac{2\pi}{5}})^2$ and $G_1(e^{j\frac{3\pi}{5}})^2$ have been eliminated since they are at a frequency of 0 rad/sec. The magnitudes of the DFTs at each stage of this process are shown in Figure 7-2.

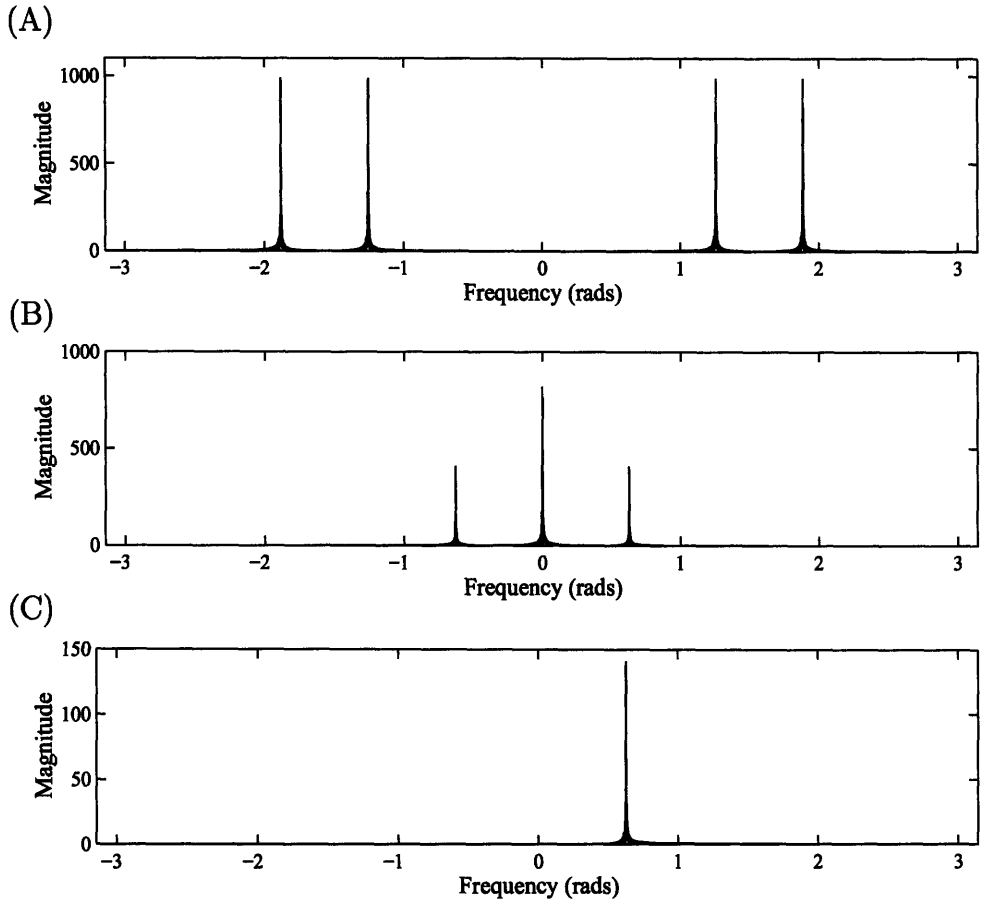

Figure 7-2: An example of the elimination of self generated noise, (A) magnitude of the DFT of $x[n]$, (B) magnitude of the DFT of $|x[n] * g_1[n]|^2$ (input to the single AM-FM estimation algorithm), and (C) magnitude of the DFT of $g_1[n] * |x[n] * g_1[n]|^2$.

If the two signals are not stationary, the noise terms are not at 0 rad/sec, although they still have a significant portion of their energy at very low frequencies. Therefore, in general, some energy of the noise terms passes through the filters and results in error in the estimates. As the spectrum of the SGN widens, the error increases. It is difficult to quantify the allowable frequency range of the SGN because there are many

factors that influence the sensitivity. For example, if the two sinusoids are close in frequency, then $e^{j(\theta_2[n]-\theta_1[n])}$ is at a low frequency near the SGN. When $|y_i[n]|^2$ passes through $G_i(e^{j\omega})$, the SGN is not reduced relative to the single AM-FM term. Another difficulty in quantifying the allowable frequency range of the SGN is that the algorithm does not break down at a certain point; its performance continually degrades as the interference from the SGN increases. The allowable frequency range of the SGN therefore depends on the error allowed in a particular application. Consequently, we use the general guideline that the frequency separation of the two sinusoids should be greater than the largest spectral component of the SGN.

7.1.3 Modifications to the Single-Sinusoid Algorithm

One modification must be made to the single-sinusoid algorithm to ensure good performance of the two-sinusoid algorithm. Recall that when the input to the single-sinusoid algorithm is real, the inverse modulation algorithm modulates the signal to a frequency, ω_c, that is as close to $\frac{\pi}{2}$ as possible. The closeness of ω_c to $\frac{\pi}{2}$ was constrained to avoid modulating the negative frequencies to positive frequencies. In the two-sinusoid case, we are even more constrained. This results from the fact the the signals that are passed to the single-sinusoid algorithm, $|y_1[n]|^2$ and $|y_2[n]|^2$, have the SGN terms that are centered at 0 rad/sec. If we leave the single-sinusoid algorithm as described in the previous chapters, the SGN will be modulated to the passband of the filters. This violates the assumption in Section 7.1.2 that most of the energy of the SGN is at low frequencies and therefore significantly reduced by the filters $G_1(e^{j\omega})$ and $G_2(e^{j\omega})$. Therefore, we do not use the inverse modulation techniques in the single-sinusoid algorithm in the two-sinusoid estimation algorithm that we have just described. In a later section, we describe a modification to the two-sinusoid algorithm that significantly reduces the SGN. Once the SGN has been reduced, we then use the inverse modulation techniques in the embedded single-sinusoid algorithm.

7.1.4 Examples of the Two-Sinusoid AM-FM Estimation Algorithm

In this section, examples of the performance of the two-sinusoid AM-FM estimation algorithm are presented to demonstrate its capabilities and limitations. As mentioned above, this algorithm does not use the iterative techniques in the embedded single-sinusoid algorithms.

We begin with a signal that consists of two sinusoids, each of them with constant AM and constant FM functions.

EXAMPLE 7.2
AM-FM estimates for the signal

$$x[n] = \cos\left(\frac{2\pi n}{5}\right) + \cos\left(\frac{3\pi n}{5}\right) \tag{7.29}$$

are shown in Figure 7-3, illustrating that when there is no modulation, which makes the transduction approximation exact, there is practically no estimation error.

An important performance measure is the estimation error as a function of the separation in frequency of the two components

EXAMPLE 7.3
For this example, the lower frequency component is held at $\frac{\pi}{2}$ rad/sec while the second signal is at $\frac{\pi}{2} + \delta$ rad/sec. More explicitly,

$$x_\delta[n] = \cos\left(\frac{\pi n}{2}\right) + \cos\left(\left[\frac{\pi}{2} + \delta\right] n\right) \qquad \text{for } \delta = \frac{\pi}{100}, \frac{\pi}{250}, \frac{\pi}{500}, \frac{\pi}{1000}. \tag{7.30}$$

The first column of Table 7.1 corresponds to a frequency separation of 50Hz for a sampling rate of 10,000 Hz. The last column of Table 7.1 corresponds to a frequency separation of 5Hz for 10,000 Hz sampling. The increase in error shown in the last column in the table is due the SGN, since no transduction error is present.

We now add modulation to the signal. In this next example, the signal consists of two sinusoids with constant amplitude modulation and sinusoidal frequency modulation. For each component, the frequency modulation is the same, the only difference being the carrier frequencies.

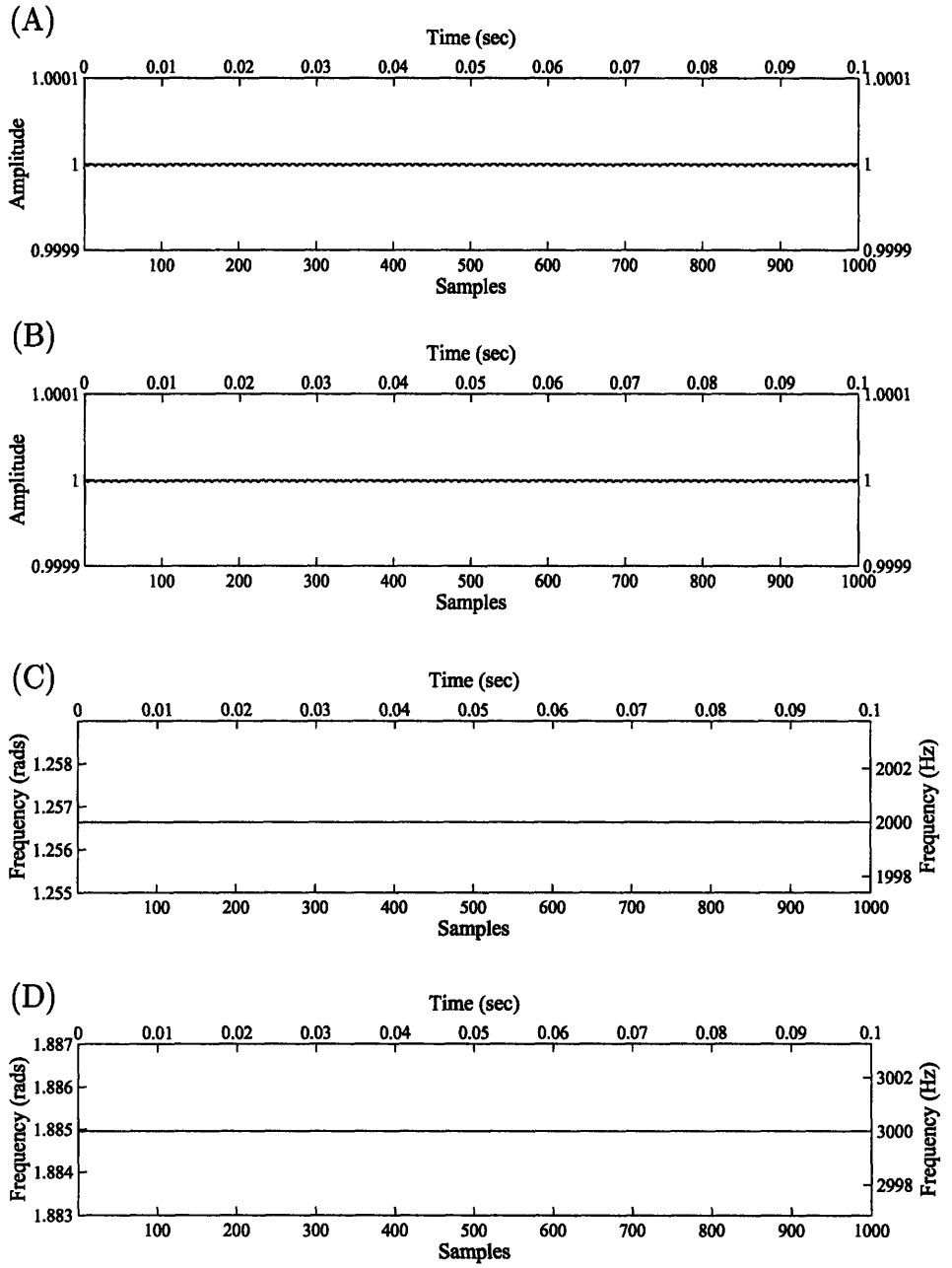

Figure 7-3: Example of two-sinusoid AM-FM estimation with constant AM and constant FM, (A) estimate of $a_1[n]$, mean square error: 1.103×10^{-12}, max deviation: 2.143×10^{-9}, (B) estimate of $a_2[n]$, mean square error: 1.363×10^{-12}, max deviation: 2.346×10^{-9}, (C) estimate of $\dot{\theta}_1[n]$, mean square error: 5.490×10^{-13} (rad/sec), max deviation: 1.079×10^{-9} (rad/sec), and (D) estimate of $\dot{\theta}_2[n]$, mean square error: 3.303×10^{-13}(rad/sec), max deviation: 8.033×10^{-10} (rad/sec).

δ	$\frac{\pi}{100}$	$\frac{\pi}{250}$	$\frac{\pi}{500}$	$\frac{\pi}{1000}$
$\hat{a}_1[n]$ mean sq. error	1.32×10^{-4}	0.019	0.085	0.324
$\hat{a}_2[n]$ mean sq. error	1.32×10^{-4}	0.019	0.085	0.324
$\hat{\dot{\theta}}_1[n]$ mean sq. error	7.09×10^{-8}	2.13×10^{-6}	9.33×10^{-6}	2.99×10^{-5}
$\hat{\dot{\theta}}_2[n]$ mean sq. error	7.01×10^{-8}	2.11×10^{-6}	1.28×10^{-5}	1.731×10^{-5}
$\hat{a}_1[n]$ max deviation	0.018	0.307	0.603	0.794
$\hat{a}_2[n]$ max deviation	0.018	0.307	0.603	0.794
$\hat{\dot{\theta}}_1[n]$ max deviation	3.45×10^{-4}	2.80×10^{-3}	4.80×10^{-3}	8.04×10^{-3}
$\hat{\dot{\theta}}_2[n]$ max deviation	3.40×10^{-4}	2.80×10^{-3}	4.65×10^{-3}	5.16×10^{-3}

Table 7.1: Mean square error and maximum deviation as a function of signal separation.

EXAMPLE 7.4

For the two-sinusoid signal,

$$x[n] = \cos\left(\frac{2\pi n}{5} + 12.5\sin\left[\frac{2\pi n}{125}\right]\right) + \cos\left(\frac{4\pi n}{5} + 12.5\sin\left[\frac{2\pi n}{125}\right]\right), \quad (7.31)$$

the AM and FM estimates are shown in Figure 7-4. The error in the estimates is due to both the FM modulation and the SGN.

In the next example, we show a signal with several types of modulation.

EXAMPLE 7.5

The signal in this example is given by

$$x[n] = \left(1 + \frac{n}{1000}\right)\cos\left(\frac{2\pi n}{5} - \frac{2\pi 25n^2}{1000^2}\right) + \left(1 + \frac{1}{2}\cos\left[\frac{\pi n}{100}\right]\right)\cos\left(\frac{3\pi n}{5} + \frac{n}{250}\sin\left[\frac{\pi n}{50}\right]\right). \quad (7.32)$$

The first component has linear AM and linear FM. The second component has sinusoidal AM and linearly increasing sinusoidal FM. The results are shown in Figure 7-5, which show that the algorithm performs well when the modulation functions are quite different from each other.

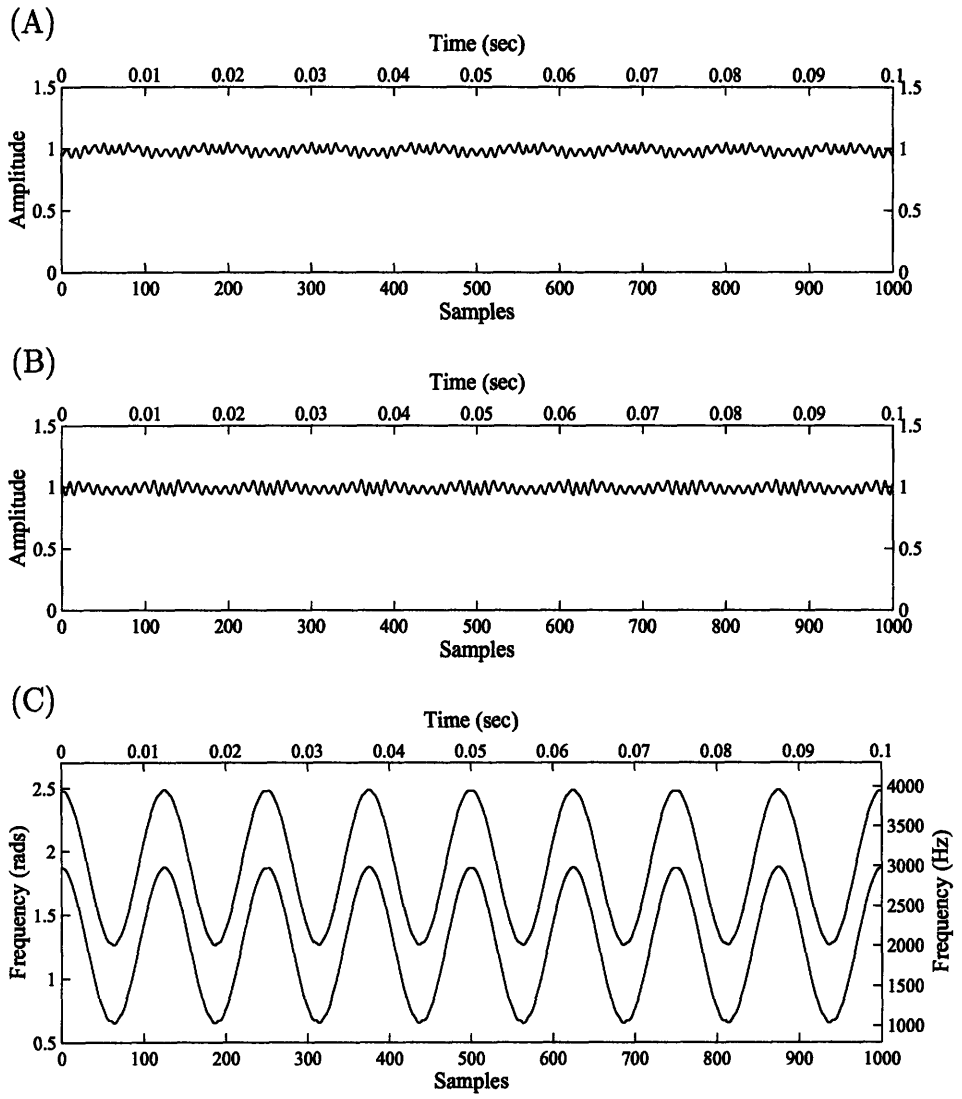

Figure 7-4: AM and FM estimates of a two component signal with constant AM and sinusoidal FM, (A) estimate of $a_1[n]$, mean square error: 1.101×10^{-3}, max deviation: 7.532×10^{-2}, (B) estimate of $a_2[n]$, mean square error: 1.202×10^{-3}, max deviation: 6.799×10^{-2}, (C) estimates of $\dot{\theta}_1[n]$ and $\dot{\theta}_2[n]$, mean square error, $\dot{\theta}_1[n]$: 2.839×10^{-4} (rad/sec), mean square error, $\dot{\theta}_2[n]$: 2.606×10^{-4} (rad/sec), max deviation, $\dot{\theta}_1[n]$: 3.752×10^{-2} (rad), max deviation, $\dot{\theta}_2[n]$: 3.616×10^{-2} (rad).

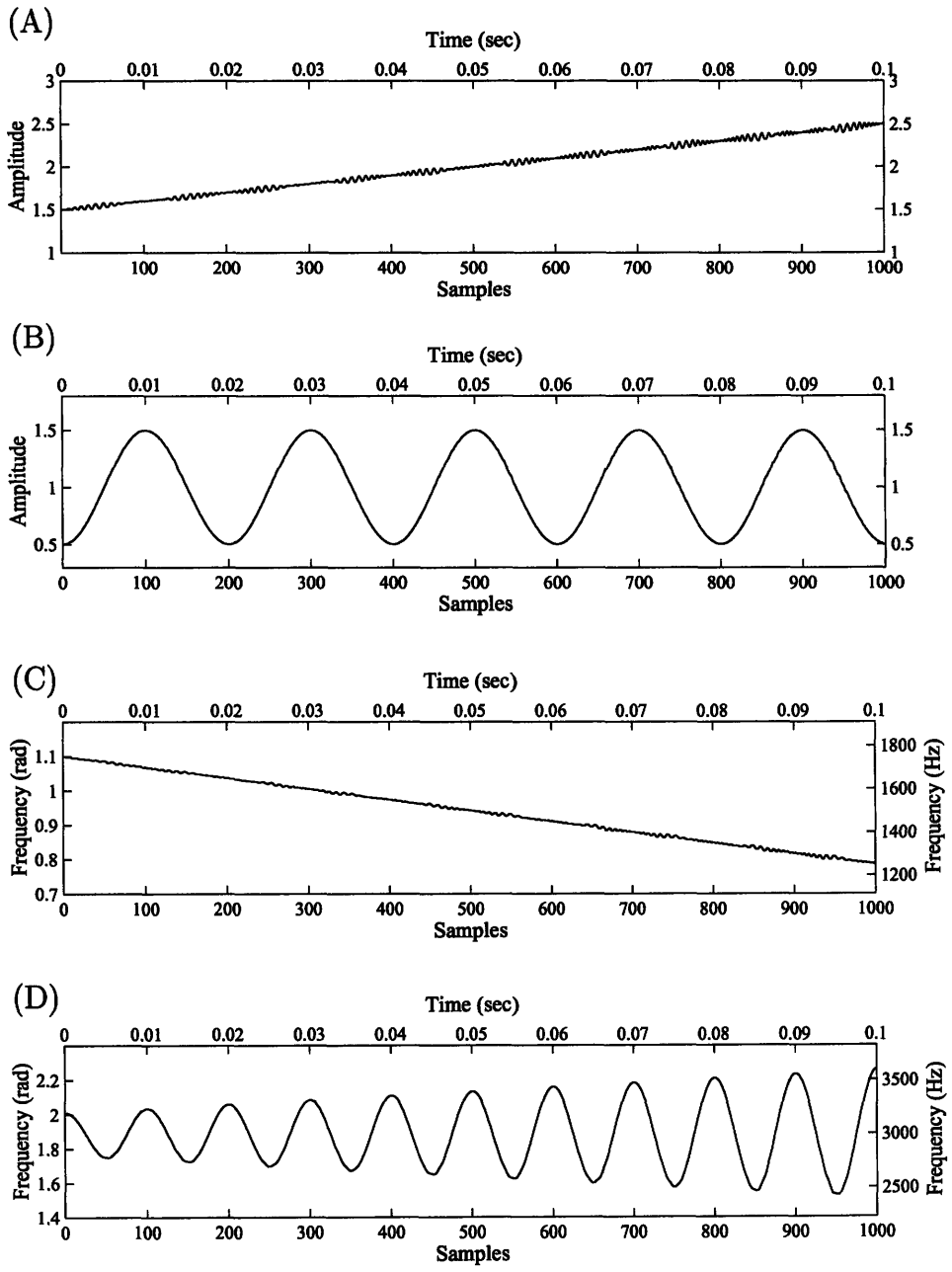

Figure 7-5: Example of two-sinusoid AM-FM estimation with AM and FM, (A) estimate of $a_1[n]$, mean square error: 2.629×10^{-4}, max deviation: 5.118×10^{-2}, (B) estimate of $a_2[n]$, mean square error: 7.048×10^{-6}, max deviation: 1.120×10^{-2}, (C) estimate of $\dot{\theta}_1[n]$, mean square error: 3.360×10^{-6} (rad/sec), max deviation: 7.460×10^{-3} (rad/sec), and (D) estimate of $\dot{\theta}_2[n]$, mean square error: 3.303×10^{-13}(rad/sec), max deviation: 1.030×10^{-2} (rad/sec).

The signal in the next example has two components that cross in frequency.

EXAMPLE 7.6
The signal is

$$x[n] = \cos\left(\frac{3\pi n}{10} + \frac{\pi n^2}{10000}\right) + \cos\left(\frac{6\pi n}{10} - \frac{\pi n^2}{10000}\right) \tag{7.33}$$

and results are shown in Figure 7-6. Since the algorithm assigns the lowest frequency estimate to $\hat{\dot{\theta}}_1[n]$, it does not show the frequency cross. Also observe that the effects of the frequency crossing is local.

In our final example, we plot the mean square error of a group of signals as both the rate of FM and the separation of the two components vary.

EXAMPLE 7.7
The group of signals in this example are given by

$$x[n] = \cos\left(\frac{\pi n}{2} - \frac{\pi\delta n}{100} + \frac{10}{\omega_m}\sin\left(\frac{2\pi\omega_m n}{1000}\right)\right) + \cos\left(\frac{\pi n}{2} + \frac{\pi\delta n}{100} + \frac{10}{\omega_m}\sin\left(\frac{2\pi\omega_m n}{1000}\right)\right), \tag{7.34}$$

where $\delta = 1, 2, \ldots, 10$, and $\omega_m = 1, 2, \ldots, 10$. At a sampling rate of 10,000Hz, this group of signals has an FM rate ranging from 10 to 100Hz, an FM range of 200Hz, and the components are separated by 100 to 1000Hz. When the frequency of the FM rate exceeds the frequency separation between the two components, the SGN has spectral components at frequencies higher than $\dot{\theta}_2[n] - \dot{\theta}_1[n]$. This causes the embedded single-sinusoid AM-FM estimation algorithms to perform poorly and results in the large error that is seen for a few cases of the signal set.

Again, it is important to note that the algorithm used in these examples used no post processing (e.g. no smoothing of the estimates).

7.2 Improvements on the Basic Algorithm

Since the two-sinusoid algorithm was based on the reduction of the two-sinusoid problem into two single-sinusoid problems, the performance of the two-sinusoid algorithm is largely influenced by the performance of the single-sinusoid algorithm. There are, however, modifications that can be made to the two-sinusoid algorithm that are independent of the single-sinusoid algorithm. First, the estimates of $\hat{a}_1[n]$, $\hat{a}_2[n]$, $\hat{\dot{\theta}}_1[n]$,

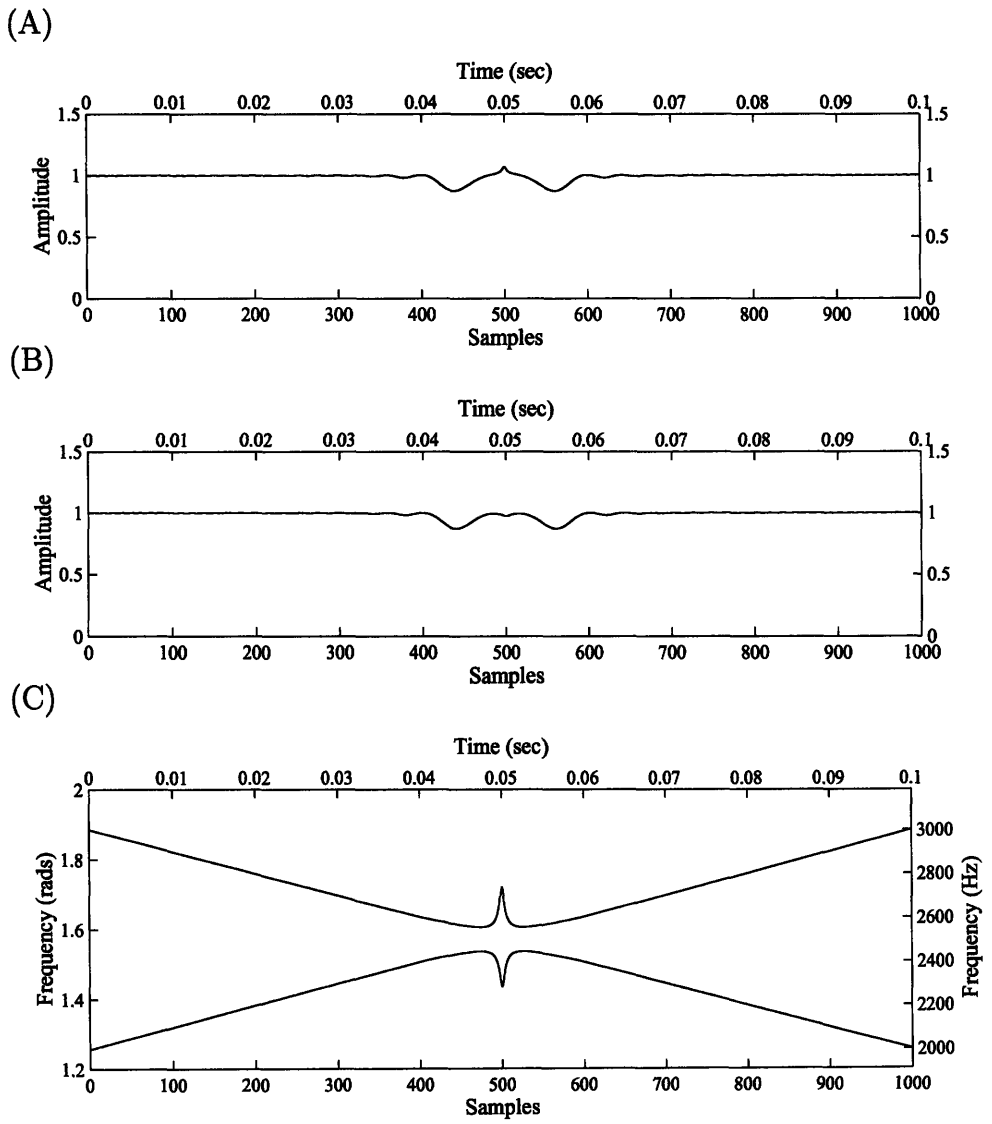

Figure 7-6: An example in which the frequencies of the two components cross, (A) amplitude estimate of first component, (B) amplitude estimate of second component, (C) frequency estimates.

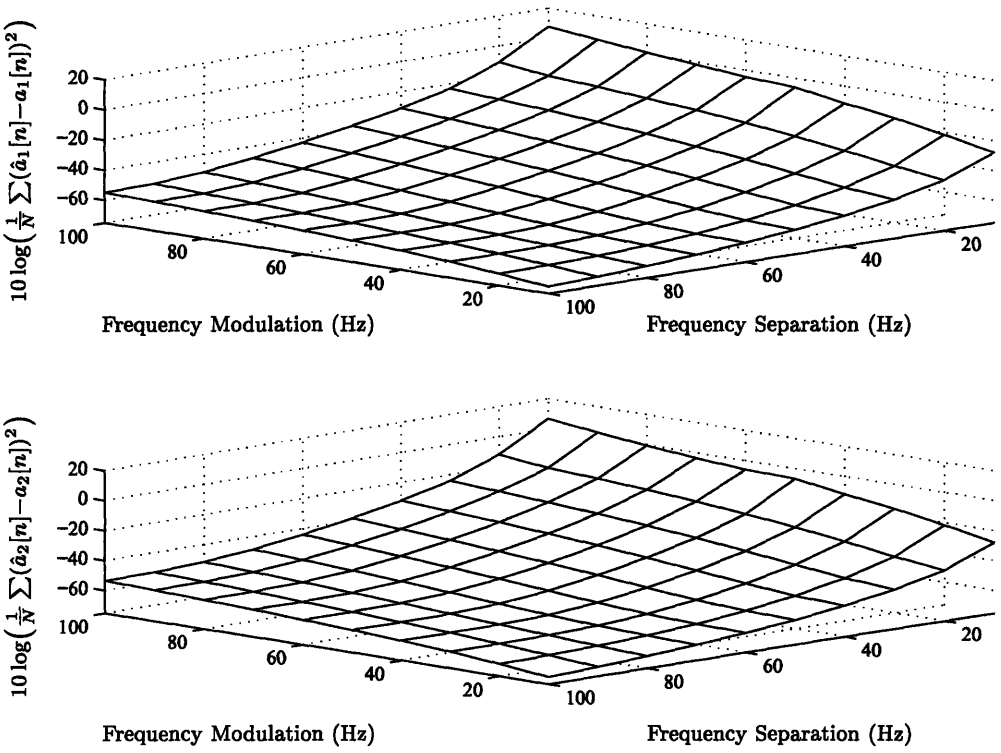

Figure 7-7: Amplitude estimate error as a function of rate of FM and component separation.

and $\hat{\dot{\theta}}_2[n]$ can be used to eliminate the noise terms $\nu_1[n]$ and $\nu_2[n]$. Second, the amplitude modulation of each component can be inverted by adaptive filtering to reduce the transduction error due to the AM.

7.2.1 Eliminating the SGN

In deriving the two-sinusoid estimation algorithm, we assumed that the SGN terms, $\nu_1[n]$ and $\nu_2[n]$, were at a low frequency and were therefore approximately filtered out in the single-sinusoid estimation algorithm. If the modulation functions contain high frequencies, this assumption becomes less valid. For example, suppose that we have a signal of the form

$$x[n] = \left[1 + .5\cos\left(\frac{2\pi n}{50}\right)\right]\cos\left(\frac{2\pi n}{5}\right) + \cos\left(\frac{3\pi n}{5}\right). \tag{7.35}$$

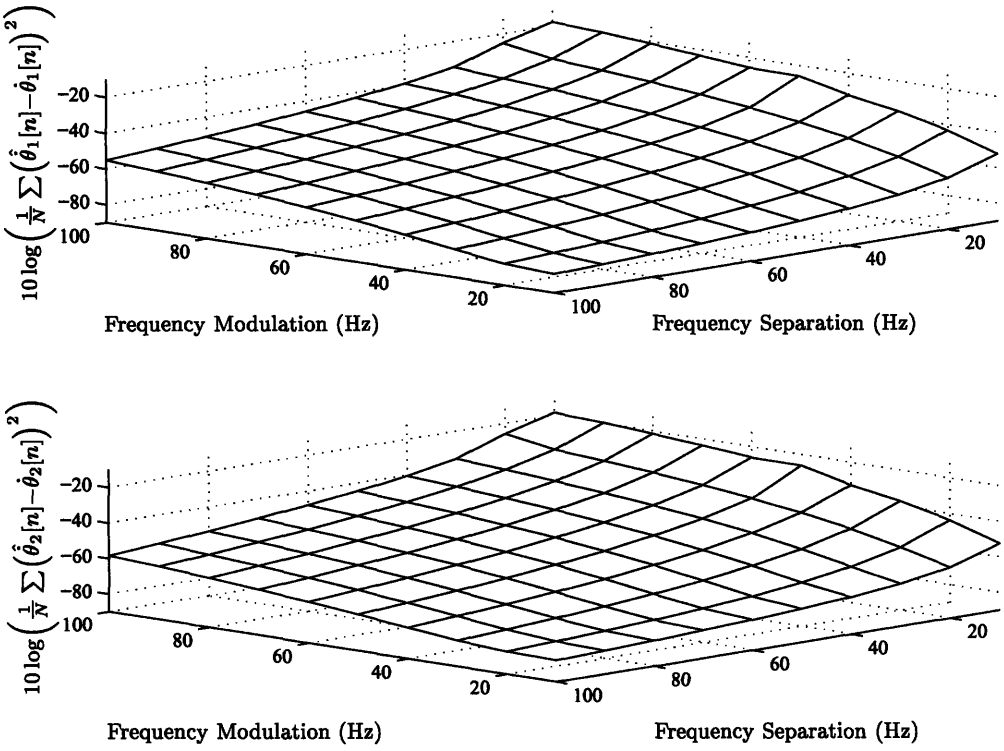

Figure 7-8: Frequency estimate error as a function of rate of FM and component separation.

The magnitude of the Fourier transform of $|g_1[n] * x[n]|^2$ is shown in Figure 7-9. Now suppose that we have obtained the AM and FM estimates from the two-sinusoid estimation algorithm. We can then estimate the SGN from Eq. (7.6) and Eq. (7.7), i.e.

$$\hat{\nu}_1[n] = a_1^2[n]G_1^2(e^{j\dot{\theta}_1[n]}) + a_2^2[n]G_1^2(e^{j\dot{\theta}_2[n]}) \tag{7.36}$$

$$\hat{\nu}_1[n] = a_1^2[n]\dot{\theta}_1^2G_1^2(e^{j\dot{\theta}_1[n]}) + a_2^2[n]\dot{\theta}_2^2G_1^2(e^{j\dot{\theta}_2[n]}), \tag{7.37}$$

and subtract this estimate from the output of filters $G_1(e^{j\omega})$ and $G_2(e^{j\omega})$. Figure 7-10 shows the block diagram with the SGN noise cancelation in place.

Recall that the presence of SGN restricted the inverse modulation in the single-sinusoid algorithm because we could not allow the SGN to be modulated to higher frequencies. Now that we have eliminated the SGN, we can use the single-sinusoid

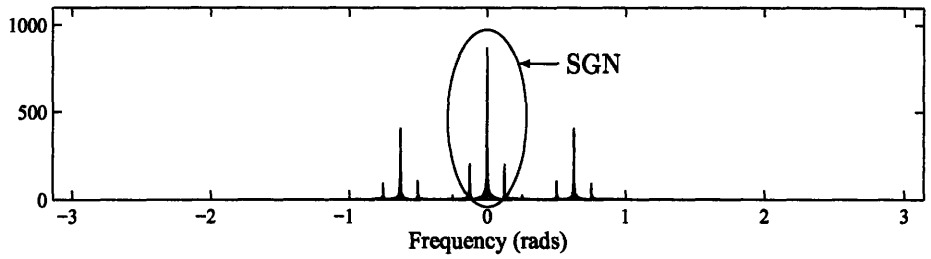

Figure 7-9: Magnitude of Fourier transform of $|g_1[n] * x[n]|^2$.

inverse modulation algorithm as it was described in Chapter 5.

We use the signal described in Eq. (7.35) to illustrate the effects of SGN cancelation. The results are shown in Figure 7-11; the SGN, circled in Figure 7-9, is essentially eliminated and the mean square error has been reduced by a factor of two.

7.2.2 Inverting the Amplitude Modulation

Inverting the modulation when the signal, $x[n]$, consists of two AM-FM sinusoids is not as straightforward as the single-sinusoid case. The difficulty arises because we cannot operate on each component of $x[n]$ independently. We can operate only on the sum of the two components. This makes inverting the FM very difficult. In order to keep the frequency separation between the two signals constant, we would need to adjust the sampling rate as a function of time to compress and stretch the spectrum of $x[n]$. Therefore, we do not address FM inversion for the two-sinusoid case in this thesis.

Inverting the AM is more difficult than in the single-sinusoid case, but less difficult than inverting the FM for the two-sinusoid case. To invert the AM, we use a pair of filters that have a linear frequency response for $\omega \in [0, \pi]$ and are unrestricted[2] for $\omega \in (-\pi, 0)$. At each time sample, using estimates from an initial pass through the

[2]The filters are unrestricted for $\omega \in (-\pi, 0)$ because when we compute the quadrature signal, the negative frequencies of $x[n]$ are eliminated.

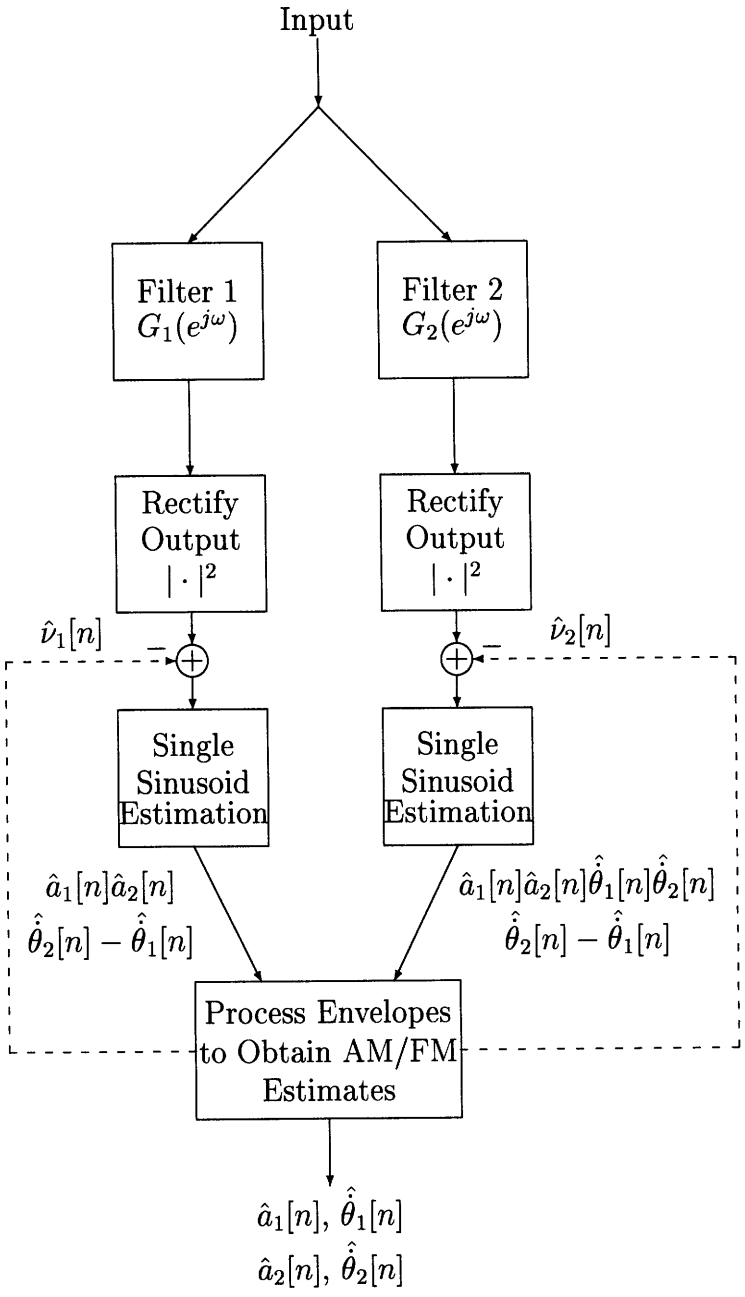

Figure 7-10: Block diagram of two-sinusoid AM-FM estimation algorithm with SGN cancelation feedback.

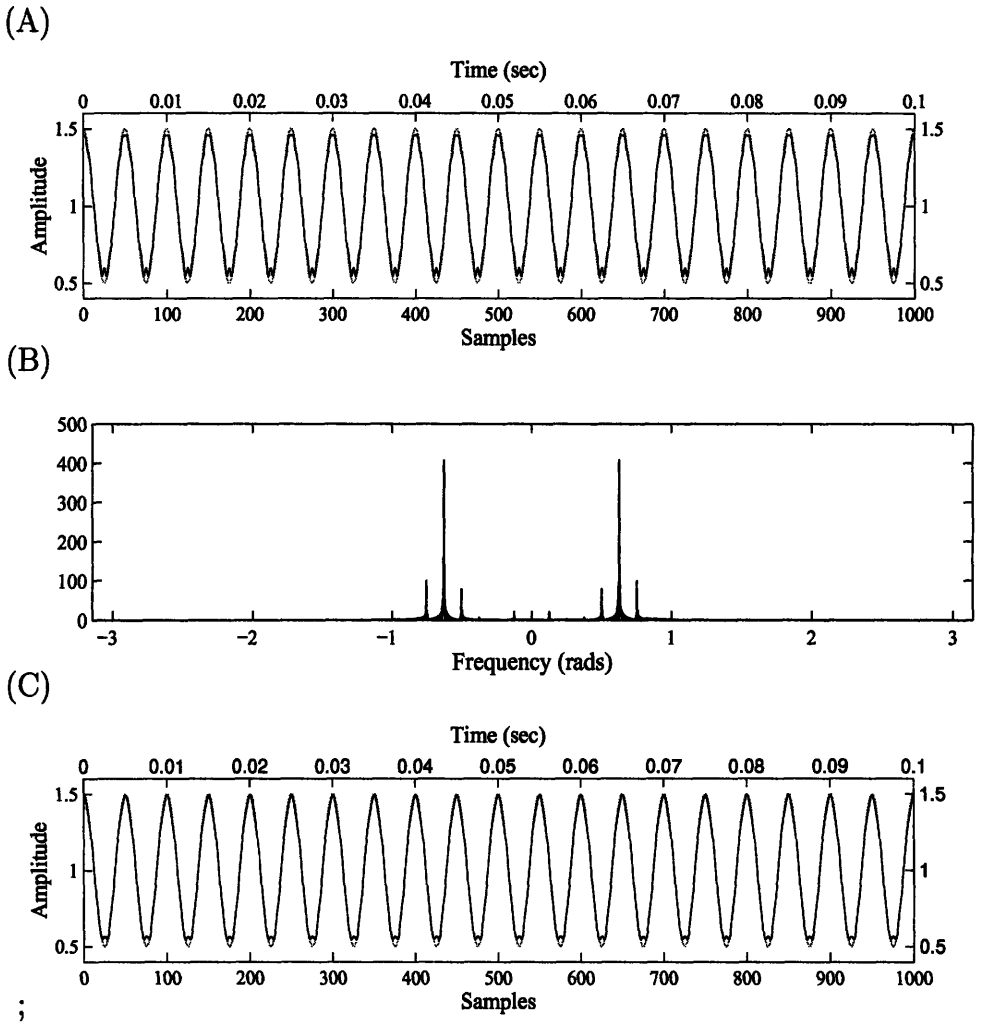

;

Figure 7-11: Example of two-sinusoid algorithm with SGN cancelation, (A) estimate of $a_1[n]$ without SGN cancelation, mean sq. error: 1.074×10^{-3}, (B) magnitude of the Fourier transform of $|g_1[n] * x[n]|^2$ after SGN has been canceled (compare with Figure 7-9), estimate of $a_1[n]$ with SGN cancelation, mean sq. error: 5.093×10^{-4}.

two-sinusoid estimation algorithm, we weight the output of the two linear filters in such a way that the amplitudes of both components are scaled to a value of one. For example, suppose that at time n_0, $a_1[n_0] = 2$, $a_2[n_0] = 3$, $\dot{\theta}_1[n_0] = \frac{\pi}{4}$, and $\dot{\theta}_2[n_0] = \frac{3\pi}{4}$. Then if we pass this signal through a filter with a frequency response, $H(e^{j\omega})$, such that $H(e^{j\frac{\pi}{4}}) = \frac{1}{2}$ and $H(e^{j\frac{3\pi}{4}}) = \frac{1}{3}$, then the output of this filter at n_0 consists of the sum of two sinusoids, each sinusoid with an amplitude equal to one. If this procedure is done at each time sample, then the amplitude modulation has been approximately eliminated (assuming the modulation estimates are close to the true modulation).

We implemented this in the following manner. First, we chose a filter with a linear frequency response for $\omega \in [0, \pi]$,

$$H_{b_1}(e^{j\omega}) = \begin{cases} \frac{\omega}{\pi} & \text{for } 0 \leq \omega \leq \pi \\ \frac{4\omega^3}{\pi^3} + \frac{6\omega^2}{\pi^2} + \frac{\omega}{\pi} & \text{for } -\pi < \omega < 0. \end{cases} \tag{7.38}$$

Over the negative frequency range, we choose $H_{b_1}(e^{j\omega})$ so that its first derivative is smooth over the enter frequency range. This smoothness results in a short impulse response. The value of $H_{b_1}(e^{j\omega})$ for $-\pi < \omega < 0$ is insignificant since the negative frequencies are eliminated by subsequent filtering. The frequency response and impulse response of $H_{b_1}(e^{j\omega})$ is shown in Figure 7-12. We then filter $x[n]$ with $H_{b_1}(e^{j\omega})$ and $H_{b_2}(e^{j\omega}) = 1 - H_{b_1}(e^{j\omega})$ to obtain the two signals $x_{b_1}[n]$ and $x_{b_2}[n]$, respectively. From the transduction approximation, these two signals can be written as

$$x_{b_1}[n] \approx a_1[n]\frac{\dot{\theta}_1[n]}{\pi}\cos(\theta_1[n]) + a_2[n]\frac{\dot{\theta}_2[n]}{\pi}\cos(\theta_2[n]) \tag{7.39}$$

$$x_{b_2}[n] \approx a_1[n]\left(1 - \frac{\dot{\theta}_1[n]}{\pi}\right)\cos(\theta_1[n]) + a_2[n]\left(1 - \frac{\dot{\theta}_2[n]}{\pi}\right)\cos(\theta_2[n]) \tag{7.40}$$

where

$$x[n] = a_1[n]\cos(\theta_1[n]) + a_2[n]\cos(\theta_2[n]) \tag{7.41}$$

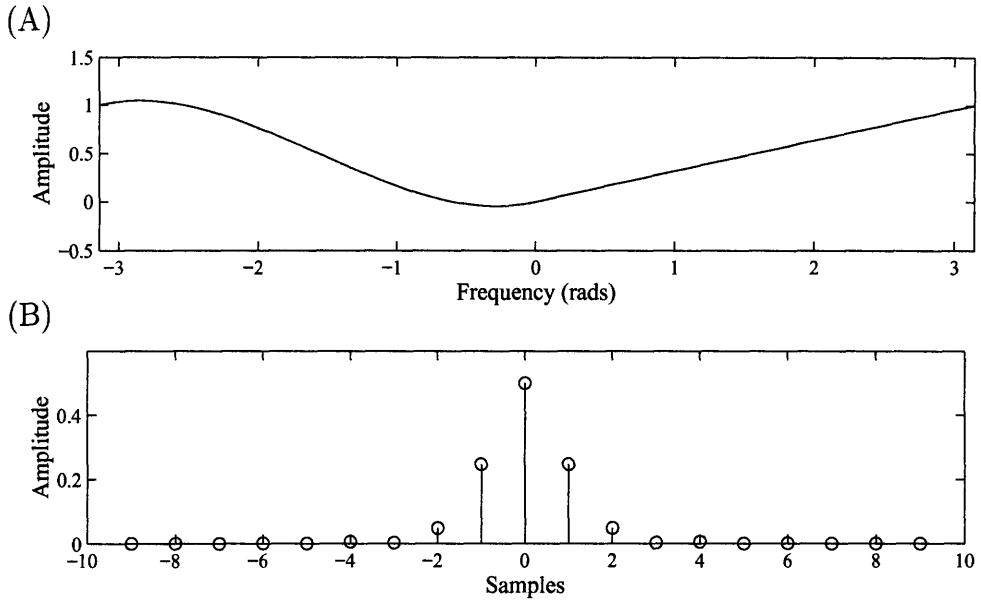

Figure 7-12: Frequency and impulse response of filter used in two-sinusoid AM inversion, (A) frequency response, (B) magnitude of impulse response.

At each time instant, we choose the appropriate weights, $b_1[n]$ and $b_2[n]$, so that

$$x_{dm}[n] = b_1[n]x_{b_1}[n] + b_2[n]x_{b_2}[n] = \cos(\theta_1[n]) + \cos(\theta_2[n]). \tag{7.42}$$

In order for this equation to hold, it must be true that

$$b_1[n]a_1[n]\frac{\dot{\theta}_1[n]}{\pi} + b_2[n]a_1[n]\left(1 - \frac{\dot{\theta}_1[n]}{\pi}\right) = 1 \tag{7.43}$$

and

$$b_1[n]a_2[n]\frac{\dot{\theta}_2[n]}{\pi} + b_2[n]a_2[n]\left(1 - \frac{\dot{\theta}_2[n]}{\pi}\right) = 1. \tag{7.44}$$

Solving for $b_1[n]$ and $b_2[n]$, we have

$$b_1[n] = \frac{a_1[n](\pi - \dot{\theta}_1[n]) - a_2[n](\pi - \dot{\theta}_2[n])}{a_1[n]a_2[n](\hat{\theta}_2[n] - \hat{\theta}_1[n])} \tag{7.45}$$

and

$$b_2[n] = \frac{a_2[n]\dot{\theta}_2[n] - a_1[n]\dot{\theta}_1[n]}{a_1[n]a_2[n](\hat{\theta}_2[n] - \hat{\theta}_1[n])}. \tag{7.46}$$

The estimates used to obtain $b_1[n]$ and $b_2[n]$ are first smoothed with a low pass filter with a cutoff frequency of $\frac{7\pi}{100}$. This is done to prevent the noise in the estimates from making the AM more severe than it was originally.

We again use the signal described in Eq. 7.35. The algorithm has both AM inversion and SGN cancelation. The results are shown in Figure 7-13. Adding the

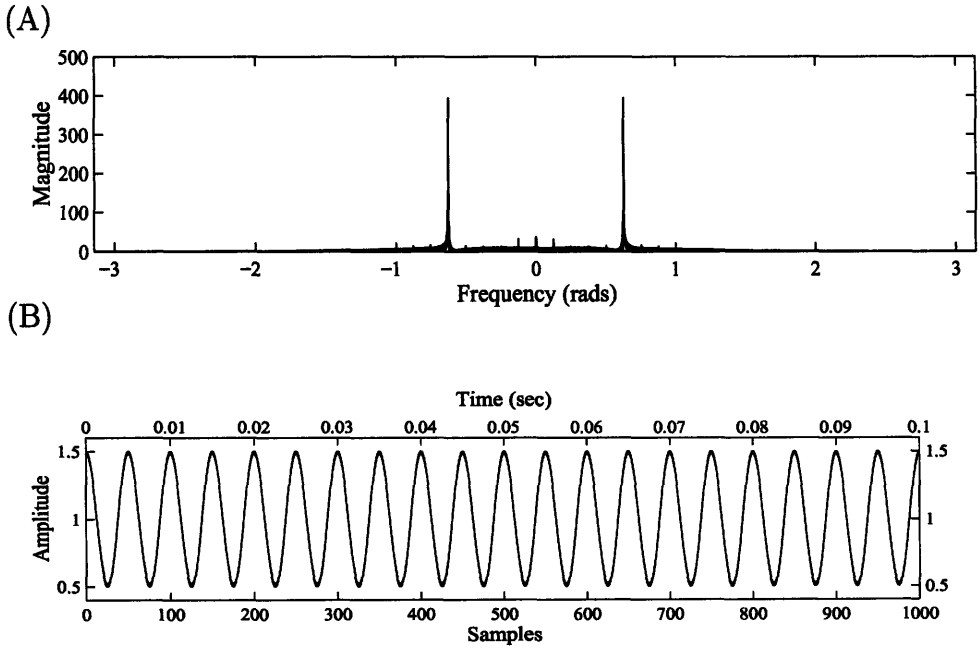

Figure 7-13: Example of two-sinusoid algorithm with SGN cancelation and AM inversion, (A) magnitude of the Fourier transform of $|g_1[n] * x[n]|^2$ after SGN has been canceled (compare with Figure 7-9 and Figure 7-11), (B) estimate of $a_1[n]$ with SGN cancelation and AM inversion, mean sq. error: 9.965×10^{-5}.

AM inversion has improved the estimate. The mean square error is reduced overall by a factor of 10.

7.3 Summary

We have proposed a method of estimating the AM and FM of a signal that is composed of two AM-FM sinusoids. We resolved the uniqueness issue by transforming the problem into two single-sinusoid AM-FM estimation problems, which we have already established have a unique solution. We then proposed modifications to the algorithm. The first modification involved estimating the SGN and then using the estimate to reduce the SGN on the next pass through the estimation algorithm. We also proposed a modification that reduces the AM of the input signal which reduces transduction error, making the transduction approximation more accurate.

Chapter 8

Multi-Component AM-FM Estimation

In the previous chapters, we obtained solutions for the AM and FM components for the cases where the signal contained one or two AM-FM sinusoids. The solution for the two-sinusoid case was obtained by reducing it to two single-sinusoid problems. We are unable to extend this approach to a signal with more than two components because this reduction of order does not occur. For example, consider a signal with three components,

$$x[n] = a_1[n]e^{j\theta_1[n]} + a_2[n]e^{j\theta_2[n]} + a_3[n]e^{j\theta_3[n]}. \tag{8.1}$$

The magnitude squared of this signal is

$$\begin{aligned} |x[n]|^2 = a_1^2[n] + a_2^2[n] + a_3^2[n] + a_1[n]a_2[n]\cos(\theta_2[n] - \theta_1[n]) + \\ a_1[n]a_3[n]\cos(\theta_3[n] - \theta_1[n]) + a_2[n]a_3[n]\cos(\theta_3[n] - \theta_2[n]), \end{aligned} \tag{8.2}$$

which consists of three AM-FM sinusoids plus SGN. We have not reduced the number of components. In fact, for signals that have more than three components, the above procedure produces *more* AM-FM components than the number with which we began.

The approach we propose is still motivated by the auditory model described in

Chapter 1, i.e. we utilize FM to AM transduction and the amplitude envelopes of the outputs of a bank of filters. The difference is that instead of closed form solutions for the AM and FM estimates, we rely on numerical techniques.

The first section of this chapter describes how to pose the problem in such a way that we can use standard numerical techniques to solve for the AM and FM functions. In the second section, we apply our approach to the single-sinusoid case and follow with a section in which we apply the approach to the two-sinusoid case. The purpose of both of these sections is to compare the performance to that of the previous chapters. In the last section, we discuss how this approach can be extended to multi-component AM-FM estimation.

8.1 Problem Formulation

AM-FM separation can be posed as a problem of finding the zeros of a system of nonlinear equations. The system of nonlinear equations results from passing the signal through a bank of filters, $H_1(e^{j\omega}), \ldots, H_N(e^{j\omega})$. If the input is a summation of M AM-FM sinusoids

$$x[n] = \sum_{k=1}^{M} a_k[n] e^{j\theta_k[n]} \tag{8.3}$$

then the transduction approximations of the envelopes of the filter outputs are

$$|y_i[n]|^2 = \sum_k \Bigg(a_k^2[n] H_i^2(e^{j\dot{\theta}_k[n]}) + \sum_{l \neq k} a_k[n] a_l[n] H_i(e^{j\dot{\theta}_k[n]}) H_i(e^{j\dot{\theta}_l[n]}) \cos(\theta_m[n] - \theta_l[n]) \Bigg). \tag{8.4}$$

Since these equations are functions of both $\theta_k[n]$ and $\dot{\theta}_k[n]$, they are a system of nonlinear differential equations. In what follows, we treat $\theta_k[n]$ and $\dot{\theta}_k[n]$ as though they were unrelated in order to simplify the algorithm. Moreover, since the system of equations involves only differences of the $\theta_k[n]$'s, we can reduce the number of

unknowns by one by defining

$$\phi_k[n] = \theta_{k+1}[n] - \theta_k[n] \qquad k = 1, 2, ..., N-1, \tag{8.5}$$

where N is the number of filters in the filter bank. This implies that

$$\theta_k[n] - \theta_l[n] = \sum_{m=l}^{k-1} \phi_m[n]. \tag{8.6}$$

We now have a function with $3M-1$ unknowns,

$$F_i(\hat{a}_1[n], \ldots, \hat{a}_M[n], \hat{\dot{\theta}}_1[n], \ldots, \hat{\dot{\theta}}_M[n], \phi_1[n], \phi_2[n], \ldots, \phi_{M-1}[n]) = |y_i[n]|^2$$
$$- \sum_k \left(\hat{a}_k^2[n] H_i^2(e^{j\hat{\dot{\theta}}_k[n]}) + \sum_{l \neq k} \hat{a}_k[n]\hat{a}_l[n] H_i(e^{j\hat{\dot{\theta}}_k[n]}) H_i(e^{j\hat{\dot{\theta}}_l[n]}) \cos(\sum_{m=l}^{k-1} \phi_m[n]) \right). \tag{8.7}$$

where M is the number of sinusoids. Therefore, we need at least $N = 3M-1$ filters to specify a solution. We know that there is at least one solution at $\hat{a}_k[n] = a_k[n]$, $\hat{\dot{\theta}}_k[n] = \dot{\theta}_k[n]$, and $\phi_k[n] = \theta_{k+1}[n] - \theta_k[n]$. Whether or not this solution is the only solution is an unresolved issue. There are known iterative algorithms, for example Newton's method and its variations, that approximate the solution to a system of nonlinear equations. We now discuss Newton's method for solving systems of nonlinear equations and how it can be applied to AM-FM estimation.

8.2 Newton's Method

Defining $\mathbf{F}(\cdot)$ as

$$\mathbf{F}(\cdot) = \begin{bmatrix} F_1(\cdot) & F_2(\cdot) & \cdots & F_N(\cdot) \end{bmatrix}^T \tag{8.8}$$

and $\mathbf{x}$ as

$$\mathbf{x} = \begin{bmatrix} \hat{a}_1[n] & \cdots & \hat{a}_M[n] & \hat{\dot{\theta}}_1[n] & \cdots & \hat{\dot{\theta}}_M[n] & \phi_{12}[n] & \phi_{13}[n] & \cdots & \phi_{(M-1)(M)} \end{bmatrix}^T, \tag{8.9}$$

we denote the solution to $\mathbf{F}(\mathbf{x})$ as $\mathbf{x}^*$ and the estimate of the solution on the kth iteration as $\mathbf{x}_k$. There are four steps that are performed at each iteration [7]:

1. If $\mathbf{x}_k$ satisfies conditions for convergence, terminate the algorithm with $\mathbf{x}^* = \mathbf{x}_k$.
2. Compute a non-zero step direction $\mathbf{p}_k$.
3. Compute a step length, α_k, such that $\mathbf{F}(\mathbf{x}_k + \alpha_k \mathbf{p}_k) < \mathbf{F}(\mathbf{x}_k)$.
4. Set $\mathbf{x}_{k+1} = \mathbf{x}_k + \alpha_k \mathbf{p}_k$, increment k, and repeat the procedure.

8.2.1 Conditions for Convergence

Since the algorithm is implemented on a digital computer and suffers from rounding errors, we cannot expect to find an *exact* solution. Therefore, we consider $\mathbf{x}_k$ to be a solution if $\|\mathbf{F}(\mathbf{x})\|^2$ is below some threshold. The thresholds varies from the single-sinusoid algorithm to two-sinusoid algorithm. For the single-sinusoid algorithm, the threshold is 1×10^{-9} and, for the two-sinusoid algorithm, the threshold is 1×10^{-3}. These values were determined experimentally.

8.2.2 Determining the Step Direction

The Newton method is derived from a linear approximation of $\mathbf{F}$ at the point $\mathbf{x}_k$. The linear approximation is obtained from the Taylor's series expansion of $\mathbf{F}(\mathbf{x}_k)$

$$\mathbf{F}(\mathbf{x}^*) \approx \mathbf{F}(\mathbf{x}_k) + J(\mathbf{x}_k)(\mathbf{x}^* - \mathbf{x}_k). \tag{8.10}$$

where $J(\mathbf{x}_k)$ is the Jacobian evaluated at $\mathbf{x}_k$. The Jacobian is defined as

$$J_k = \begin{bmatrix} \frac{\partial f_1(\boldsymbol{x}_k)}{\partial x_1} & \frac{\partial f_1(\boldsymbol{x}_k)}{\partial x_2} & \cdots & \frac{\partial f_1(\boldsymbol{x}_k)}{\partial x_n} \\ \frac{\partial f_2(\boldsymbol{x}_k)}{\partial x_1} & \frac{\partial f_2(\boldsymbol{x}_k)}{\partial x_2} & \cdots & \frac{\partial f_3(\boldsymbol{x}_k)}{\partial x_n} \\ \vdots & \vdots & & \vdots \\ \frac{\partial f_n(\boldsymbol{x}_k)}{\partial x_1} & \frac{\partial f_n(\boldsymbol{x}_k)}{\partial x_2} & \cdots & \frac{\partial f_n(\boldsymbol{x}_k)}{\partial x_n} \end{bmatrix} \tag{8.11}$$

Since $\mathbf{x}_{k+1} = \mathbf{x}_k + \alpha_k \mathbf{p}_k$, we want $\mathbf{p}_k$ to approximate $\mathbf{x}^* - \mathbf{x}_k$. Since $\mathbf{F}(\mathbf{x}^*) = 0$, we have from Eq. (8.10)

$$\mathbf{p}_k = -J^{-1}(\mathbf{x}_k)\mathbf{F}(\mathbf{x}_k) \tag{8.12}$$

8.2.3 Determining the Step Length

There are many ways to determine the step length. The condition that must be met is

$$\|\mathbf{F}(\mathbf{x}_k + \alpha_k \mathbf{p}_k)\|^2 < \|\mathbf{F}(\mathbf{x}_k)\|^2 \tag{8.13}$$

In terms of convergence rate, the optimal approach would be to minimize $\|\mathbf{F}(\mathbf{x}_k + \alpha_k \mathbf{p}_k)\|^2$ with respect to α_k. This is a fairly complex nonlinear problem in itself. Since, at this point, we are not interested in fast convergence, we do not concern ourselves with an optimal method. Instead, we use a more brute-force approach – at each iteration we start with an α_k such that $\|\alpha_k \mathbf{p}_k\|_2 = 0.1$, which we choose based on experimentation. If the condition in Eq. (8.13) is satisfied, we use the current α_k. If the condition is not satisfied, we reduce α_k by a factor of 0.9 and then re-evaluate $\mathbf{F}(\mathbf{x}_k + \alpha_k \mathbf{p}_k)$, repeating this procedure if the condition is still not satisfied.

8.3 Newton's Method and Multi-Component AM-FM Estimation

In Section 8.1, we described how the AM-FM estimation problem can be posed as a problem of finding the zeros of a set of nonlinear functions. The nonlinear functions resulted from passing the signal through a bank of filters and approximating the envelopes of the filter outputs with the transduction approximation. In this section, we describe the choice of filters and the implementation.

8.3.1 Filter Choice

In the algorithms of previous chapters, we used the constraint $G_2(e^{j\omega}) = \omega G_1(e^{j\omega})$. We again have constraints between filters and they arise because we calculate the inverse of the Jacobian. In order for the Jacobian to be invertible, the vectors formed by the $3M-1$ partial derivatives of $F_i(\mathbf{x}_k)$ and $F_l(\mathbf{x}_k)$ must be independent for all $i \neq l$ and all $a_i[n] > 0$, $\dot{\theta}[n] \in [0,\pi]$, and $\phi_i[n] \in [0,\pi]$. It is not obvious how this constraint carries over to the filter choice. However, we can make one important observation. We *cannot* use a bank of filters with a linear spectral shape if there is more than one AM-FM sinusoid. This constraint results from the fact that we must use at least five filters when there is more than one sinusoid. If the filters have a linear spectral shape, then the output of one of the filters can be determined from a linear combination of two other filter outputs. In other words, the filter outputs are not linearly independent and therefore no new information is obtained from using more than two filters that have a linear spectral shape. One way to determine if a valid set a filters has been chosen is to confirm that the eigenvalues of the Jacobian are non-zero for all $a_i[n] > 0$, $\dot{\theta}_i[n] \in [0,\pi]$, and $\phi_i[n] \in [0,\pi]$.

We also desire to keep the equations for the filters simple in order to determine the Jacobian. This conflicts with our desire to use a filter that has a short impulse response[1]. We can avoid these difficulties by pre-filtering the input and estimating

[1]Even using filters as in the previous chapter, i.e. $G_1(e^{j\omega}) = \frac{1}{2}(1-cos(2\omega))$, becomes cumbersome when calculating the Jacobian.

the AM-FM functions of the resulting pre-filtered signal. Once the AM-FM functions of the filtered signal have been obtained, the AM-FM functions of the original signal can be easily determined. Figure 8-1 illustrates this approach.

To obtain the AM and FM functions of the original signal, $x[n]$, we first observe that the pre-filtering did not change the frequencies present in $x[n]$. In other words, filtering does not change the FM. Therefore, the FM estimates obtained from $x_f[n]$ are also estimates of the FM of $x[n]$. The amplitude functions, $a_i[n]$, of $x[n]$ are scaled by $P(e^{j\dot{\theta}_i[n]})$, so they can be obtained from the amplitude estimates of $x_f[n]$ by dividing by $P(e^{j\dot{\theta}_i[n]})$. Viewing the system as a pre-filter cascaded with a bank of filters allows us to design filters with short impulse responses and to simultaneously choose filters that are simple so that calculating the Jacobian is still practical.

8.4 Newton's Method Applied to the Single AM-FM Sinusoid

We now return to the problem of estimating the AM and FM functions when the input is of the form

$$x[n] = a[n]\cos(\theta[n]). \tag{8.14}$$

We can specify the filters as before. The pre-filter is given by

$$P(e^{j\omega}) = \begin{cases} \frac{1}{2}(1-\cos(2\omega)) & 0 \le \omega \le \pi \\ 0 & -\pi < \omega < 0 \end{cases} \tag{8.15}$$

and the two filters in the filter bank are given by

$$H_1(e^{j\omega}) = \begin{cases} 1 & 0 \le \omega \le \pi \\ 0 & -\pi < \omega < 0 \end{cases} \tag{8.16}$$

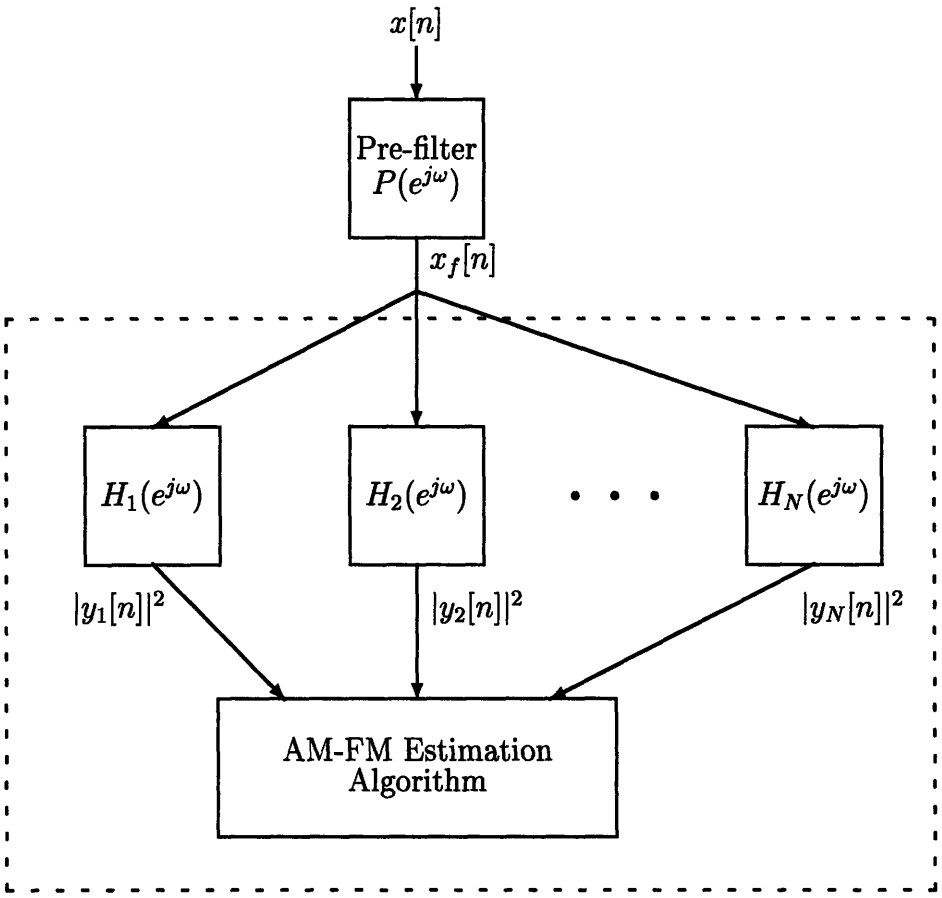

Figure 8-1: Block diagram showing the relation between the pre-filtering stage and the AM-FM estimation algorithm.

and

$$H_2(e^{j\omega}) = \begin{cases} \omega & 0 \le \omega \le \pi \\ 0 & -\pi < \omega < 0 \end{cases} \tag{8.17}$$

With these particular filter choices, the multivariate function, $\mathbf{F}(\mathbf{x})$, becomes

$$\mathbf{F}(\mathbf{x}, n) = \begin{bmatrix} F_1(\hat{a}[n], \hat{\dot{\theta}}[n]) \\ F_2(\hat{a}[n], \hat{\dot{\theta}}[n]) \end{bmatrix} = \begin{bmatrix} \hat{a}^2[n] - |y_1[n]|^2 \\ \hat{a}^2[n]\hat{\dot{\theta}}^2[n] - |y_2[n]|^2 \end{bmatrix} \tag{8.18}$$

and from Eq. (8.11), the Jacobian is

$$J(\mathbf{x}, n) = \begin{bmatrix} 2a[n] & 0 \\ 2\dot{\theta}^2[n]a[n] & 2\dot{\theta}[n]a^2[n] \end{bmatrix} \tag{8.19}$$

In the following example, our test signal is the same as that of Example 4.4.

EXAMPLE 8.1
For the signal

$$x[n] = \left[1 + .7\cos\left(\frac{\pi n}{20}\right)\right]\cos\left(\frac{\pi n}{2} + 2\sin\left(\frac{\pi n}{10}\right)\right), \tag{8.20}$$

results are shown in Figure 8-2. The performance is close to that of the first single-sinusoid estimation algorithm of Chapter 4.

8.5 Newton's Method Applied to Two AM-FM Sinusoids

The case with two AM-FM sinusoids present in the input was also described and implemented in a previous chapter. Recall that the input is of the form

$$x[n] = a_1[n]\cos(\theta_1[n]) + a_2[n]\cos(\theta_2[n]). \tag{8.21}$$

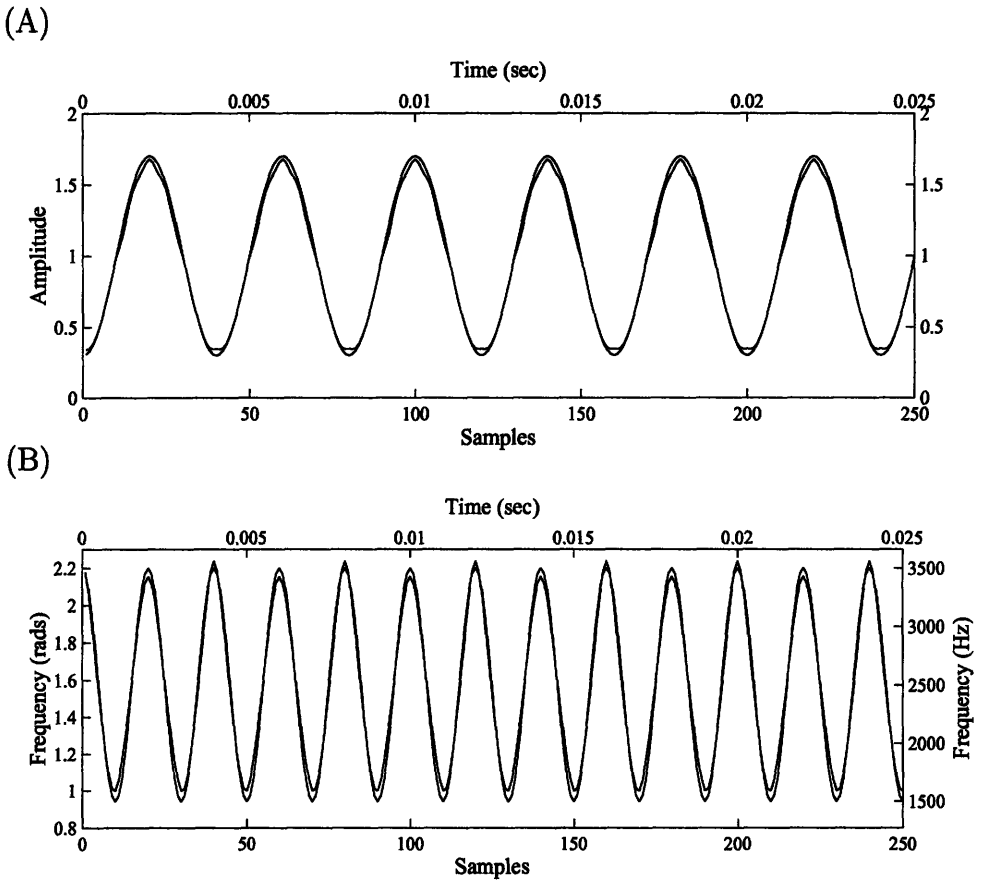

Figure 8-2: Example of Newton's method applied to single-sinusoid AM-FM estimation, (A) amplitude estimate, mean square error: $1.424 \times 1-^{-3}$, max deviation: 6.784×10^{-2}, (B) frequency estimate, mean square error: 2.860×10^{-3} (rad^2/sec), max deviation: 1.009×10^{-1} (rad).

We have chosen the same pre-filter as Eq. (8.15). The five filters are expressed as

$$H_1(e^{j\omega}) = \begin{cases} 1 & 0 \leq \omega \leq \pi \\ 0 & -\pi < \omega < 0 \end{cases} \qquad H_2(e^{j\omega}) = \begin{cases} \omega^{\frac{1}{4}} & 0 \leq \omega \leq \pi \\ 0 & -\pi < \omega < 0 \end{cases} \tag{8.22}$$

$$H_3(e^{j\omega}) = \begin{cases} \omega^{\frac{1}{2}} & 0 \leq \omega \leq \pi \\ 0 & -\pi < \omega < 0 \end{cases} \qquad H_4(e^{j\omega}) = \begin{cases} \omega^{\frac{3}{4}} & 0 \leq \omega \leq \pi \\ 0 & \pi < \omega < 0 \end{cases}$$

$$H_5(e^{j\omega}) = \begin{cases} \omega & 0 \leq \omega \leq \pi \\ 0 & -\pi < \omega < 0 \end{cases}$$

which are chosen for ease in determining the Jacobian. We now show an example of the performance of this approach.

EXAMPLE 8.2

The input signal is given by

$$x[n] = \left[1 + .2\sin\left(\frac{\pi n}{125}\right)\right]\cos\left(\frac{2\pi n}{5} + 10\sin\left(\frac{\pi n}{250}\right)\right) + \left[1 - .3\cos\left(\frac{3\pi n}{500}\right)\right]\cos\left(\frac{3\pi n}{5} - \frac{\pi n^2}{25000}\right). \quad (8.23)$$

The results are shown in Figure 8-3. Although the performance is slightly inferior to that of the two-sinusoid AM-FM estimation algorithm presented in Chapter 7, these results indicate that this approach can be applied to AM-FM estimation successfully.

8.6 Extension to Multi-Component Case

The procedures that we described in this chapter can be extended to the multi-component case. There are a few issues that must be addressed before implementation. First, the amount of computation increases dramatically for each additional component. For example, the inverse of the Jacobian is repeatedly calculated until the algorithm converges and this repeated calculation occurs at each sample point. Since the Jacobian is a $(3M-1) \times (3M-1)$ matrix, M being the number of sinusoids, calculating the inverse of the Jacobian becomes very computationally expensive. There are more efficient variations of Newton's method that do not require this calculation at every iteration and these methods are desirable for the case of multiple sinusoids. Second, we need to better understand how the choice of filters affects performance. Last, and most important, we need to establish whether or not this approach allows for a *unique* solution.

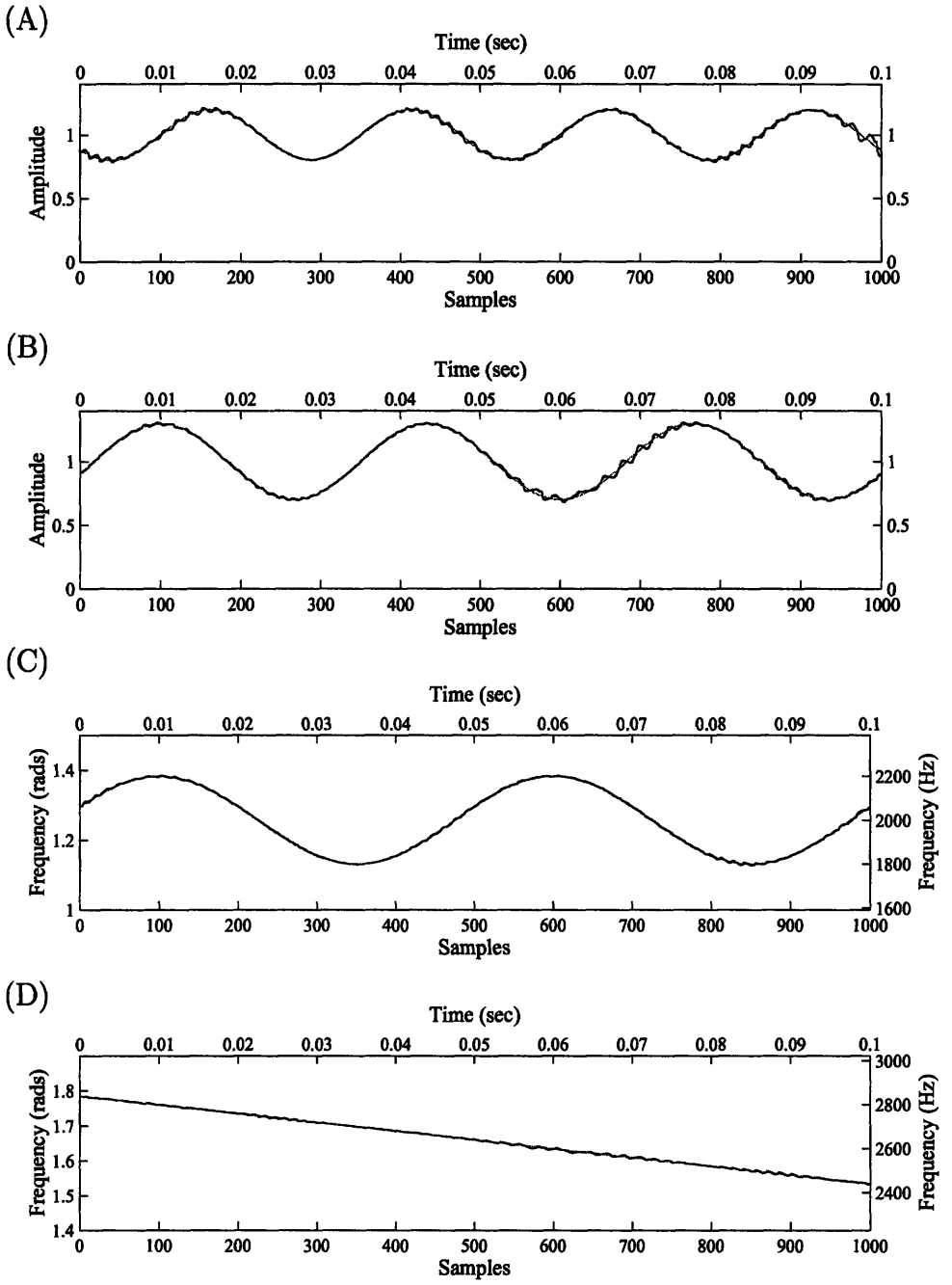

Figure 8-3: Estimates (solid lines) obtained from two-sinusoid AM-FM estimation using Newton's method, (A) estimate of $a_1[n]$, mean square error: 1.618×10^{-4}, max deviation: 6.079×10^{-2}, (B) estimate of $a_2[n]$, mean square error: 1.415×10^{-4}, max deviation: 4.320×10^{-2}, (C) estimate of $\dot{\theta}_1[n]$, mean square error: 2.772×10^{-6} rad^2/sample, max deviation: 5.325×10^{-3} rad, (D) estimate of $\dot{\theta}_2[n]$, mean square error: 2.302×10^{-6} rad^2/sample, max deviation: 5.649×10^{-3} rad.

8.7 Summary

In this chapter, we described an approach to AM-FM estimation for signals with multiple AM-FM components that utilizes FM to AM transduction to obtain a system of nonlinear equations which is solved with standard numerical techniques. We implemented this approach for the cases where the input consists of one or two AM-FM sinusoids and gave examples. We then discussed a few of the unresolved issues with this approach for the case of three or more sinusoids.

Chapter 9

Conclusions

9.1 Summary of Thesis

Our goal in this thesis was to estimate the AM and FM of the sinusoidal components of a signal. Our approach was motivated by the early stages of auditory processing. There were three fundamental properties of the auditory system that provided this motivation: (1) the input signal is processed with a bank of broad, overlapping filters, (2) the output of these filters is rectified, and (3) there is FM to AM transduction.

The first half of the thesis described our approach to AM-FM estimation for the case where the input is a single AM-FM sinusoid. Although some similar work has been performed [14, 13, 16], we proposed and implemented improvements to the approach; furthermore, the single-sinusoid algorithm provided the foundation for extending the algorithm to the case where the input consists of two AM-FM sinusoids. Our improvements involved using the AM and FM estimates to "invert" the modulation of the signal and then applying the algorithm to the demodulated signal. By doing this, we showed experimentally that the transduction error was reduced on successive iterations, resulting in improved AM-FM estimates.

The inverse modulation technique required that we modulate the signal to a frequency, ω_c, in order to keep the signal in the passband of the filters. To determine the optimal choice for ω_c, we considered separately how ω_c influences performance in terms of transduction error and additive noise. To perform this analysis, we devel-

oped a new frequency-domain approach to analyze filters with respect to transduction error.

We then proposed a method to estimate the AM and FM functions when the input signal is assumed to be a sum of two AM-FM sinusoids. We showed that this problem can be reduced to two single-sinusoid AM-FM estimation problems. We also improved this algorithm by both canceling the SGN and inverting the AM. We gave several examples which showed that the algorithm works under a wide range of AM-FM signals.

The last topic of the thesis was the extension of the transduction-based approach to the more general multi-component AM-FM estimation problem. We showed that the approach used for the two-sinusoid case, i.e. reducing the problem to a lower-order problem, does not work. We therefore proposed the use of standard numerical approaches to solve the set of nonlinear equations that result from taking the magnitude of the filter bank outputs. We gave examples for the single- and two-sinusoid case and outlined the approach for more than two components.

9.2 Suggestions for Future Work

This thesis has shown that FM to AM transduction is a useful approach to AM and FM estimation. There are several aspects of the algorithms presented that can be improved upon or which require further investigation.

Improving Filter Selection

One of the key factors in choosing the particular transduction filters was analytic simplicity. Therefore, these filters are likely not "optimal". There are two complementary criterion to use when choosing The transduction filters. First, the results obtained by Bovik et al. [3] show that in order to reduce transduction error, the impulse response of the filter should be as short in duration as possible[1]. As we established in Chapter 6, another requirement is that the frequency response of the filters are maximally flat

[1]See Eq. (3.11).

over the frequency range of the inputs. The filters cannot have a completely flat spectral shape, however, because such filters do not transduce the FM to AM. Therefore, we face a trade-off between simplicity, spectral shape, and impulse response length. The other aspect of the filter choice is the relationship among the filters. Recall in the one- and two-sinusoid cases, we chose $G_2(e^{j\omega}) = \omega G_1(e^{j\omega})$, for analytic simplicity. Again, there is a trade-off between analytic simplicity, spectral shape, and the impulse response length of $G_1(e^{j\omega})$ and $G_2(e^{j\omega})$.

Multi-Component Extensions

In Chapter 8, we proposed a method using standard numerical techniques to estimate the AM and FM functions when the signal is consists of more than two AM-FM sinusoids. We did not show that this approach produces a unique solution; this result needs to be established. Despite the issue with uniqueness, we implemented the methods for the cases of one and two sinusoids. For the single-sinusoid case, the algorithm converged to the "true" solution with performance comparable to that of the single-sinusoid AM-FM estimation algorithm of Chapter 4. The two-sinusoid algorithm also converged to the "true" solution, but its performance was somewhat inferior than that of the two-sinusoid AM-FM estimation algorithm of Chapter 7. One factor that possibly contributes to the inferior performance may be the filter choice. Since we required the Jacobian, which involves taking the derivatives of products of the frequency response of the filters, we kept the filters simple. In doing so, we may have chosen filters that are poorly suited for this task. If the uniqueness results can be established, then a multi-component algorithm needs to be implemented. We have done some preliminary experimentation with a three-sinusoid algorithm and had difficulties with convergence. We are unsure if this is caused by the manner in which the algorithm has been implemented or because there is not a unique solution.

Signal Detection

In all of the algorithms presented in this thesis, it was assumed that number of components of a signal remained the same throughout the duration of the signal. Since many signals we are interested in analyzing, such as speech, do not have the

same number of components at every instant, it is desirable to have the algorithms detect these changes.

Convergence of Inverse Modulation

In Chapter 5, we showed experimentally that inverting the modulation with estimates of the AM and FM significantly reduced the estimation error. A current area of investigation is proving that this technique converges to the exact AM and FM functions.

Signal Separation

In Chapter 7, we showed that when the frequency separation of the two components becomes small and the modulation increases in rate, the error in the estimates increases significantly. This is a result of the SGN having spectral components which are passed to the embedded single-sinusoid algorithm. The SGN cannot be canceled in these cases because the initial estimates contain such large errors and therefore give poor SGN estimates. We are currently investigating alternative approaches to SGN cancelation that work under a wider range of conditions.

Error Reduction by Multiple Filters

In the algorithms presented in this thesis, we have used the minimum number of filters necessary. A possible approach to reduce the error is to use many filters and exploit the redundancy to obtain improved AM-FM estimates. For example, we could average the estimates obtained from several algorithms using different filter sets.

Filtering Additive Noise

After obtaining the FM estimates, we can filter the signal to remove any noise that does not lie in the frequency range of the signal and then re-apply the algorithm. Preliminary experimentation indicates that this technique significantly reduces sensitivity to additive noise.

Bibliography

[1] E.H. Armstrong. A method of reducing disturbances in radio signaling by a system of frequency modulation. In *Proc. of Institute of Radio Engineers*, volume 24, pages 689–740, May 1936.

[2] B. Boashash. Estimating and interpreting the instantaneous frequency of a signal. In *Proc. IEEE*, volume 80, pages 519–568, April 1992.

[3] A.C. Bovik, J.P. Havlicek, and M.D. Desai. Theorems for discrete filtered modulated signals. In *Proc. IEEE Int. Conf. on Acoustics, Speech, and Signal Processing*, Minneapolis, Minnesota, April 1993.

[4] Leon Cohen. *Time-Frequency Analysis.* Prentice Hall PTR, Englewood Cliffs, NJ, 1995.

[5] John P. Costas. Residual signal analysis. *Proceedings of the IEEE*, 68(10):1351–1352, October 1980.

[6] John P. Costas. Residual signal analysis - a search and destroy approach to spectral estimation. In *Proceedings of the First ASSP Workshop on Spectral Estimation*, pages 6.5.1–6.5.8, August 1981.

[7] Philip E. Gill, Walter Murray, and Margaret H. Wright. *Practical Optimization.* Academic Press, New York, NY, 1981.

[8] J.L. Goldstein. Auditory spectral filtering and monaural phase perception. *J. Acoust. Soc. Am.*, 41(2):458–479, 1967.

[9] R. Kumaresan, A.G. Sadasiv, C.S. Ramalingam, and J. F. Kaiser. Instantaneous nonlinear operators for tracking multicomponent signal parameters. In *Proc. IEEE Sixth SP Workshop on Statistical Signal and Array Processing*, pages 404–407, Victoria, B.C., Canada, 1992.

[10] Petros Maragos, James F. Kaiser, and Thomas F. Quatieri. Energy separation in signal modulations with application to speech analysis. *IEEE Transactions on Signal Processing*, 41(10):3024–3051, 1993.

[11] Petros Maragos, James F. Kaiser, and Thomas F. Quatieri. On amplitude and frequency demodulation using energy operators. *IEEE Transactions on Signal Processing*, 41(4):1532–1550, 1993.

[12] Petros Maragos and Alexandros Potiamanos. Higher order differential energy operators. *IEEE Signal Processing Letters*, 2:152–154, 1995.

[13] Robert M^{c}Eachern. How the ear really works. In *Proc. of the IEEE-SP Int. Symp. on Time-Frequency and Time-Scale Analysis*, pages 437–440, Victoria, B.C., Canada, October 1992.

[14] Robert M^{c}Eachern. Hearing it like it is - audio signal processing the way the ear does it. *DSP Applications*, pages 35–47, February 1994.

[15] A.V. Oppenheim and R.W. Schafer. *Discrete-Time Signal Processing.* Prentice Hall, Englewood Cliffs, NJ, 1989.

[16] T.F. Quatieri, T.E. Hanna, and G.C. O'Leary. AM-FM separation using auditory-motivated filters. *IEEE Trans. on Speech and Audio Processing*, 1997. To be published in Sept/Nov. Also in *Proc. IEEE Int. Conf. on Acoustics, Speech, and Signal Processing*, Atlanta, GA, May 1996.

[17] C. S. Ramalingam. *Analysis of Non-Stationary, Multi-Component Signals with Applications to Speech.* PhD thesis, University of Rhode Island, Kingston, RI, January 1995.

[18] Kourosh Saberi and Ervin R. Hafter. A common neural code for frequency- and amplitude-modulated sounds. *Nature*, 374(6):537–539, April 1995.

[19] Balasubramaniam Santhanam and Petros Maragos. Energy demodulation of two-component AM-FM signals with application to speaker separation. In *Proc. Intl. Conf. Acoust., Speech, and Sig. Proc.*, Atlanta, 1996.

[20] George B. Thomas. *Calculus and Analytic Geometry.* Addison-Wesley Pub. Co., Reading, MA, 4th edition, 1968.